A LOW COST FREE DRIFTING POSITION TRANSMITTER FOR THE MEASUREMENT OF THE THERMOCLINE PROPERTIES

CANDIDATE NAME:

SEBASTIEN QUEHIN

AWARD:

M.Eng BY RESEARCH (MODE A)

INSTITUTION:

GALWAY-MAYO INSTITUTE OF TECHNOLOGY

SUPERVISOR:

Dr. PATRICK DELASSUS

Submitted to the National Council for Education Awards, July 2000

ABSTRACT

This thesis describes the work undertaken in the conception of a vehicle able to observe the thermocline, the temperature and the salinity from the sea surface to 200m deep. This work includes the mechanical design of the device, termed a "ballast system" or "subsurface profiler" and the control of its velocity. This profiler is able to accommodate sensors capable of collecting such data (temperature and salinity). These sensors are provided by Sea-Sense Ltd, Galway. The profiler is designed to be disposable, auto-controlled and located by satellites in order to eliminate the recovery cost. It is designed to achieve at least two hundred cycles from the sea surface to 200m deep. Furthermore, the profiler velocity must be controlled accurately and as close as possible to $0.05 m.s^{-1}$.

Once the mechanical design and the selection of the appropriate sensors mounting components are achieved, the mechanical strength of the profiler, using appropriate materials, is evaluated at 200m deep where the pressure is relatively high (about 20 bars).

The profiler velocity is simulated via a motor, which pumps (discharges) water in order to become heavier (lighter).

Tools such as mechanical design automation software, finite element analysis and dynamical simulation systems software were employed to provide a solution to each problem through this project.

ACKNOWLEDGEMENTS

I am greatly indebted to a number of people for their contributions throughout this project.

Firstly, I would like to thank Dr. PATRICK DELASSUS, my project supervisor for giving me the opportunity to undertake this project.

I would also like to thank him for his advice, criticism and knowledge throughout these 21 months.

Special thanks are due to MARCEL CURE for his assistance in oceanography, GEORGE ANDERSON for his help in control theory and GERALD MacMICHAEL for his advice.

TABLE OF CONTENTS

I- INTRODUCTION 1

II- OCEANOGRAPHY

1-MATHEMATICAL EQUATIONS 5

2-CLASSIFICATION OF FORCES AND MOTIONS 6

A-Wind-driven circulation 6

B-Thermohaline circulation 6

3-HORIZONTAL CIRCULATION 7

A-Ekman spiral 7

B-Geostrophic currents 8

4-VERTICAL CIRCULATION 10

A-Thermohaline circulation 10

B-Wind-induced circulation 11

C-Langmuir circulation 12

5-PROPERTIES OF SEAWATER 14

A-Pressure 14

B-Temperature 14

C-Salinity 15

D-Density 16

6-CONCLUSION 17

III- DESIGN

1-INTRODUCTION 19

2-EXISTING DEVICES 20

A-Instruments connected directly to the vessel 21

B-Free-fall sensors 21

C-Sensors fixed in position 23

D-Measurement using tracked devices 23

3-SELECTION 25
4-OTHER SOLUTIONS 27
A-Thermodynamic solution 27
B-Airship solution 29
C-Change in mass solution 30
5-CONCLUSION 31

IV- DYNAMICS OF THE PROFILER
1-INTRODUCTION 33
2-GENERAL EQUATIONS OF MOTION OF UNDERWATER VEHICLES 33
3-EQUATIONS OF MOTION APPLIED TO THE REAL PROFILER 36
A-Assumptions 36
B-Linearisation of the drag force 37
C-Quantity of water required 40
D-Acceleration and deceleration 47
4-CONCLUSION 50

V-PUMP DESIGN
1-INTRODUCTION 52
2-LEADING PARAMETERS 53
3-DIFFERENTIAL PISTON 54
A-Foam and gas 54
B-Belleville washers 55
C-Heavy-duty spring 57
D-Conclusion 58
4-BALL SCREW 58
A-Transformation of rotary motion into piston translation 58
B-Selection of the ball screw 59
C-Conclusion 62
5-CONCLUSION 63

VI-MOTOR SELECTION

1-INTRODUCTION 65

2-TORQUE 65

3-MOTOR SELECTION 66

A-Stepper motor 66

B-High torque motor 66

C-Sketch of the internal device 70

4-BATTERY SELECTION 71

5-CONCLUSION 75

VII-MATERIAL AND SHAPE OF THE PROFILER

1-INTRODUCTION 77

2-MATERIAL 77

A-External shape 77

B-Mechanical properties of Epoxy and fibreglass 77

C-Pump 78

D-Corrosion prevention 78

3-SHAPE 81

A-Influence of the profiler volume 81

B-Shamrock shape 82

C-Cylindrical shape 83

4-STRESS ANALYSIS OF THE EXTERNAL SHAPE 84

A-Shamrock shape 84

B-Cylindrical shape 86

5-BEARING SUPPORT 87

A-Without web 88

B-With web 89

6-STRESS ANALYSIS OF THE CYLINDER FIXATION: 90

7-CONCLUSION 93

VIII-CONTROL DESIGN OF THE PROFILER

1-INTRODUCTION 95

2-SELECTION OF THE CONTROL METHOD 95

A-Mathematical method 95
B-Pressure difference method 96
C-Selection 98
3-ARMATURE CONTROL VERSUS FIELD CONTROL 99
4-SIGNAL CONDITIONING 99
5-TACHOMETER 100
6-BLOCK DIAGRAM 100
7-STABILITY 101
A-Assumptions 101
B-Definition 102
C-Condition of a stable system 102
D-Determination of the system stability 105
E-Conclusion 108
8-SIMULATION 108
9-CONCLUSION 115

IX-STABILITY OF THE SUBMERGED AND FLOATING PROFILER
1-INTRODUCTION 117
2-STABILITY 117
3-CONCLUSION 121

X-OVERALL CONCLUSION 122

APPENDIX A: INTERNATIONAL EQUATION OF STATE OF SEAWATER 131

APPENDIX B: BALL SCREW VELOCITY AND TIME PER DUTY 133

APPENDIX C: TIME AND AMPERAGE REQUIRED PER DUTY 144

APPENDIX D: OUTPUT CHARACTERISTICS OF THE MOTOR 153

APPENDIX E: NOMENCLATURE 164

CHAPTER I:

INTRODUCTION

The information about the upper parts of the ocean obtained in recent years by earth-orbiting satellites is immense. Measurements are made over vast areas of the ocean surface. Satellites have greatly improved the accuracy of position fixing, but satellite sensors are only able to obtain measurements at the ocean surface. Properties deeper than a metre or so are undetected. Then more conventional methods of measurement are necessary to probe the ocean depths. Numerous researches in seas are achieved daily, which purposes are wide and diverse. The most common are fish studies for fishermen to locate easily shoals, topography of the seabed, petrol research and properties of the seawater. Indeed, sea property changes can help to explain the circulation of water masses as well as the migration of fishes, the alteration of pollution and so on.

The purpose of this project is to design a free drifting profiler capable of housing and displacing sensors that are used to measure certain properties of the sea. These sensors are mounted into a steel cylinder of 90mm in diameter and 515mm long. The properties to measure by the sensors include the salinity, the temperature and the pressure. Salinity and temperature are typical characteristics of seawater while pressure measurement is a way of controlling the profiler depth. Regions having a steep temperature gradient, usually occurring above 200m deep, are called thermoclines. The observation of these thermoclines must also be achieved by the profiler. The three main classifications of thermoclines are as follows:

•Diurnal thermocline: It can form anywhere, provided there is enough heating during the day, though it only occurs at depths down to about 10-15m, and temperature differences across it does not normally exceed 1-2°C.

•Seasonal thermocline: The temperature and the depth of the mixed surface layer show seasonal variations in mid-latitudes. During winter, when surface temperatures are low and conditions at the surface are rough, the temperature profile can be effectively vertical. In summer, as surface temperatures rise, a seasonal thermocline often develops at depths of about 150m with temperature differences exceeding 10°C.

•Permanent thermocline: This thermocline is deeper and always present.

The profiler must dive and resurface from the sea surface to 200m deep in order to measure the desired characteristics and to observe the different thermoclines. The profiler must have a vertical velocity of 0.05 $m.s^{-1}$ (velocity desired by Sea-Sense Ltd) and must achieve 200 cycles over a period of 4 months (1 cycle is equivalent to one return). This is equivalent to one cycle in just over 2 hours. Then the profiler will drift for about 30 hours before achieving another cycle.

While floating at the sea surface, the profiler will relay data to a shore station. The use of "off the shelf" components for the Global Positioning System (GPS) and Argos satellite relay will ensure a low production cost. This is essential given that there is a likelihood that the device might be lost. Indeed with ship charter costs of up to £50,000 per day, the profiler will be considered disposable, so the recovery costs can be eliminated.

Aim and objectives:

- Literature review including oceanography and existing devices

- Selection of the appropriate design:

  Selection of the appropriate design among the existing designs and the possible new concepts. This part also includes the selection of the appropriate components.

- Methods to reduce the energy consumption:

  Possible ways to reduce the energy required and selection of the optimal method.

- Shape and material analysis:

  Selection of the most hydrodynamic shape able to withstand the external pressure at 200m deep.

- Control:

  Selection of the optimal way to control the motor in order to get an actual profiler velocity as close as possible to 0.05$m.s^{-1}$.

CHAPTER II:

OCEANOGRAPHY

1-MATHEMATICAL EQUATIONS

The ocean is a very complex system that is difficult to predict since many parameters have to be taken into account [1] .

Ocean circulation is deeply dependent on:

- The atmosphere and climate (wind, solar radiation)
- The moon (tidal motions)
- The location (Coriolis force)
- Characteristics of the water (temperature, salinity)

The equations of motion are[2]:

$$\text{Acceleration} = (\text{pressure} + \text{gravity} + \text{frictional} + \text{tidal})\text{forces/unit mass}$$

$$\begin{cases} \dfrac{du}{dt} = -\alpha \times \dfrac{\partial p}{\partial x} + 2\Omega\sin(\phi \times v) - 2\Omega\cos(\phi \times w) + Fx \\ \dfrac{dv}{dt} = -\alpha \times \dfrac{\partial p}{\partial y} - 2\Omega\sin(\phi \times u) + Fy \\ \dfrac{dw}{dt} = -\alpha \times \dfrac{\partial p}{\partial z} - g + 2\Omega\cos(\phi \times u) + Fz \end{cases}$$

Eqn. II.1

Where:

u,v,w: orthogonal velocities in the x,y and z direction

x: East to west direction

y: North to south direction

z: Vertical direction (upward)

α: Specific volume ($1/\rho$)

p: Pressure

Ω: Angular velocity of earth about its axis

ϕ: Geographic latitude

Fi: Other forces components (frictional, tidal)

These equations are very difficult to solve since many unknowns are present. Moreover, the intention is not to solve them nor to find current velocities at a given time and at a given place, but to understand the ocean currents qualitatively.

2-CLASSIFICATION OF FORCES AND MOTIONS

The forces can be divided into two classes [3]:

•Primary (which cause motion):

1-Gravitation

2-Wind stress

3-Atmospheric pressure

4-Seismic (from sea bottom)

•Secondary (which result from motion):

1-Coriolis force

2-Friction

These two kinds of motion are, as written before, difficult to understand and a simple classification will be given:

A-Wind-driven circulation

This circulation is set in motion by moving air masses. This motion is confined primarily to *horizontal movement* in the upper waters and plays a major role in transporting excess heat from the tropics to the heat-deficient higher latitudes.

B-Thermohaline circulation

This has a significant *vertical component*. It is initiated at the ocean surface in high latitudes by temperature and salinity conditions that produce a high-density mass, which sinks and spreads slowly beneath the surface waters. The layer separating the wind driven circulation from the deep thermohaline circulation is the pycnocline. Nevertheless, these systems do communicate across the pycnocline in a way that is only now being recognised[4].

Horizontal and vertical motions will be studied separately in the attempt to further understand the ocean circulations.

3-HORIZONTAL CIRCULATION

A-Ekman spiral

Ekman explained in 1902 quantitatively what Nansen observed four years before [2]: The currents do not follow the direction of the wind but are deflected to the right from 20° to 40° in the northern hemisphere (left in the southern one). In his theory, Ekman assumed the surface current flowing at 45° to the right (Figure II-1) [5].

There are no homogeneous water columns in existence in the ocean, and movements actually occurring, as a result of wind stress on the surface, will deviate from this idealised picture.

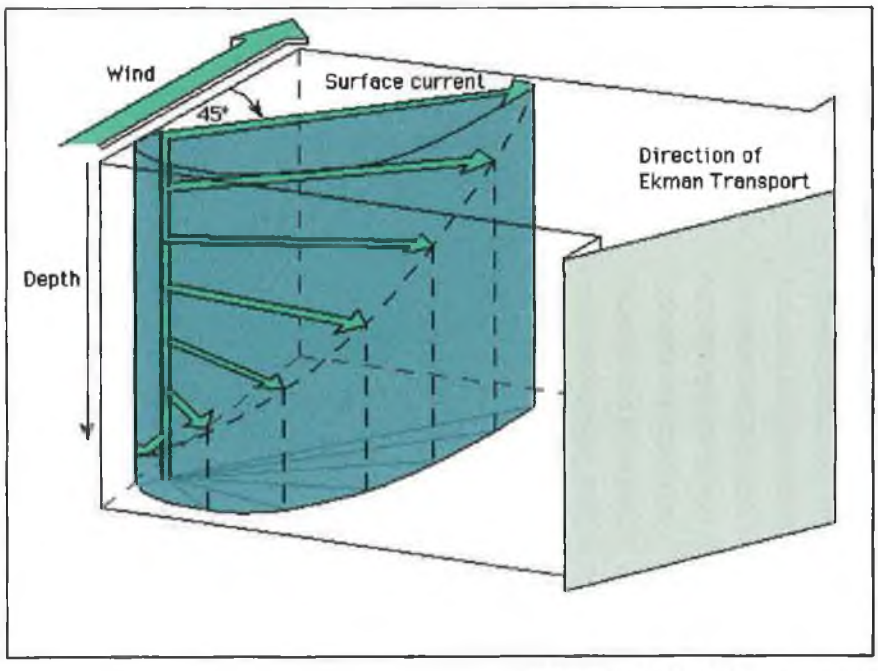

Figure II-1 Ekman spiral

However this theory is not reliable and not accurate since too many assumptions are used [2] :

-No boundaries

-Infinitely deep water

-Constant kinematic eddy viscosity

-Barotropic condition i.e. homogeneous water and sea surface level

-Constant Coriolis parameter

B-Geostrophic currents

Considering the subtropical gyre in the north Atlantic ocean and remembering the Ekman layer, a clockwise rotation in the northern hemisphere will tend to produce a subtropical convergence and pilling up of water in the centre of that gyre. Within all subtropical gyres, hills of water that rise as much as 2m above the water level can be found. Then gravitational force acts on individual particles of water balancing with the Coriolis force. This motion around the hill is called geostrophic current.

Again, this idealised flow would exist if there were no friction. Owing to the friction between water molecules, the water follows a path that moves it gradually down the slope of the hill. The apex of the hill formed within the rotating gyre is not in the centre of that gyre. The highest part of each hill is located closer to the western boundary of the gyre (figure II-2).

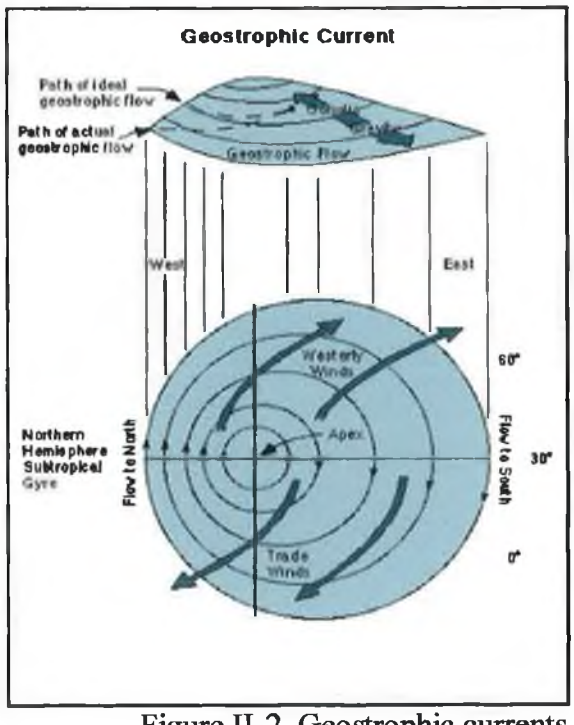

Figure II-2 Geostrophic currents

The causes of westward intensification are complex and will not be explained. Western boundary currents commonly flow 10 times faster and to greater depths than eastern boundary currents.

To conclude with the horizontal currents, some data collected during several current researches are shown below.

Data, shown in table II-1, was collected by two stations 50 km apart. Station A was 41°55'N, 50°09W and Station B was 41°28'N, 50°09W [2], these locations are in the mid-latitudes of the Atlantic:

Depth (m)	**Velocity ($m.s^{-1}$)**
0	0.26
25	0.27
50	0.28
75	0.29
100	0.29
150	0.28
200	0.24

Table II-1 Horizontal currents according to depth

In Figure II-3 [6], four examples of horizontal velocities in the mixed layer from the sea surface to 150m deep in November 1982 are shown:

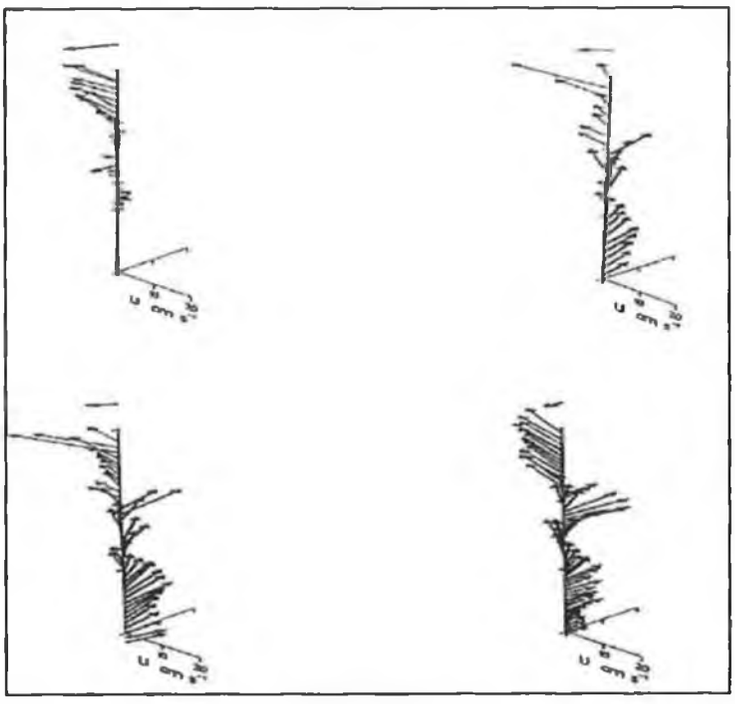

Figure II-3 Horizontal currents in the mixed layer

To know the drift of the profiler, a constant horizontal profiler drift of $0.25 m.s^{-1}$ will be assumed due to the horizontal water current. Hence, depending on the time taken (t) to sink form 0 to 200m, the profiler will not be able to drift further than 0.25t in the horizontal direction, as shown in Figure II-4:

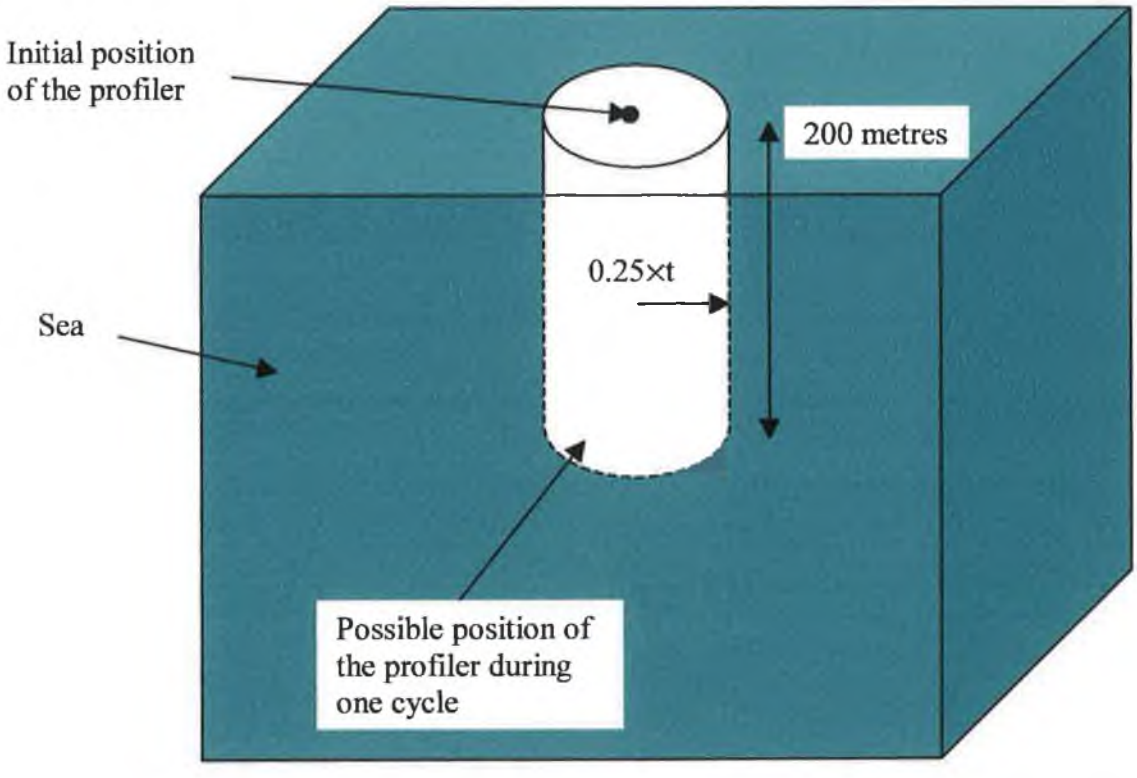

Figure II-4 Maximum profiler drift

4-VERTICAL CIRCULATION

This circulation is of great interest since the profiler has to dive and resurface. Indeed the vertical component will modify the magnitude of the drag force.

A-Thermohaline circulation

Vertical mixing of ocean water is achieved primarily through the sinking and rising of water in high latitudes: Norwegian sea, Irminger and Labrador sea (the Weddel sea in the southern hemisphere).

This occurs only in high latitude areas since the water column has a gravitational stability sufficiently neutral to allow vertical movements of large masses of water [2].

Salinity appears to have a very minimal effect on the movement of water masses in the lower latitudes because high salinity water will not sink. This is due to their temperatures that are high enough to maintain a low density for the surface water mass. In such areas, a strong halocline (salinity gradient) may be found. This kind of velocity occurs much deeper than 200m deep. Away from these high latitudes, recent measurements indicate vertical velocities of the order of 10^{-4} ms^{-1} (about 10m a day) [2][4]

B-Wind-induced circulation

Upwelling, see figure II-5, occurs in areas where the surface flow of water is away from this area. If volume is to be conserved and horizontal surface flows bring insufficient water into the area, water must come from beneath the surface to replace the volume that has been displaced. Downwelling occurs where pilled-up water is found and causes the sinking of surface water.

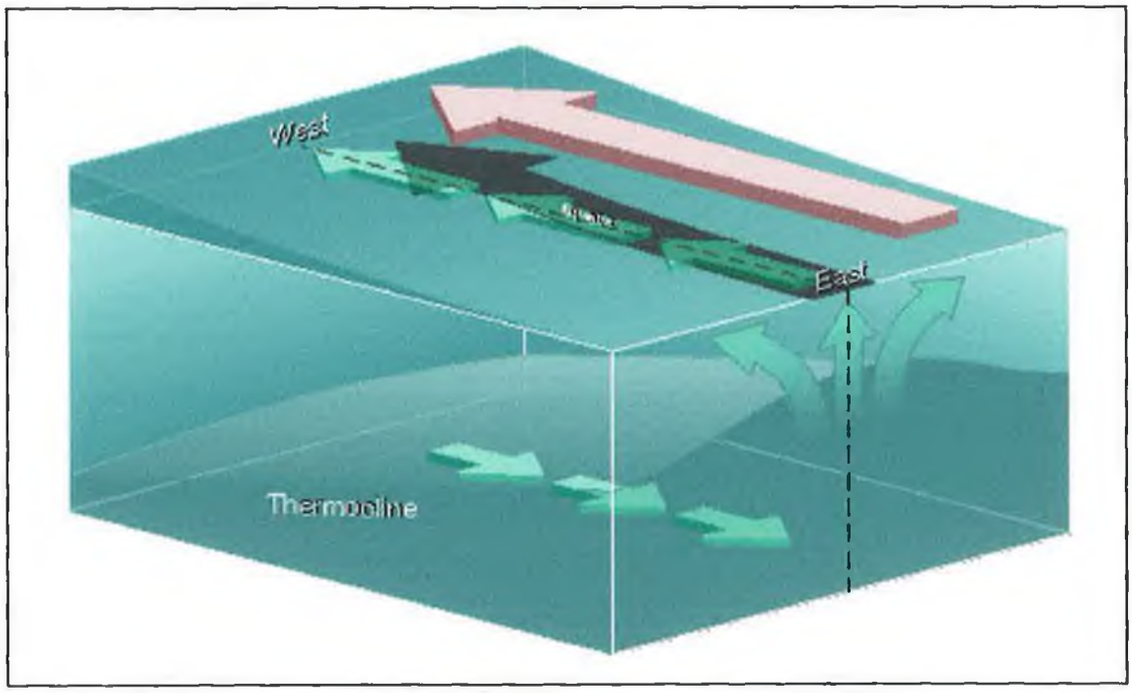

Figure II-5 Upwelling

C-Langmuir circulation

Langmuir circulations are helical roll vortices, as shown in figure II-6 [8]. They appear after the onset of winds greater than 3 ms^{-1} (Although some circulations have been found for slower wind [6]). They are a potentially important mechanism for the downward transfer of wind-generated momentum and consequent mixing of heat and momentum through the surface layer.

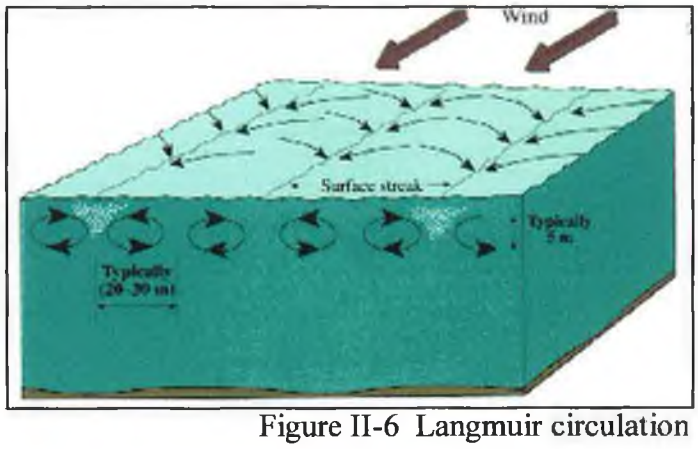

Figure II-6 Langmuir circulation

Several researches have been done in the ocean to find the intensity of the vertical current and their depth of penetration. Depending on the season and of the wind velocity, very different data have been found. Moreover for the same conditions, a different Langmuir circulation can be found.

For example, Robert A. Weller and James F. Price realised that "in December 1982 the strongest downwelling was observed during the strongest wind. In May 1983, though the winds were the same strength as the strongest winds of December 1982, weaker downwelling was observed that did not penetrate deeply into the mixed layer" [6].

Also from the data collected, Robert A. Weller and James F. Price conclude that downwelling velocities are strong away from the surface.

In figure II-7a and II-7b [6], it can be seen that downwelling velocities of 0.25 $m.s^{-1}$ are found between 15 and 30m deep with strongest speeds in winter.

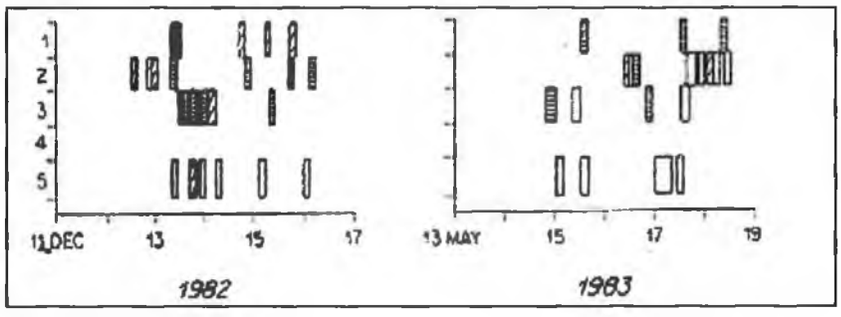

Fig.II-7a Fig.II-7b

Key:

- Depth: 1: Sea surface, 2:0-15m, 3:15-30m, 4: Fixed depth of 20m, 5: Fixed to 30m.
- Downwelling speeds (darkest first): >25$cm.s^{-1}$, 15-25$cm.s^{-1}$, 5-15$cm.s^{-1}$, <5$cm.s^{-1}$.

Downwelling velocities of 20 cms^{-1} can easily occur at 23m deep (in figure II-8 [6]).

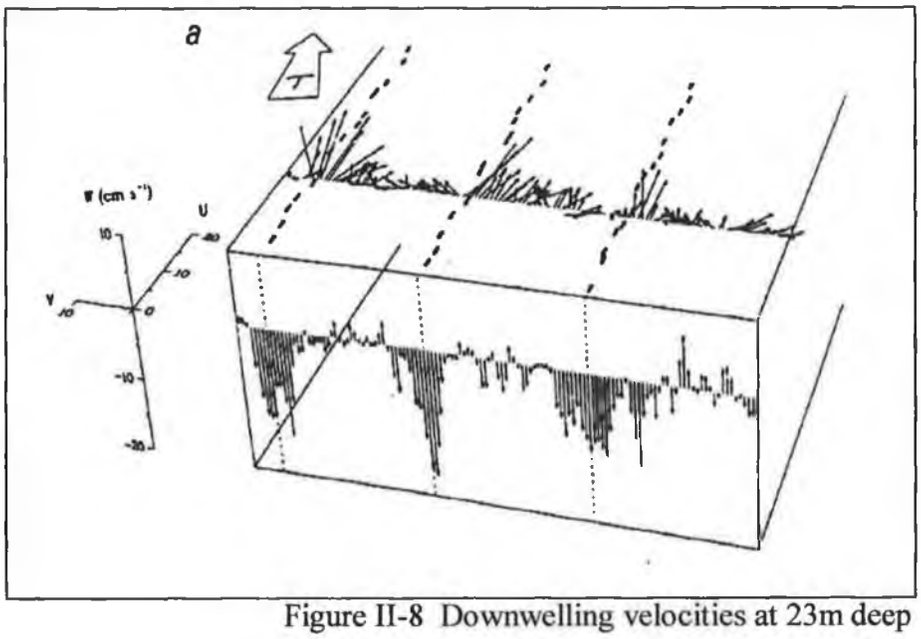

Figure II-8 Downwelling velocities at 23m deep

As can be seen, the upward velocities are much slower with maximum amplitude of 7 to 8 $cm.s^{-1}$.

5-PROPERTIES OF SEAWATER

The physical properties of seawater are pressure, temperature and salinity. All of these properties are important in order to understand the variations of seawater density since it will have a big influence on the profiler:

A-Pressure

It increases with depth as a linear function assuming a constant density.

$$\text{Pressure} = \text{density} \times \text{gravity} \times \text{depth} \qquad \text{Eqn. II-2}$$

For the upper 200m layer, the pressure will vary from 0 bar at the sea surface to 20 bars at 200m deep.

B-Temperature

About 90% of the world's oceans have temperatures in the range –2 to 10°C (away from the surface where warmer water can be found). An increase in temperature will decrease the density since this volume will tend to expand. Moreover, the relationship between density and temperature is non-linear, and density is less sensitive to temperature changes at low temperatures than at high ones.

The ocean has a well-mixed surface layer where the water temperatures are relatively constant. Below the mixed layer is the thermocline, (Figure II-9) [7] a zone where temperature changes rapidly with depth. Below this thermocline, the temperature is relatively uniform with depth, showing only a small decrease in the ocean bottom. The temperature structure of the upper ocean varies during the year. During summer the surface water is warmer. As warmer water is less dense than cold one, this warm water remains at the surface and the water column is "stable". There is little wind so the mixed layer is shallow, as is the thermocline.

During winter, cooler temperatures and wind from storms cool the surface waters. This increases the density of the surface water, which then sinks to a level of similar density.

This combination of cooling and wind mixing causes a deep mixed layer. In spring the water warms again and the thermocline reforms.

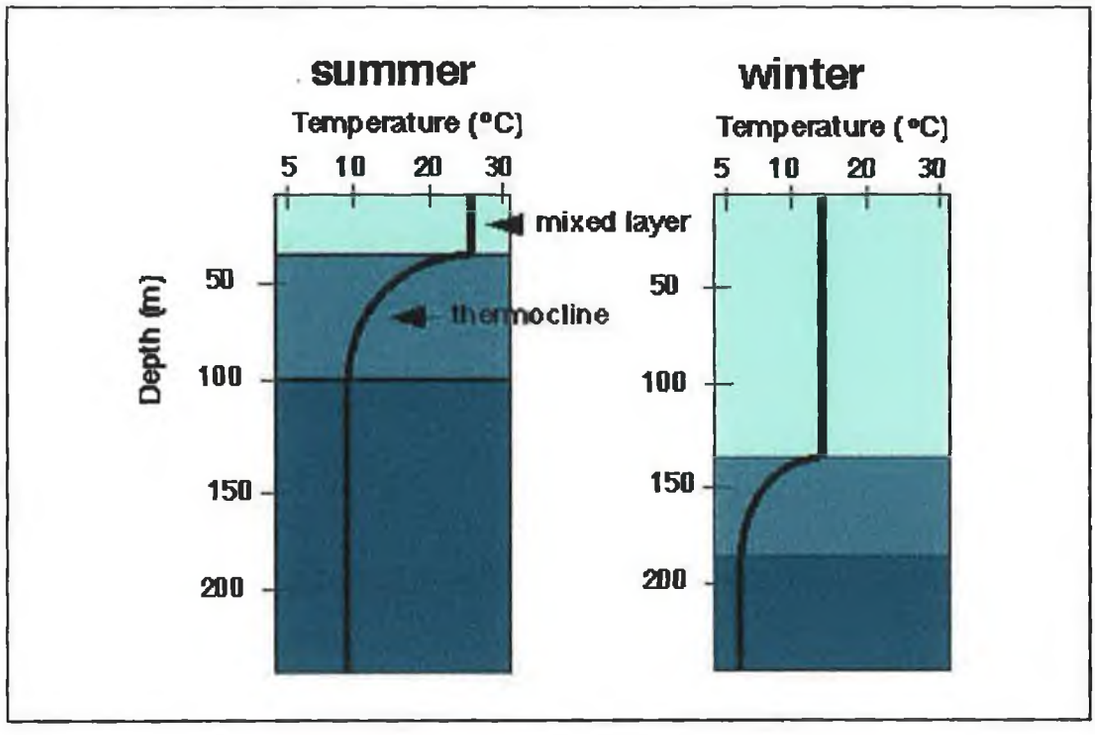

Figure II-9 Thermocline

C-Salinity

An average value for the salinity is $35^{o}/_{oo}$ (35g per kilogram). However salinity lower than $20^{o}/_{oo}$ may be found in the vicinity of rivers or melting ice [2]. Salinity varies with depth in the ocean, but it is very different from a region to another. In rainy regions, surface water will be diluted by fresh water in rain. Hence the surface water will have a lower salt content than deep water. In arid regions, evaporation of surface water makes the water left saltier than the underlying water. Therefore, the halocline (density variation due to salinity variation) can go either from high salinity to low salinity, or the other way around, or it may not exist at all.

D-Density

Temperature and salinity mainly control density. Warm water is less dense than cold water, and salty water is denser than fresh water.

Because the temperature varies more than salinity, there is usually a strong pycnocline at the same depth as the thermocline (Figure II-10).

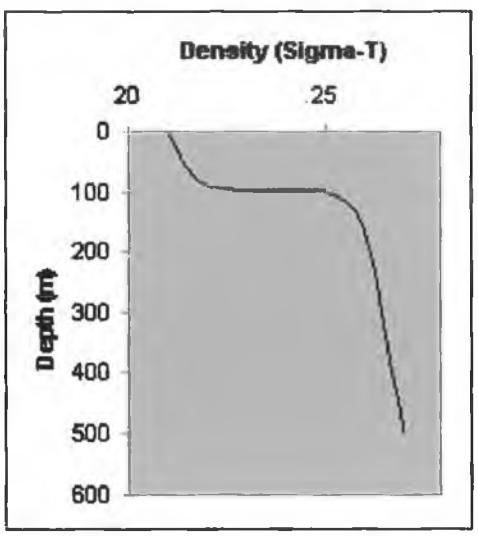

The density ρ is usually denoted Sigma-t (σ) where $\sigma = \rho - 1000$

Figure II-10 Density variation

A formula, called International Equation of State of Sea-water (IES 80), enables high accuracy in calculating seawater density as a function of salinity (S), temperature (T) and pressure (p in bars). This equation (shown in appendix A) was determined empirically in a series of laboratory measurements.

6-CONCLUSION

This chapter was not intended to create or to invent anything but to explain sea motions. In fact, this area has still to be discovered since very little is known. Only experiments carried out in sea can give reasonable results.

Concerning the profiler dynamics, two results prevail to know the profiler drift: the maximum velocities in the horizontal and vertical direction. Indeed, from the maximum vertical velocity, the maximum drag force applied on the profiler can be determined, while the maximum horizontal velocity will give an indication of the maximum drift of the profiler during one cycle.

Table II-2 summarises the maximum current velocities as a function of depth in both vertical and horizontal directions. These values are very simplified but will be used in the dynamics chapter in order to simulate the worst sea current conditions.

Current direction	**Magnitude**
Horizontal	$0.25 m.s^{-1}$
Vertical	From sea surface to 30m deep: $\pm 0.2 m.s^{-1}$
	From 30 to 200m deep: $\pm 0.1 m.s^{-1}$

Table II-2

CHAPTER III:

DESIGN

1-INTRODUCTION

Marine research requires investment in ships and technological improvements for the science to develop. Also novel measurements are necessary to provide further insights into ocean process. Ships have always been essential for marine studies but they are expensive so other methods of observing the ocean are evolving. In this chapter, the main possible designs to collect the desired data will be discussed. Then the selection of the appropriate design will be achieved. The main criteria of selection are shown in figure III-1.

The most important criterion is that the profiler must be a new concept.

A low cost and the independence of the profiler are, even if less important, necessary. Indeed, it must not be too expensive to allow its manufacturing in the future. Its independence is also very important to enable the profiler to work on its own.

Finally the profiler must be disposable to eliminate the recovery cost. It must also be capable of drifting freely. This means that it can not be fixed in position, and the energy required must be reduced as much as possible.

Remote sensing instruments will not be discussed because they are not appropriate.

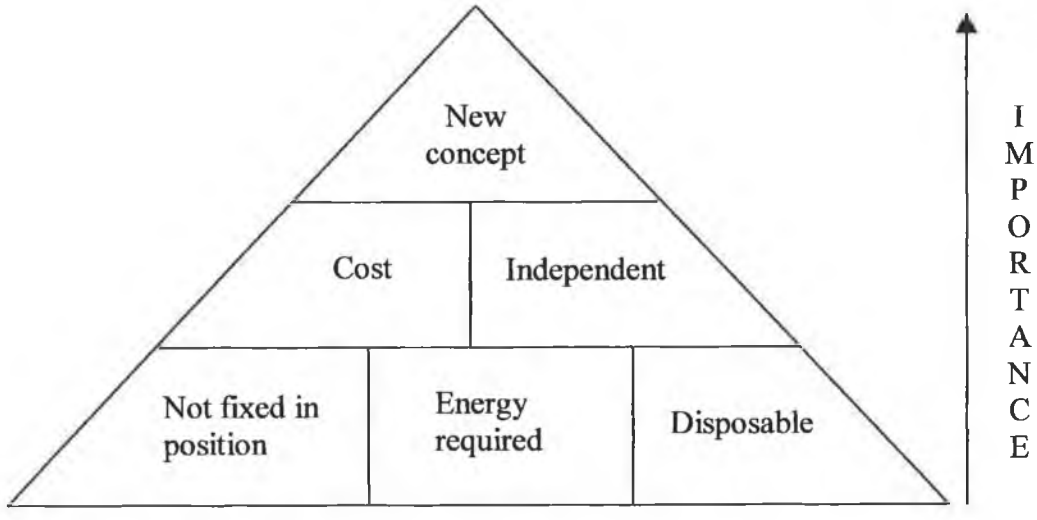

Figure III-1

2-EXISTING DEVICES

Figure III-2 [8] shows the four main kinds of existing measurement devices. The first one consists of sensors directly connected to a vessel, the second concept is free-fall sensors, the third one is made up of sensors fixed in position and the last one is using a tracked device.

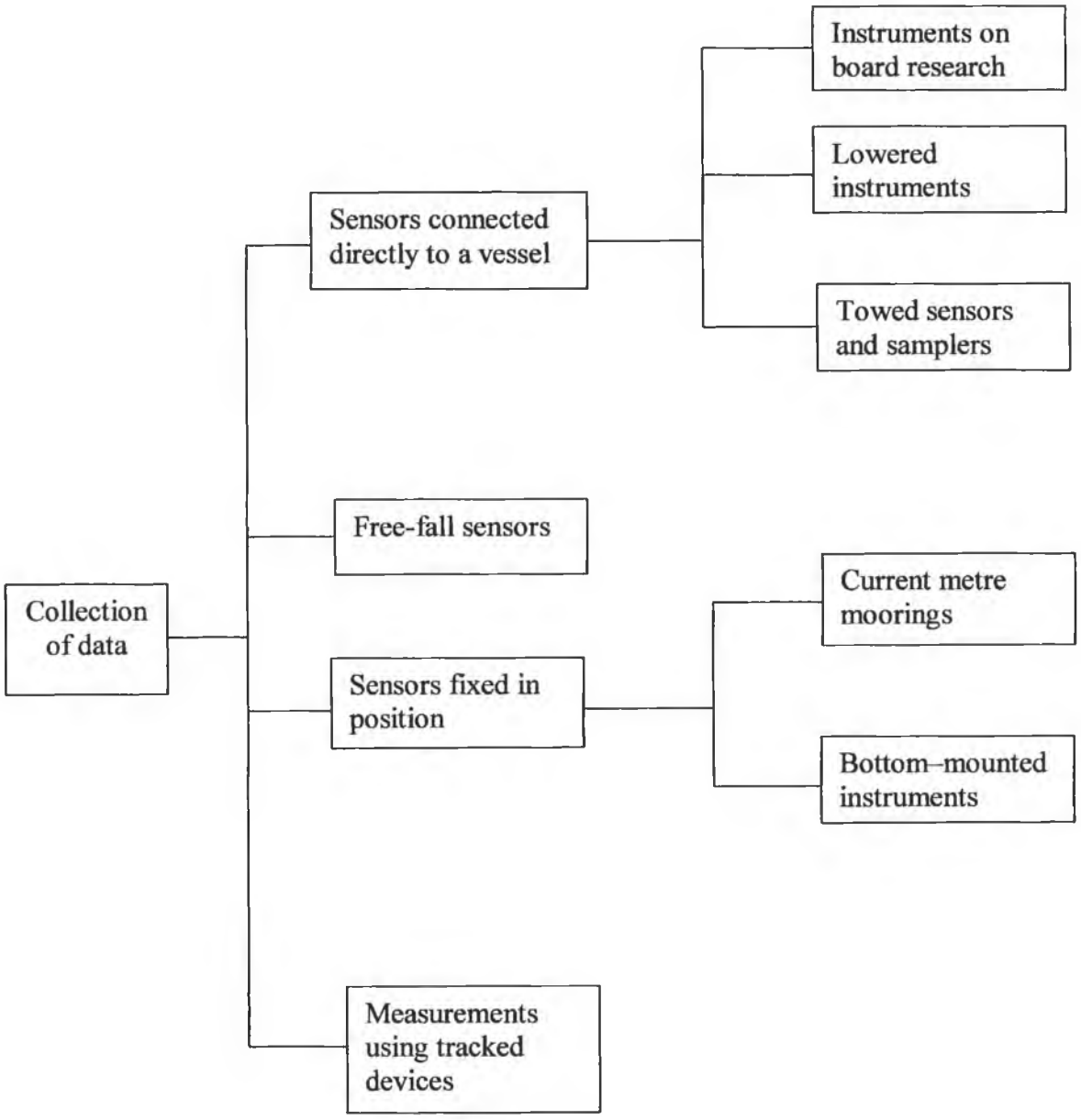

Figure III-2

A-Instruments connected directly to the vessel

• Instruments on board research vessels provide fundamental measurements of the ocean. Data is collected from the vessel while underway.

• Lowered instruments are lowered from stationary ships. Such system shed light on the global-scale circulation of the deep ocean.

• Towed sensors and samplers. Because the two solutions mentioned previously are costly in ship time, engineers have devised vehicles that can be towed behind a ship to give continuous coverage while underway. Figure III-3 shows the PRIMER (from Seasoar labs) towed vehicle.

Figure III-3 Primer vehicle

B-Free-fall sensors

The sensors are released from a research vessel allowing it to free-fall due to its own weight before recovery by line. Figure III-4 shows a High Resolution Profiler, developed by a team at Woods Hole Oceanographic Institution, USA.

Figure III-4 High Resolution Profiler

This design consists of a floating part, a cable and the sensor support (figure III-5). As it is heavier than the displaced water, the sensor support sinks. When the desired depth is reached, the winch stops unwinding. The opposite procedure is achieved when resurfacing is required. The collected data (temperature and salinity) are transmitted to the floating part via the cable. The floating part can transmit these data to a ship or a station.

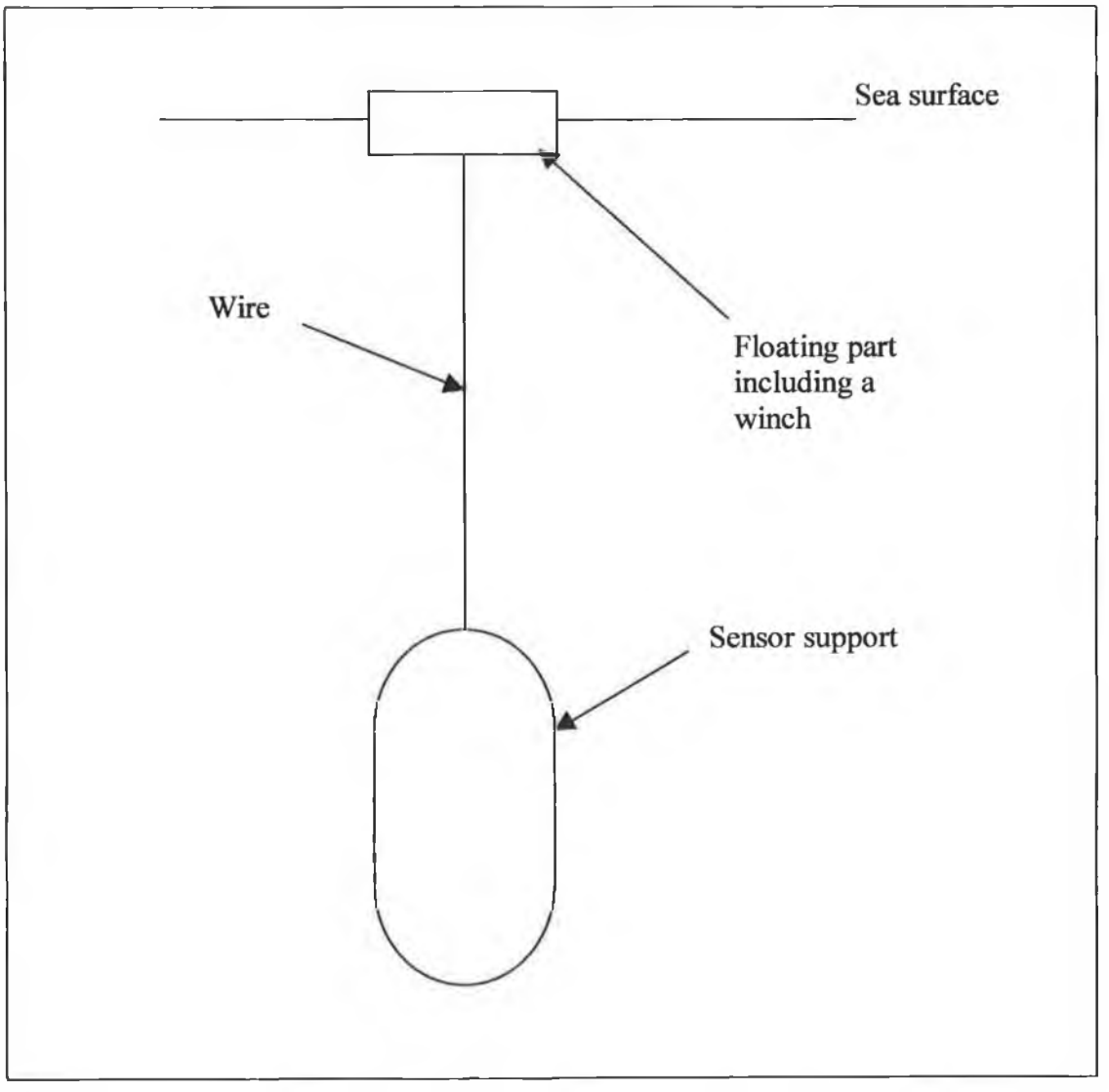

Figure III-5

C-Sensors fixed in position

Another possible way of measuring the sea properties can be achieved by a subsurface buoy anchored to the seabed as shown in figure III-6. Many salt, temperature and pressure sensors can be installed all along the cable. Its main disadvantages are that it always measures at the same location. These anchored buoys are also vulnerable to damage or displacement by fishing trawls.

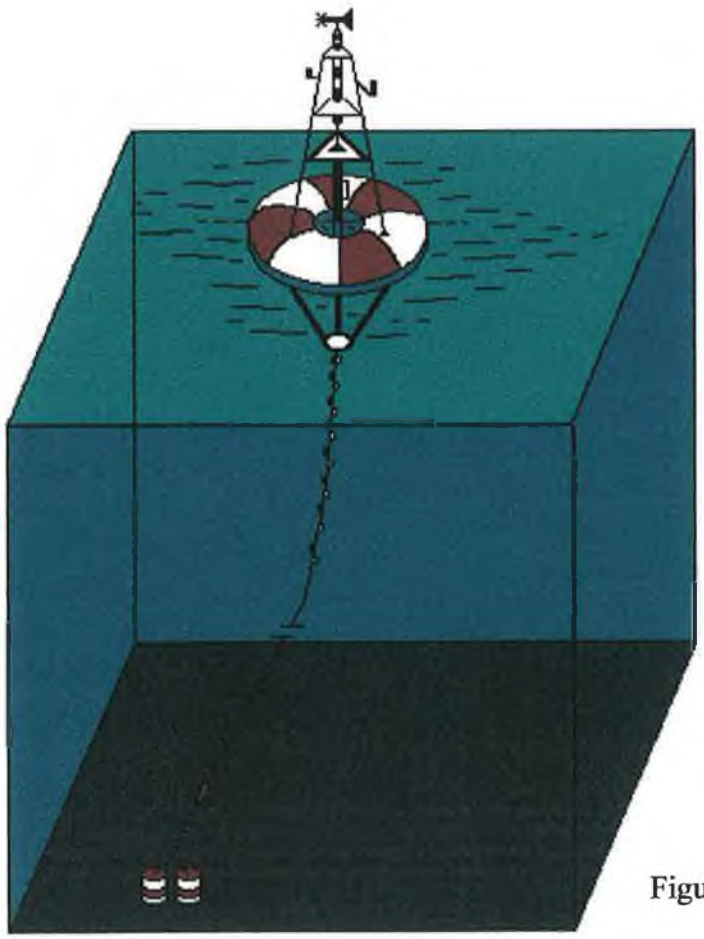

Figure III-6 Sensors fixed in position

D-Measurement using tracked devices

The newest method of collecting data comes from the ALACE (Autonomous Lagrangian Circulation Explorer) float [9] as shown in figure III-7. It drifts at a desired depth and comes back to the surface every twenty days to send information about its

position via an ARGOS platform location and data transmission satellite system. The devices can operate as deep as 2000m deep.

Figure III-7 ALACE float

The buoyancy change is performed by changing the effective volume of the float. An electrically driven hydraulic pump moves oil from the reservoir (internal to the float) to an external bladder. Only one institution, the Scripps Institution of Oceanography, La Jolla, California, USA, builds and deploys such devices. This relatively new technology is the most popular for such devices.

Explanation of the change of volume design:

The inner mass of the float remaining constant, this principle uses the change of volume of the float to dive or resurface, as shown in figure III-8. By increasing its volume, the mass of displaced water becomes greater then the upward thrust is increased. Thus the float rises to the surface. To make it dives, the volume is decreased, then the mass of displaced water is reduced. Consequently the float sinks.

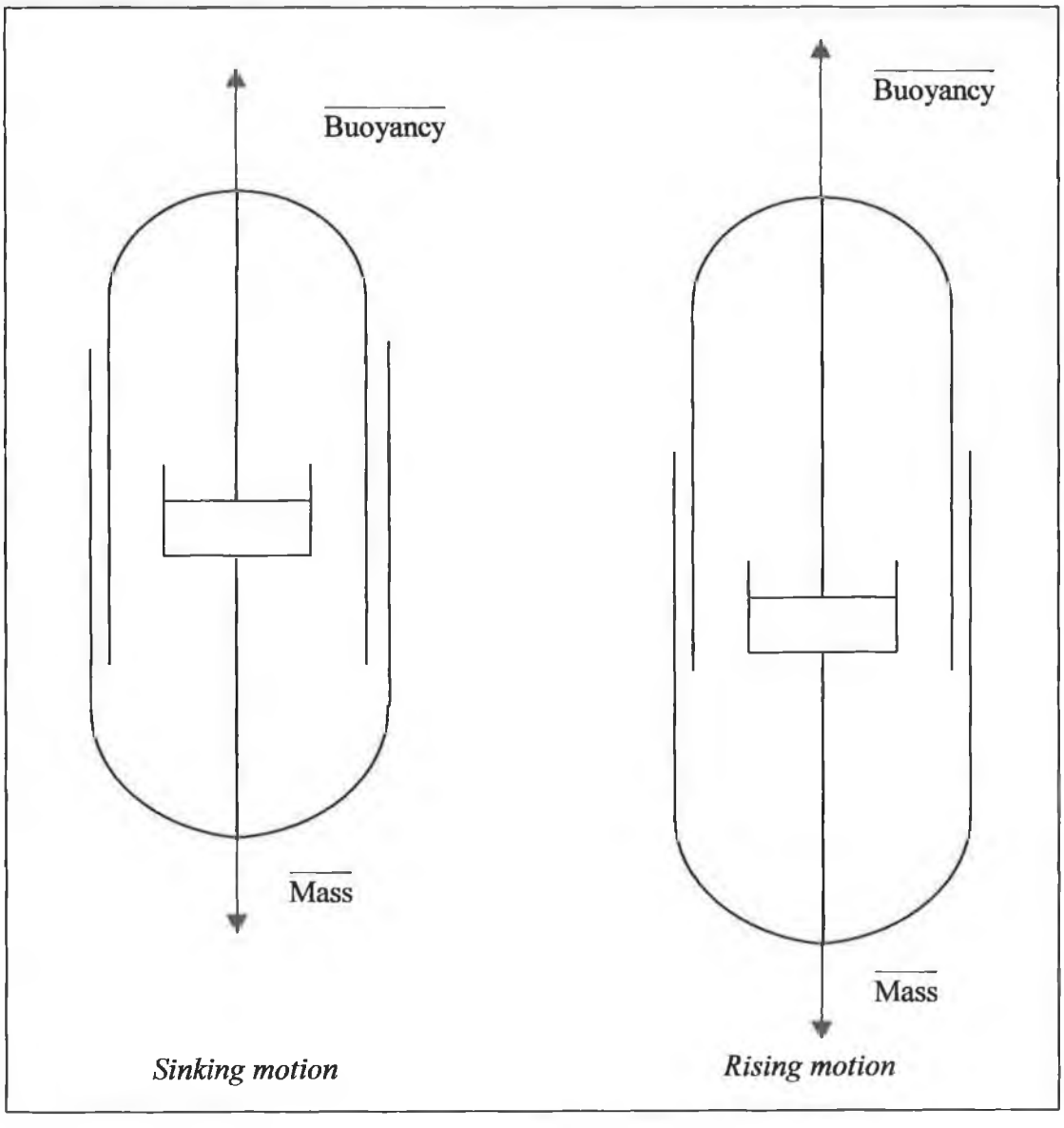

Figure III-8 Change of volume design

3-SELECTION

From the four different types of system, only the last one is suitable. For the three others, at least one important criterion can not be achieved. Table III-1 summarises the criteria that can not be fulfilled according the type of system.

The device choice is focussed on the tracked devices. However, the change of volume like the ALACE system will not be studied since it has already been researched and is a viable technology.

Type of system / Criteria	Sensors directly connected to a vessel	Free-fall sensors	Sensors fixed in position	Measurement using tracked devices
New concept	X	X	X	Newest of the four concepts
Low cost	X	X		
Independent	X	X		
Not fixed in position			X	
Energy requirement			Own power source	Own power source
Disposable	X	X	X	

Table III-1 Selection

Note that for the following table a cross means that the criterion is not fulfilled.

Firstly, sensors that are dependent on a vessel are not suitable since their main disadvantage is their cost due to ship requirement.

Concerning the sensors fixed in position, their mechanical design is very basic. However, the aim is to measure at different locations. Moreover, this design involves recovery cost.

Finally, only one possible design remains from this selection. Measurement systems using tracked devices are the most suitable. Indeed they are independent, disposable, and innovative.

4-OTHER SOLUTIONS

Three different possibilities are interesting to study further: a thermodynamic concept, the principle of an airship under the sea and the profiler design used for submarines, i.e. change of mass by pumping or releasing water.

Each of these solutions will first be described and the final choice from these three solutions will be carried out.

Note: the external profiler shape is studied in chapter VII.

A-Thermodynamic solution

This solution consists of a gas tank inside the profiler that is warmed up or cooled (figure III-9). When this gas is warmed up, its volume increases thereby increasing the profiler volume. Thus, the buoyancy force increases too and the profiler resurfaces. When sinking motion is required, the gas is cooled down and the profiler volume decreases.

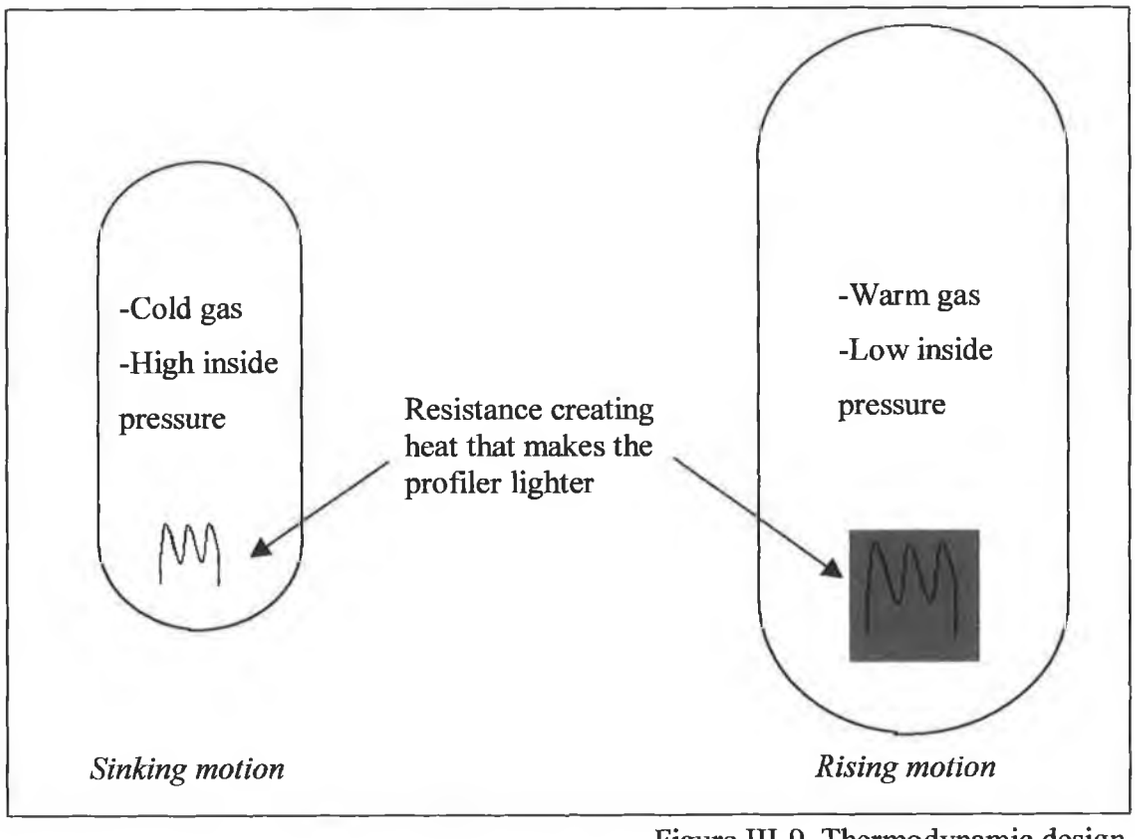

Figure III-9 Thermodynamic design

Assuming an ideal gas such as air, its properties at two different states are related to each other by (for a fixed mass):

$$\frac{p_1 \times V_1}{T_1} = \frac{p_2 \times V_2}{T_2}$$ Eqn. III-1 [10]

Where:

p_1: Pressure in Pa at the sea surface

V_1: Volume in m^3 at the sea surface

T_1: Temperature in K at the sea surface

p_2: Pressure at 200m deep

V_2: Volume at 200m deep

T_2: Temperature at 200m deep

The aim is to determine the volume ratio, using equation III-1, assuming that the gas expands when warmer. This will enable the profiler to resurface. A range of temperatures from 1°C (when sinking) to 100°C (when resurfacing) will be assumed. To work, it is imperative that the volume when sinking is smaller to reduce its buoyancy.

Then assuming: p_1: 10^5 Pa (atmospheric pressure)

T_1: 100+273=373K

$p_2 > 2\times10^6$ Pa (external pressure at 200m deep)

T_2: 1+273=274K

The ratio is:

$$\frac{V_1}{V_2} = \frac{p_2 \times T_1}{p_1 \times T_2} = \frac{(2\times10^6)\times 373}{10^5 \times 274}$$

$$\frac{V_1}{V_2} = 27.23$$

This means that the volume at 200m deep will be 27.23 times smaller. It seems unrealistic to find a way of designing a mechanical device having such volume variations.

B-Airship solution

This design is easier in principle since only few components are necessary. First of all, the profiler sinks due to its own weight until 200m deep (the profiler is heavier than the water displaced). When the desired depth is reached, a balloon of a light gas is released having the consequence to increase the buoyancy force (figure III-10).

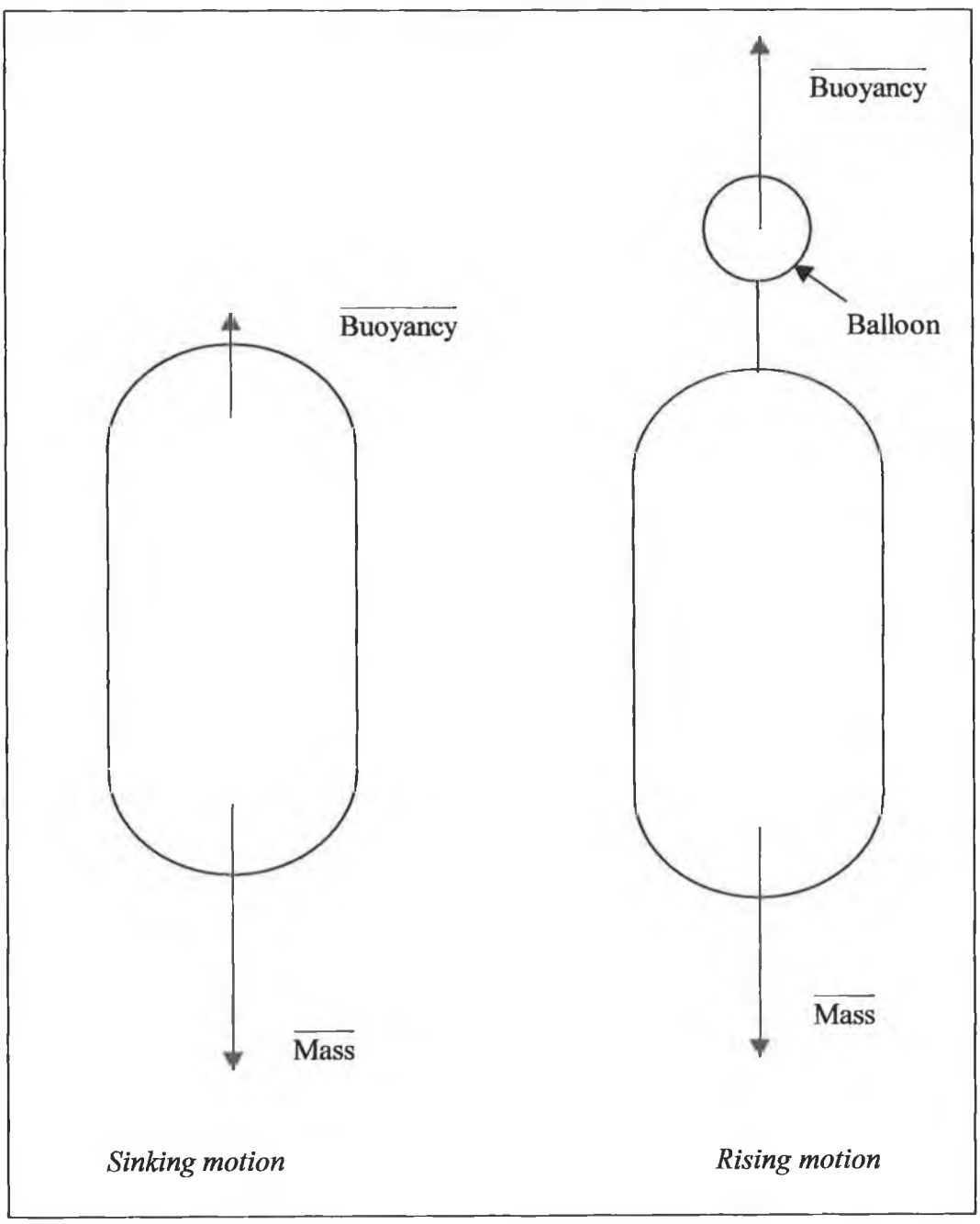

Figure III-10 Airship design

C-Change in mass solution

The final solution is to pump water inside the profiler to increase its own weight (figure III-11). When the profiler has pumped water and is heavier than the displaced water, it sinks. When the final depth is reached, some water is released from the profiler to make it lighter[11]. Hence it resurfaces.

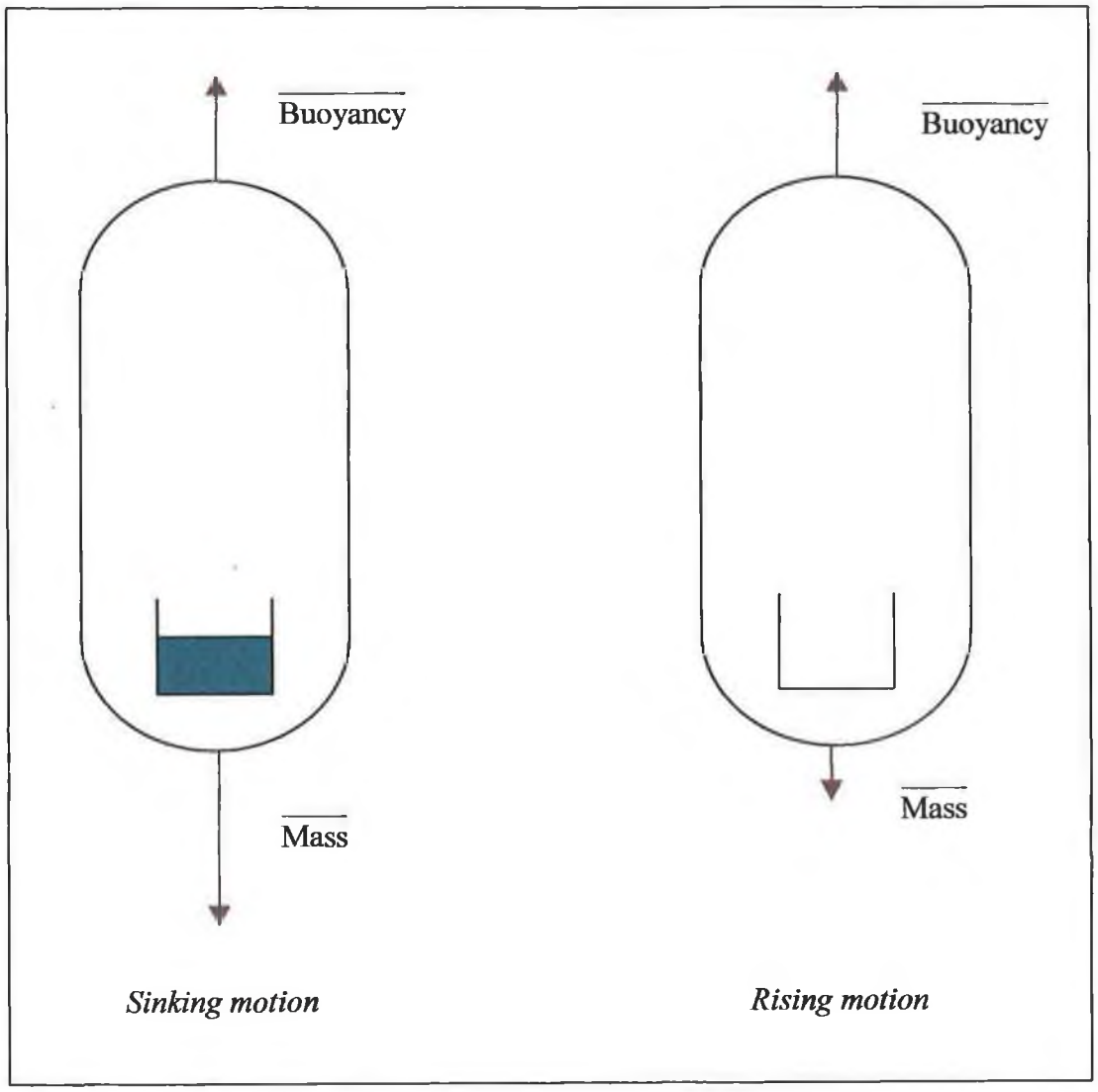

Figure III-11 Change in mass design

5-CONCLUSION

From the three described solutions, only the last one will be studied further.

The change of volume design seems only possible by using an actuator. Indeed the volume variations are too large to achieve through heating a gas inside the profiler. Moreover, even if it is not proven, the time required to cool the gas could be very long involving a slow dynamical response.

The second solution (use of balloons) is very interesting due to its simplicity. However, each cycle requiring a different balloon involves the necessity of two hundred balloons. This would be too cumbersome. In fact this technology could be suitable for only few cycles.

The change of mass solution is interesting. Indeed this concept is used for submarines but not for the kind of profiler under study. This solution is probably the most suitable according to our requirement. However, the main difference with a submarine is that a submarine uses propellers to move.

All along my research, I have not found any relevant documentation about the chosen method of moving the profiler. Indeed, the three most common methods are the instruments connected directly to the vessel, the change of buoyancy by changing the volume of the profiler and the propelled devices. For such devices, relevant literature is available compared with our method.

In chapter IV, the dynamics of the profiler must be undertaken in order to determine the quantity of water that has to be pumped to get the $0.05 m.s^{-1}$ vertical velocity.

However, one shall underline that some calculations require data from the following chapters. For example, the profiler volume and the profiler projected area, also related to the size of the motor and the battery must be known to perform the profiler dynamics. Another example is that the motor selection is related to the torque to overcome, itself related to the piston area hence to the piston volume. Consequently a parameter change affects several other parameters.

CHAPTER IV:
DYNAMICS OF THE PROFILER

1-INTRODUCTION

This chapter deals with the dynamics of the profiler. According to the chosen solution, both the appropriate initial mass of the profiler and the amount of water required to sink or rise must be calculated. Knowing that surface waves have depth effects down to about 30m deep [12] depending on the atmospheric conditions, their influence will be neglected in order to simplify the complex mathematical model [2].

The dynamics equation will be a differential equation. The Laplace transformation will be used to solve it. Indeed "it is probably the best tool for solving differential equations with constant coefficients, especially if a particular solution satisfying given initial conditions is required" [13]. However, because the Laplace transformation transforms differential equations in the time domain into the s domain, the equation must be linear [14].

In our case, the initial conditions are the depth (h) and the velocity (h').

2-GENERAL EQUATIONS OF MOTION OF UNDERWATER VEHICLES [15]

The general equations of dynamics of the underwater vehicle in the three dimensional Cartesian co-ordinate system connected with the vehicle's hull may be formulated as follows [15]:

$$\begin{cases} \dfrac{d\vec{P}}{dt} + \vec{\omega} \times \vec{P} = \vec{F} \\ \dfrac{d\vec{K}}{dt} + \vec{\omega} \times \vec{K} + \vec{V} \times \vec{P} = \vec{M} \end{cases} \qquad \text{Eqn. IV - 1}$$

Where :

$\vec{V}^T = [V_x, V_y, V_z]$: linear velocity vector

^{T} : for the transposed matrix

$\vec{\omega}^T = [\omega_x, \omega_y, \omega_z]$: angular velocity vector

$\vec{P}^T = [P_x, P_y, P_z]$: momentum vector of the system hull and additional mass of water

$\vec{K}^T = [K_x, K_y, K_z]$: moment of momentum vector of the system and additional mass of water

$\vec{F}^T = [F_x, F_y, F_z]$: resultant vector of external forces acting on vehicle

$\vec{M}^T = [M_x, M_y, M_z]$: resultant vector of moments of external forces acting on vehicle

Components of $\vec{P}$ and $\vec{K}$ may be derived from the kinetic energy E_k of the vehicle shape and additional mass of water. The total kinetic energy of the vehicle moving in the water environment may be written as follows:

$$E_k = \frac{1}{2}[V_x V_y V_z \omega_x \omega_y \omega_z] \begin{bmatrix} m+\lambda_{11} & 0 & 0 & 0 & 0 & 0 \\ 0 & m+\lambda_{22} & 0 & 0 & 0 & \lambda_{26} \\ 0 & 0 & m+\lambda_{33} & 0 & \lambda_{35} & 0 \\ 0 & 0 & 0 & I_{xx}+\lambda_{44} & 0 & 0 \\ 0 & 0 & \lambda_{53} & 0 & I_{yy}+\lambda_{55} & 0 \\ 0 & \lambda_{62} & 0 & 0 & 0 & I_{zz}+\lambda_{66} \end{bmatrix} \begin{bmatrix} V_x \\ V_y \\ V_z \\ \omega_x \\ \omega_y \\ \omega_z \end{bmatrix}$$

Eqn. IV-2

Where:

- m: mass of the vehicle
- I_{xx}, I_{yy}, I_{zz}: principal moments of inertia of the vehicle's hull
- I_x, I_y, I_z: moments of inertia of the vehicle's hull
- λ_{ij}: coefficients of mass and moments of additional mass of water

(Also called added mass [16])

Setting:

$$\begin{cases} m_x = m+\lambda_{11} \\ m_y = m+\lambda_{22} \\ m_z = m+\lambda_{33} \\ I_x = I_{xx}+\lambda_{44} \\ I_y = I_{yy}+\lambda_{55} \\ I_z = I_{zz}+\lambda_{66} \end{cases}$$

Eqn. IV-3

the kinetic energy takes the following form:

$$E_k = \frac{1}{2} \times \left(m_x \times V_x^2 + m_y \times V_y^2 + m_z \times V_z^2 + I_x \times \omega_x^2 + I_y \times \omega_y^2 + I_z \times \omega_z^2\right) + \lambda_{26} \times V_y \times \omega_z + \lambda_{35} \times V_z \times \omega_y$$

Eqn. IV-4

Knowing that P_i and K_i are the derivatives of the kinetic energy with respect of V_i and ω_i respectively as shown in equation IV-5:

$$\begin{cases} P_x = \dfrac{\delta E_k}{\delta V_x} \\ P_y = \dfrac{\delta E_k}{\delta V_y} \\ P_z = \dfrac{\delta E_k}{\delta V_z} \end{cases} \qquad \begin{cases} K_x = \dfrac{\delta E_k}{\delta \omega_x} \\ K_y = \dfrac{\delta E_k}{\delta \omega_y} \\ K_z = \dfrac{\delta E_k}{\delta \omega_z} \end{cases} \qquad \text{Eqn. IV - 5}$$

The derivatives of the kinetic energy (equation IV - 4) with respect to the velocity gives P and K as follows:

$$\begin{cases} P_x = m_x \times V_x \\ P_y = m_y \times V_y + \lambda_{26} \times \omega_z \\ P_z = m_z \times V_z + \lambda_{35} \times \omega_y \end{cases} \quad \text{and} \quad \begin{cases} K_x = I_x \times \omega_x \\ K_y = I_y \times \omega_y + \lambda_{35} \times V_z \\ K_z = I_z \times \omega_z + \lambda_{26} \times V_y \end{cases} \qquad \text{Eqn. IV - 6}$$

By using the vectors $\vec{P}$ and $\vec{K}$ of equation IV-6, equation IV-1 yields:

$$\begin{cases} m_x \times \dfrac{dV_x}{dt} - m_y \times \omega_z \times V_y + m_z \times \omega_y \times V_z + \lambda_{35} \times \omega_y^2 - \lambda_{26} \times \omega_z^2 = \sum F_x \\ m_y \times \dfrac{dV_y}{dt} + \lambda_{26} \times \dfrac{d\omega_z}{dt} - m_x \times \omega_z \times V_x + m_z \times \omega_x \times V_z - \lambda_{35} \times \omega_y \times \omega_z = \sum F_y \\ m_z \times \dfrac{dV_z}{dt} + \lambda_{35} \times \dfrac{d\omega_y}{dt} - m_y \times \omega_x \times V_y + m_x \times \omega_y \times V_x + \lambda_{26} \times \omega_x \times \omega_z = \sum F_z \\ I_x \times \dfrac{d\omega_x}{dt} + (\lambda_{26} + \lambda_{35}) \times (\omega_y \times V_y - \omega_z \times V_z) = \sum M_x \\ I_y \times \dfrac{d\omega_y}{dt} + \lambda_{35} \times \dfrac{dV_z}{dt} + \omega_x \omega_y (I_x - I_z) + V_x V_z \times (m_x - m_z) - \lambda_{26} \omega_x V_y - \lambda_{35} \omega_y V_z = \sum M_y \\ I_z \times \dfrac{d\omega_z}{dt} + \lambda_{26} \times \dfrac{dV_y}{dt} + \omega_x \omega_y (I_y - I_x) + V_x V_y \times (m_y - m_x) + \lambda_{35} \omega_x V_z + \lambda_{26} \omega_z V_x = \sum M_z \end{cases}$$

Eqn. IV-7

3-EQUATIONS OF MOTION APPLIED TO THE REAL PROFILER

A-Assumptions

It is assumed that the horizontal profiler velocities (V_x and V_y) and angular velocities of the profiler about the three axis (ω_x, ω_y, ω_z), each of them generated by the sea currents, do not have any effect on the vertical profiler velocity since little is known about these currents [17]. These five components are therefore assumed to be equal to zero. Therefore equation IV-7 becomes:

$$m_z \times \frac{dV_z}{dt} = \sum F_z \qquad \text{Eqn. IV - 8}$$

Four different forces act on the profiler. Indeed the weight, the drag force, the buoyancy and the force due to the water current must be taken into account.
Figure IV-1 represents the free-body diagram of the profiler when sinking [11]. When resurfacing, the drag force changes direction (downward). Sea currents being unpredictable, each direction must be analysed.

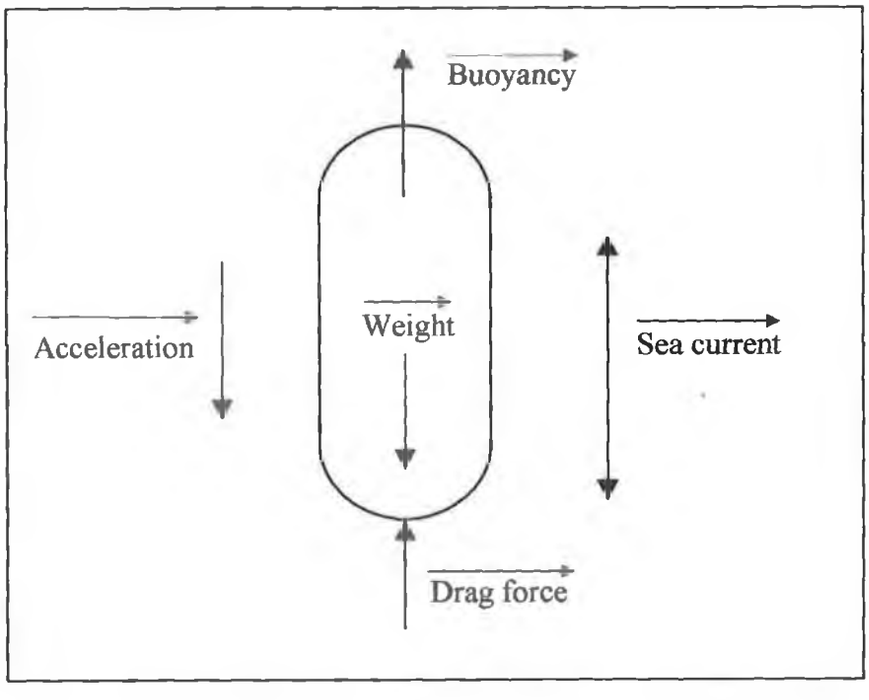

Figure IV-1 Free body diagram

Then equation IV-8 gives:

$$\bullet\ m_z \times \frac{dV_z}{dt} = \text{weight} - \text{drag} - \text{buoyancy} \pm \text{water current}$$

$$\bullet\ (\text{mass} + \text{added mass}) \times \frac{d^2z}{dt^2} = (\text{mass} \times g) - \left(\frac{1}{2} \times \rho_{water} \times A \times c_d \times \left(\frac{dz}{dt}\right)^2\right)$$

$$- (\text{volume profiler} \times \rho_{water} \times g) \pm \left(\frac{1}{2} \times \rho_{water} \times A \times c_d \times v_c^2\right) \qquad \text{Eqn. IV - 9}$$

Where:

-A: Projected area of the profiler

-c_d: Drag coefficient, equal to 0.8. This coefficient which depends on the Reynolds number is twice smaller (0.4) [[18] ; [19]]. But for safety reasons, it will be taken over its actual magnitude.

-ρ_{water}: water density, assumed to be constant. (1020kg.m^{-3})

-v_c: Water current

-Velocity to reach equal to 0.05m.s^{-1}

-z: Displacement in the vertical direction

-t: Time

-Magnitude of the water current v_c, shown in table IV-1:

Depth range	**Maximal water vertical velocity v_c**
From 0 to 30m	±0.2m.s^{-1}
From 30 to 200m	±0.1m.s^{-1}

Table IV-1

-Added mass=50kg (Very little is known about this coefficient but it is usually taken as half of the actual mass [18]).

B- Linearisation of the drag force

Figure IV-2 shows the actual behaviour of the drag force according to the velocity. Since the drag force is non-linear, equation IV-8 is a second order differential equation with a non-linear coefficient.

In order to solve this equation using the Laplace transform, the drag must be linearized [[14]; [20]] as shown in figure IV-2.

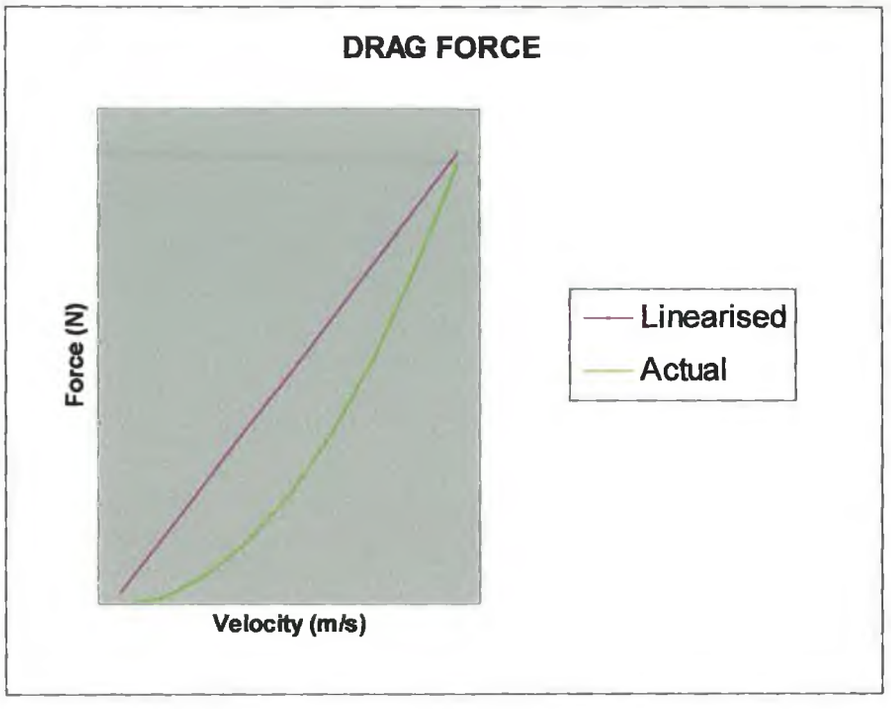

Figure IV-2 Linearisation of the drag force

This process allows the transformation of equation IV-9 into equation IV-10:

$$(\text{mass} + \text{added mass}) \times \frac{d^2z}{dt^2} = \text{mass} \times g - \frac{1}{2} \times \rho_{water} \times A \times c_d \times \left(\alpha + \beta \times \frac{dz}{dt} \right)$$
$$- \text{volume profiler} \times \rho_{water} \times g \pm \frac{1}{2} \times \rho_{water} \times A \times c_d \times v_c^{\,2} \qquad \text{Eqn. IV-10}$$

Where α and β are two coefficients to be determined.

Note: with $\alpha \neq 0$, the initial drag force is also different than zero. However, this coefficient is very small for such small velocities and has very little effect on the dynamics of the profiler.

The line minimising the squared distances between the n actual points of a given set of data points and their approximated location is the best-fitting line [[13]; [14]]. A line having this property is said to fit the data in the least squares line.

The least squares method:

Then using this method the drag force becomes: $F = \alpha + \beta \times v$

Where:

$$\alpha = \frac{(\sum F)(\sum v_2) - (\sum v)(\sum vF)}{n\sum v_2 - (\sum v)^2} \quad \text{and} \quad \beta = \frac{n\sum vF - (\sum v)(\sum F)}{n\sum v_2 - (\sum v)^2} \qquad \text{Eqn. IV-11}$$

V: Velocity ($m.s^{-1}$)

F: Force (N)

Using Mathematica[21], α and β can be calculated as shown below. Note that the projected area is determined in chapter VII and appendix E.

```
Clear[ρ, area, cd, curve, v, finalvelocity, table, line]
ρ = 1020;
area = 0.89621;
cd = 0.8;
curve = 1/2 × ρ × area × cd × v^2;
finalvelocity = 0.05;
table = Table[{v, curve}, {v, 0, finalvelocity, 0.01}];
line = Fit[table, {1, v}, v]
Plot[{curve, line}, {v, 0, finalvelocity}, AxesLabel -> {velocity [m / s], Force [N]}];

-0.0130846 + 1.96268 v
```

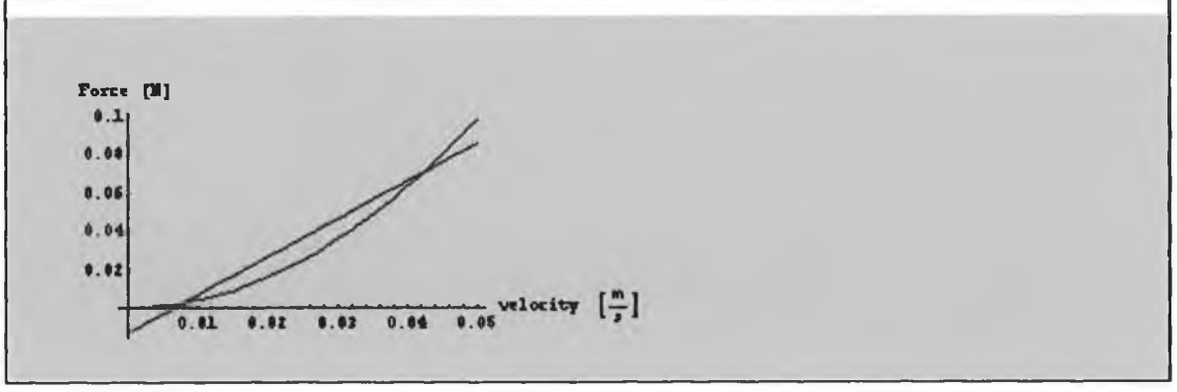

Then α=-0.0130846N and β=1.96268kg.s^{-1}.

Note: A density ρ of 1030 kg.m^{-3} leads almost to the same result since a water density variation of 10 kg.m^{-3} is negligible. It would represent a density change of about 1%.

In order to determine if this approximation is acceptable, i.e. assuming that the induced error remains within a range of ±20%. In table IV-2, the exact values, approximate values and percent error are present.

Velocity $m.s^{-1}$	Actual Force	Approximated force	Percentage error
0.04	0.063N	0.065N	3.17 %
0.05	0.098N	0.085N	13 %

Table IV-2 Induced error

The simplification using the least squares method is acceptable since the induced error is within the range. Thus, equation IV-10 is solvable using α and β. The quantity of water required to dive (rise) having a velocity of $0.05m.s^{-1}$ can therefore be calculated.

C-Quantity of water required

Knowing α and β, equation IV-9 is solvable. Therefore the quantity of water required to sink or rise having a velocity of $0.05m.s^{-1}$ can be performed. Initially, the initial mass of the profiler must be determined. This amount can be found when the profiler rises at a velocity of at least 0.05m/s with the worst conditions (maximum water counter current v_c=0.2m/s). Using the Laplace transform, equation IV-10 gives:

$$(\text{mass} + \text{added mass})s^2Y(s) = \left(\frac{\text{mass} \times g}{s}\right) - \left(\frac{1}{2} \times \rho_{water} \times A \times c_d \times \left(\frac{\alpha}{s} + \beta s Y(s)\right)\right)$$
$$- \left(\frac{\text{volume profiler} \times \rho_{water} \times g}{s}\right) \pm \left(\frac{\rho_{water} \times A \times c_d \times v_c^{\,2}}{2s}\right) \qquad \text{Eqn.IV - 12}$$

Mathematica procedure:

Once the initial mass of the profiler determined empirically (p41), the amount of water to pump (discharge) can be calculated (p42). The first step is to transform the differential equation into its Laplace transform (Lap1**i**: Lap1**A** for the worst conditions (counter sea-water current) and Lap1**B** for the best ones). Once in the s-domain, Lap1i is transformed into Lap2i by including the initial conditions. This equation is solved and multiplied by s in order to get the velocity instead of the displacement. Velocity**A** and Velocity**B** are the equations to solve (depending on the conditions). Finally, the amount of water Δ_m required can be calculated assuming a $0.05m.s^{-1}$-profiler velocity.

Using Mathematica, the initial mass of the profiler is calculated as follows:

```
Velocity with inital mass (worst case);
<< Calculus`LaplaceTransform`
Clear[addedmass, pwater, area, volume, vc, g, cd, buoyancymass,
 massballast, m, α, β, h, lap1h, s, t, lap2h, lap3h, lap4h, velocityh]
addedmass = 50;
pwater = 1020;
area = 0.09621;
volume = 9.9418×10^(-2);
vc = 0.2;
g = 9.81;
cd = 0.8;
buoyancymass = volume×pwater;
massballast = 100.8;
α = -0.0130846;
β = 1.96268;
lap1h =
 LaplaceTransform[(addedmass + massballast)×h''[t] == -massballast×g + buoyancymass×g -
    1/2×pwater×(area)×cd×(α+β×h'[t]) - 1/2×pwater×(area)×cd×vc^2, t, s];
lap2h = lap1h/. {LaplaceTransform[h[t], t, s] -> laphh, h[0] -> 0, h'[0] -> 0};
lap3h = laphh/. First[Solve[lap2h == 0, laphh]];
lap4h = lap3h×s;
velocityh = InverseLaplaceTransform[lap4h, s, t];
t = 100;
velocityh
```

```
0.0634957
```

Note:
- The velocity depends on the time but when t=100 seconds the terminal velocity is reached (It is, in fact, the case after several seconds).
- For every calculation, the z direction will be taken positive with the acceleration direction. (If the profiler is sinking, z positive from the sea surface to deep water, and if the profiler is resurfacing, z positive from deep water to sea surface).

The calculated appropriate initial mass, 100.8kg is acceptable. Indeed, being in the worst conditions, the upward velocity is 0.0634957m.s^{-1}. This means that the profiler is light enough to resurface in any circumstance when empty of water. Moreover this amount is close to the "buoyancy mass"(101.4kg). This will save energy since it will avoid pumping useless water.

However, α and β were assumed for a velocity of 0.05 $m.s^{-1}$. This means that the actual velocity is smaller than 0.0634957$m.s^{-1}$ but higher than 0.05 $m.s^{-1}$.

To conclude, the initial mass of the profiler will be 100.8kg.

From the sea surface to 30m deep:

Having the initial mass of the profiler, the determination of the quantity of water required to sink from 0 to 30 meters deep can be achieved. From this calculation, the amount of water Δ_m is determined for v_c taken in both directions.

```
FROM 0 TO 30 m;
<<Calculus`LaplaceTransform`
Clear[addedmass, pwater, area, volume, vc, g, cd, buoyancymass, massballast, Δm, α, β, h,
 lap1A, s, t, lap2A, lap3A, lap4A, velocityA, lap1B, lap2B, lap3B, lap4B, velocityB]
addedmass = 50;
pwater = 1020;
area = 0.89621;
volume = 9.9418 × 10^(-2);
vc = 0.2;
g = 9.81;
cd = 0.8;
buoyancymass = volume × pwater;
massballast = 100.8 + Δm;
α = -0.0130846;
β = 1.96268;
lap1A =
 LaplaceTransform[(addedmass + massballast) × h''[t] == massballast × g - buoyancymass × g -
    1 / 2 × pwater × (area) × cd × (α + β × h'[t]) - 1 / 2 × pwater × (area) × cd × vc^2, t, s];
lap2A = lap1A /. {LaplaceTransform[h[t], t, s] -> lapHA, h[0] -> 0, h'[0] -> 0};
lap3A = lapHA /. First[Solve[lap2A == 0, lapHA]];
lap4A = lap3A × s;
velocityA = InverseLaplaceTransform[lap4A, s, t];
lap1B =
 LaplaceTransform[(addedmass + massballast) × h''[t] == massballast × g - buoyancymass × g -
    1 / 2 × pwater × (area) × cd × (α + β × h'[t]) + 1 / 2 × pwater × (area) × cd × vc^2, t, s];
lap2B = lap1B /. {LaplaceTransform[h[t], t, s] -> lapHB, h[0] -> 0, h'[0] -> 0};
lap3B = lapHB /. First[Solve[lap2B == 0, lapHB]];
lap4B = lap3B × s;
velocityB = InverseLaplaceTransform[lap4B, s, t];
t = 100;
FindRoot[velocityA - 0.05, {Δm, 0}]
FindRoot[velocityB - 0.05, {Δm, 0}]

{Δm → 1.10673}

{Δm → 0.78662}
```

If v_c is going upward, then a quantity of 1.1kg is required to get a 0.05 $m.s^{-1}$ velocity. However, if v_c is tale wind, less water is required. This amount would be 0.786kg.

From 30 to 200m deep:

Another calculation must be achieved for the range 30 to 200m deep. Indeed the water current v_c decreases from 0.2$m.s^{-1}$ to 0.1$m.s^{-1}$. Refer to table IV-1 for more information about v_c.

```
FROM 30 TO 200 m;
<<Calculus`LaplaceTransform`
Clear[addedmass, pwater, area, volume, vc, g, cd, buoyancymass, massballast, Δm, α, β, h,
 lap1A, s, t, lap2A, lap3A, lap4A, velocityA, lap1B, lap2B, lap3B, lap4B, velocityB]
addedmass = 50;
pwater = 1028;
area = 0.09621;
volume = 9.9418 × 10^(-2);
vc = 0.1;
g = 9.81;
cd = 0.8;
buoyancymass = volume × pwater;
massballast = 100.8 + Δm;
α = -0.0130846;
β = 1.96268;
lap1A =
 LaplaceTransform[(addedmass + massballast) × h''[t] == massballast × g - buoyancymass × g -
    1 / 2 × pwater × (area) × cd × (α + β × h'[t]) - 1 / 2 × pwater × (area) × cd × vc^2, t, s];
lap2A = lap1A /. {LaplaceTransform[h[t], t, s] -> laphA, h[0] -> 0, h'[0] -> 0};
lap3A = laphA /. First[Solve[lap2A == 0, laphA]];
lap4A = lap3A × s;
velocityA = InverseLaplaceTransform[lap4A, s, t];
lap1B =
 LaplaceTransform[(addedmass + massballast) × h''[t] == massballast × g - buoyancymass × g -
    1 / 2 × pwater × (area) × cd × (α + β × h'[t]) + 1 / 2 × pwater × (area) × cd × vc^2, t, s];
lap2B = lap1B /. {LaplaceTransform[h[t], t, s] -> laphB, h[0] -> 0, h'[0] -> 0};
lap3B = laphB /. First[Solve[lap2B == 0, laphB]];
lap4B = lap3B × s;
velocityB = InverseLaplaceTransform[lap4B, s, t];
t = 100;
FindRoot[velocityA - 0.05, {Δm, 0}]
FindRoot[velocityB - 0.05, {Δm, 0}]

{Δm → 0.98669}

{Δm → 0.906662}
```

In this second case, since v_c is smaller with depth, the force to overcome is therefore smaller. Less water is then required if the same velocity is desired. In the worst case 0.98kg of water has to be pumped from the initial mass (100.8kg). This means that water must be released from the previous state (1.1-0.98= 0.12kg) if the $0.05 m.s^{-1}$ velocity is desired.

From 200 to 30m deep:

Similarly, when resurfacing is required, the required amount of water is:

```
FROM 200 TO 30 m;
<<Calculus`LaplaceTransform`
Clear[addedmass, pwater, area, volume, vc, g, cd, buoyancymass, massballast, Δm, α, β, h,
 lap1A, s, t, lap2A, lap3A, lap4A, velocityA, lap1B, lap2B, lap3B, lap4B, velocityB]
addedmass = 50;
pwater = 1020;
area = 0.09621;
volume = 9.9418×10^(-2);
vc = 0.1;
g = 9.81;
cd = 0.8;
buoyancymass = volume×pwater;
massballast = 100.8 + Δm;
α = -0.0130846;
β = 1.96268;
lap1A =
 LaplaceTransform[(addedmass + massballast)×h''[t] == -massballast×g + buoyancymass×g -
    1/2×pwater×(area)×cd×(α + β×h'[t]) - 1/2×pwater×(area)×cd×vc^2, t, s];
lap2A = lap1A /. {LaplaceTransform[h[t], t, s] -> lapHA, h[0] -> 0, h'[0] -> 0};
lap3A = lapHA /. First[Solve[lap2A == 0, lapHA]];
lap4A = lap3A×s;
velocityA = InverseLaplaceTransform[lap4A, s, t];
lap1B =
 LaplaceTransform[(addedmass + massballast)×h''[t] == -massballast×g + buoyancymass×g -
    1/2×pwater×(area)×cd×(α + β×h'[t]) + 1/2×pwater×(area)×cd×vc^2, t, s];
lap2B = lap1B /. {LaplaceTransform[h[t], t, s] -> lapHB, h[0] -> 0, h'[0] -> 0};
lap3B = lapHB /. First[Solve[lap2B == 0, lapHB]];
lap4B = lap3B×s;
velocityB = InverseLaplaceTransform[lap4B, s, t];
t = 100;
FindRoot[velocityA - 0.05, {Δm, 0}]
FindRoot[velocityB - 0.05, {Δm, 0}]

{Δm→ 0.22603}

{Δm→ 0.306058}
```

An actual mass of either 101.026kg (100.8+0.226) or 101.1kg (100.8+0.306) is required depending on the direction of v_c.

From 30m deep to the sea surface:

In this final case, v_c is as in the first state assumed as $0.2 m.s^{-1}$.

```
FROM 30 TO 0 m;
<<Calculus`LaplaceTransform`
Clear[addedmass, pwater, area, volume, vc, g, cd, buoyancymass, massballast, Δm, α, β, h,
 lap1A, s, t, lap2A, lap3A, lap4A, velocityA, lap1B, lap2B, lap3B, lap4B, velocityB]
addedmass = 50;
pwater = 1020;
area = 0.09621;
volume = 9.9410 × 10^(-2);
vc = 0.2;
g = 9.81;
cd = 0.8;
buoyancymass = volume × pwater;
massballast = 100.8 + Δm;
α = -0.0130046;
β = 1.96268;
lap1A =
 LaplaceTransform[(addedmass + massballast) × h''[t] == -massballast × g + buoyancymass × g -
    1/2 × pwater × (area) × cd × (α + β × h'[t]) - 1/2 × pwater × (area) × cd × vc^2, t, s];
lap2A = lap1A /. {LaplaceTransform[h[t], t, s] -> lapHA, h[0] -> 0, h'[0] -> 0};
lap3A = lapHA /. First[Solve[lap2A == 0, lapHA]];
lap4A = lap3A × s;
velocityA = InverseLaplaceTransform[lap4A, s, t];
lap1B =
 LaplaceTransform[(addedmass + massballast) × h''[t] == -massballast × g + buoyancymass × g -
    1/2 × pwater × (area) × cd × (α + β × h'[t]) + 1/2 × pwater × (area) × cd × vc^2, t, s];
lap2B = lap1B /. {LaplaceTransform[h[t], t, s] -> lapHB, h[0] -> 0, h'[0] -> 0};
lap3B = lapHB /. First[Solve[lap2B == 0, lapHB]];
lap4B = lap3B × s;
velocityB = InverseLaplaceTransform[lap4B, s, t];
t = 100;
FindRoot[velocityA - 0.05, {Δm, 0}]
FindRoot[velocityB - 0.05, {Δm, 0}]

{Δm → 0.105988}

{Δm → 0.4261}
```

Finally, an actual mass of either 100.905kg or 101.226kg is required depending on the direction of v_c.

Again v_c having a bigger influence than from 200 to 30m deep, more water must be released in order to make the profiler lighter.

Table IV-3 summarises in the worst case the quantities of water required:

Depth range	**Actual mass**	**Relative change**
From 0 to 30m	100.8+1.10673≈101.9kg	**+1.1kg**
From 30 to 200m	100.8+0.90666.2≈101.7kg	-0.2kg
From 200 to 30 m	100.8+0.22603≈101kg	-0.7kg
From 30 to 0m	100.8+0.105988≈100.9kg	-0.1kg

Table IV-3

The maximum amount of required water is 1.1 kg. Hence a "pumping capacity" of at least 1.1kg is necessary.

However, because the water density (ρ) changes with depth, location, temperature and salinity contents, the buoyancy also varies. Assuming that the density varies from 1020 to1030kg.m^{-3}, the buoyancy will vary from:

Buoyancy "mass" = volume of displaced water$\times\rho$ Eqn. IV-13

With: volume $=9.9418\times10^{-2}$ m^3

$$(9.9418\times10^{-2})\times1020 < \text{Buoyancy mass} < (9.9418\times10^{-2})\times1030$$

$$101.4\text{kg} < \text{Buoyancy mass} < 102.4\text{kg}$$

Therefore, the variation of buoyancy is 1kg.

Then the capacity must be:

From dynamics: 101.9-100.8 =1.1kg

From buoyancy: =1kg

=2.1kg

Minimal capacity of water to pump =2.1kg.

Because of all the assumptions made, a safety coefficient is added. **Hence the water capacity will be assumed to be at least 3kg**.

D-Acceleration and deceleration

It is essential to know the quantity of water required in each of the four cases. This will allow the determination of the capacity of the piston.
However, it is also very important to calculate both the acceleration and the deceleration in order to determine the time required to reach $0.05 m.s^{-1}$ and $0\ m.s^{-1}$ respectively.

Using the same process as for the determination of water required, both velocities are calculated as a function of time in order to find the acceleration and deceleration. In this calculation, the acceleration will also be dependent on the water current v_c.

Assumptions:

- For the acceleration, the initial conditions are:

  Displacement $h[0]=0m$

  Velocity $h'[0]=0m.s^{-1}$

- For the deceleration, the initial conditions are:

  Displacement $h[0]=0m$

  Velocity $h'[0]=0.05m.s^{-1}$

- The ranges for the graph shown on page 48 are:

  Time from 0 to 15 seconds

  Water current:

  Acceleration: from -0.2 to $0.2m.s^{-1}$ (minus sign for opposite direction)

  Deceleration: from -0.1 to $0.1m.s^{-1}$

- Actual mass of the profiler:

  When accelerating: mass = 100.8+1.10673kg (Refer to page 42)

  When decelerating: mass = 100.8+0.22603kg (Refer to page 44)

3DPLOT OF THE VELOCITY AS A FUNCTION OF TIME AND WATER CURRENT (ACCELERATION MOTION)

```
<< Calculus`LaplaceTransform`
Clear[addedmass, area, g, α, β, cd, ρwater, volume,
 buoyancymass, massballast, h, t, lap, lap1, laph, lap2, lap3, velocity, vc]
addedmass = 50;
area = 0.09621;
g = 9.81;
α = -0.0130046;
β = 1.96268;
cd = 0.6;
ρwater = 1020;
volume = 9.9418 × 10^-2;
buoyancymass = volume × ρwater;
massballast = 100.0 + 1.10673;
lap = LaplaceTransform[(addedmass + massballast) × h''[t] == +massballast × g - buoyancymass × g -
    1/2 × ρwater × (area) × cd × (α + β × h'[t]) - 1/2 × ρwater × (area) × cd × (vc × Abs[vc]), t, s];
lap1 = lap /. {LaplaceTransform[h[t], t, s] -> laph, h[0] -> 0, h'[0] -> 0};
lap2 = laph /. First[Solve[lap1 == 0, laph]];
lap3 = lap2 × s;
velocity = InverseLaplaceTransform[lap3, s, t];
Plot3D[velocity, {t, 0, 15}, {vc, -0.2, 0.2}, PlotPoints → 40,
 Mesh → False, AxesLabel → {"time", "water current", "ballast velocity"}];
```

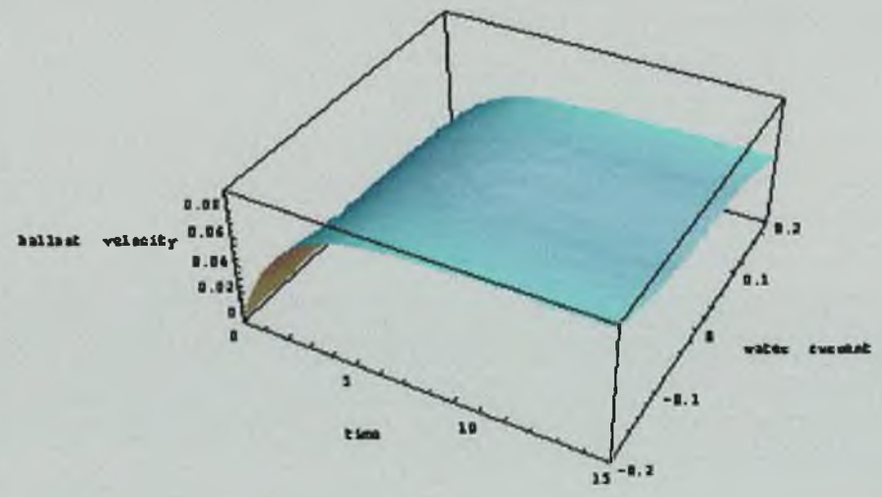

3DPLOT OF THE DECELERATION AS A FUNCTION OF TIME AND WATER CURRENT (DECELERATION MOTION)

```
<<Calculus`LaplaceTransform`
Clear[addedmass, area, g, α, β, cd, ρwater, volume,
 buoyancymass, massballast, h, t, lap, lap1, laph, lap2, lap3, velocity, vc]
addedmass = 50;
area = 0.09621;
g = 9.81;
α = -0.0130946;
β = 1.96268;
cd = 0.8;
ρwater = 1020;
volume = 9.9418 × 10^-2;
buoyancymass = volume × ρwater;
massballast = 100.8 + 0.22603;
lap = LaplaceTransform[(addedmass + massballast) × h''[t] == +massballast × g - buoyancymass × g -
    1/2 × ρwater × (area) × cd × (α + β × h'[t]) - 1/2 × ρwater × (area) × cd × (vc × Abs[vc]), t, s];
lap1 = lap /. {LaplaceTransform[h[t], t, s] -> laph, h[0] -> 0, h'[0] -> 0.05};
lap2 = laph /. First[Solve[lap1 == 0, laph]];
lap3 = lap2 × s;
velocity = InverseLaplaceTransform[lap3, s, t];
Plot3D[velocity, {t, 0, 10}, {vc, -0.1, 0.1}, PlotPoints → 40,
 Mesh → False, AxesLabel → {"time", "water current", "ballast velocity"}];
```

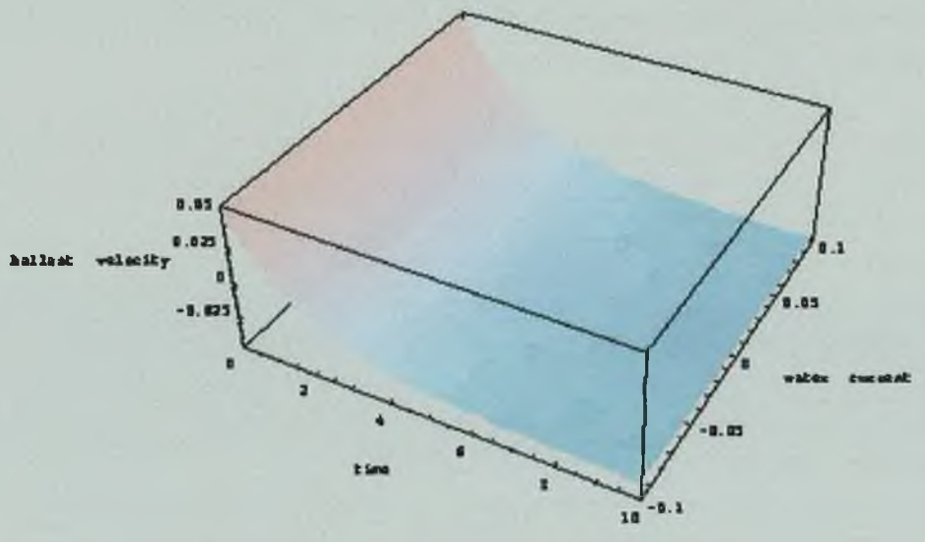

In both cases, after less than ten seconds the final conditions are reached. This means that the profiler will rapidly attain $0.05m.s^{-1}$ or $0m.s^{-1}$ once the water has been pumped or released respectively.

4-CONCLUSION

Due to the difficulty in solving the complete dynamics equation, the drag force had to be linearised. With this simplification, the quantity of water to be pumped or discharged can be calculated. A quantity of 1.1kg of water is necessary for the profiler to sink or resurface in the worst conditions.

The volume of the profiler is another important parameter. Indeed a large volume would displace a large amount of water. Hence a large quantity of water would have to be pumped due to this density variation. In our case, a capacity of one kilogram is required. Finally an error is generated because of the simplifications made. Therefore for safety reasons, the storage capacity will be 3kg of water instead of the 2.1kg calculated.

It must be noticed that a $0.2m.s^{-1}$ vertical sea water velocity (in the worst conditions) would not lead to the same profiler velocity. Indeed, the drag force acting on the profiler would slow down the profiler. Hence a $0.05m.s^{-1}$ profiler velocity can be reached even if strong counter currents occur. More water would just have to be pumped (the difference between 1.1kg and 0.78kg of page 42 from 0 to 30m deep).

To get a larger velocity of the profiler, the projected area of the external shape must be reduced as much as possible. Indeed a smaller projected area will reduce the drag force. Consequently a reduced amount of water would be needed. The shape must also be hydrodynamic to reduce the drag coefficient and hence the drag force magnitude. Therefore the energy required will be reduced. This is why the existing ballast systems are very long, have a small projected area and a hemispheric end.

As an example a sphere for the external shape would not be suitable. Indeed the water density variation on the volume would have a greater influence (many litres to pump) on such a shape. Moreover a sphere also has a large projected area. Both these disadvantages would lead to a huge amount of energy required.

CHAPTER V:

PUMP DESIGN

1-INTRODUCTION

The aim of this chapter is to design a pump having a capacity of 3kg of water. Because the energy required to release water at 200m deep is huge due to the high pressure, it becomes necessary to find a way to save energy. Indeed it seems impossible to create energy; solar energy would require huge panels, a turbine would increase significantly the profiler volume, the complexity of the profiler and would also alter the hydrodynamic shape.

Several possibilities to save energy will be described and the most appropriate will be chosen. The main idea is to design a differential piston creating a counter-force. This counter-force reduces the force required by the motor, hence leads to a reduction in the energy. This will be achieved by assuming an acceptable torque created by the motor. Indeed the torque will directly lead to the motor selection achieved in chapter VI.

Finally the transformation of the angular velocity of the motor into the piston translation will be discussed. Again, in order to save energy, the friction involved must be very low.

Figure V-1 represents the conceptual design of the pump. When water must be pumped or discharged, the motor rotates clockwise or anti-clockwise (respectively). This enables the piston to translate after the transformation of the angular velocity into piston translation.

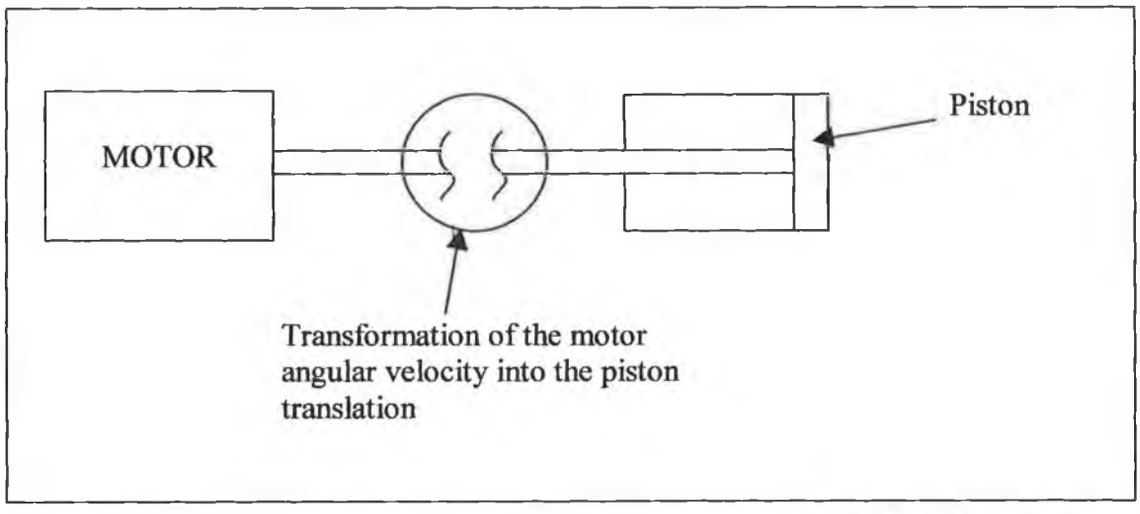

Figure V-1 Pump design

2-LEADING PARAMETERS

Two different parameters must be reduced as much as possible. The first one is the work required from the motor while the second parameter is the torque that the motor must overcome [[22][23]].

$$\text{Work} = \frac{F \times l}{\eta_p \times \eta_t} = \frac{(\rho \times g \times h) \times (\pi \times r^2) \times l}{2 \times \pi \times \eta_p \times \eta_t}$$

$$\text{Torque} = \frac{F_{max} \times \text{lead}}{2 \times \pi \times \eta_p \times \eta_t} = \frac{(\rho \times g \times 200) \times (\pi \times r^2) \times \text{lead}}{2 \times \pi \times \eta_p \times \eta_t} \qquad \text{Eqn. V-1}$$

Where:

F: Force acting on the piston due to the external pressure (N)
l: Pumping (discharging) length (m)
η_p: Piston efficiency
η_t: Efficiency of the transformation of motion device
ρ: Density of water ($kg.m^{-3}$)
g: Acceleration due to gravity ($m.s^{-2}$)
h: Depth (m)
r: Piston radius (m)
lead: lead screw of the transformation of motion device (m)

The possibilities to reduce the work required from the motor are twofold. The first one is to reduce r or l. However, knowing that the piston volume must be 2.93×10^{-3} m^3 to have a 3kg capacity (assuming a seawater density of $1025 kg.m^{-3}$), a reduction of r or l would involve an increase of l or r respectively in order to keep the same volume. Then the second and only possible way is to reduce as much as possible F is by introducing a counter-force.

Concerning the torque, the only way to reduce it is to decrease the lead screw or the piston radius. In order to find an appropriate motor, the highest torque must not exceed 4N.m. Indeed a torque of 4N.m is at the top end of torque output for a DC motors.

3-DIFFERENTIAL PISTON

This idea is to create a counter-force $\overrightarrow{F2}$ that would reduce the force required from the motor (figure V-2).

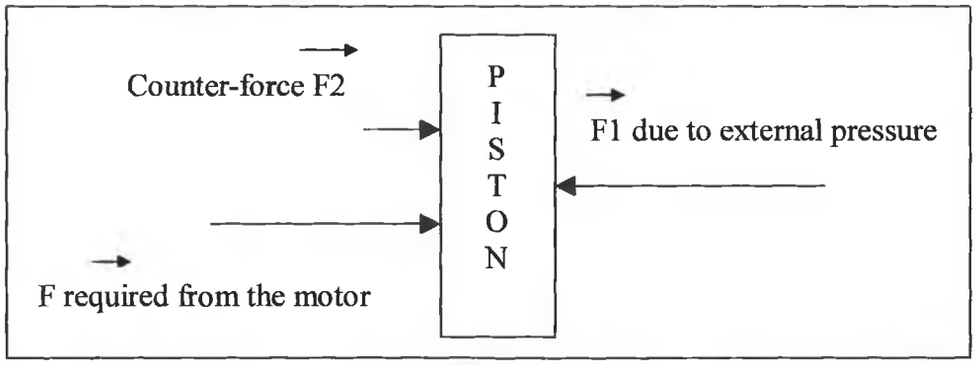

Figure V-2 Differential piston

The four main possibilities to create the counter-force are:

1- The use of foam
2- The use of a gas
3- The use of Belleville washers
4- The use of a spring

A-Foam and gas [24]

Although foam and gas can withstand high pressure, they are not suitable because of their highly non-linear behaviour under pressure. Indeed it would be very difficult to control the piston displacement. The force due to the external pressure is linear (F= piston area$\times \rho \times g \times h$), where the only variable is the depth h. Then it is more suitable for the counter-force to be linear.

Figure V-3 represents first the force due to the external pressure behaviour (black line). It can be seen that this behaviour is linear (function of depth). The yellow curve represents the gas or foam behaviour. This behaviour is highly non-linear.

In order to control the motor easily, it is more appropriate for the counter-force (pink line) to be linear.

Therefore, the gas or foam solution is not appropriate.

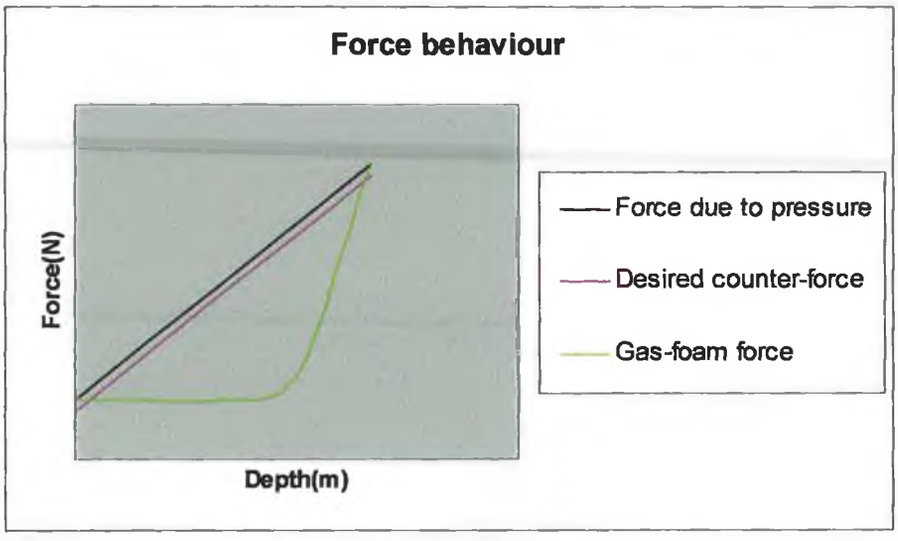

Figure V-3

B-Belleville washers

This solution appears to be more reliable even if especial care has to be taken. Indeed, although they do not have a linear behaviour, it will be seen that depending on the inside height/thickness ratio (h/t), their behaviour tends to be linear[25].

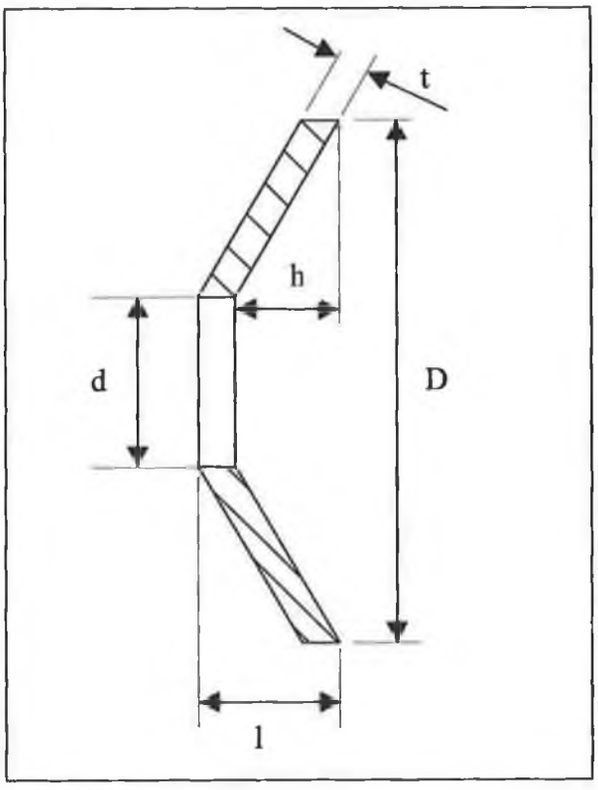

t: Thickness
h: Inside height
d: Internal diameter
D: External diameter
l: Height

Figure V-4 Belleville washer

They are used to provide very high loads with small deflections. Three kinds of combinations can be realised either in parallel, series or combination of the two. Used in series, the deflection becomes the number of washers multiplied by the deflection of one washer, and the load of the stack is equal to that of one washer. The load of a parallel stack is equal to the load of one washer multiplied by the number of washers, and the deflection of the stack is that of one washer.

In a combination of both series and parallel, both the deflection and the load are increased. To get a quasi-linear behaviour, the ratio h/t has to be nearly 0.4. For a ratio equal or above 1, the non-linearity becomes obvious and annoying for the system (figure V-5).

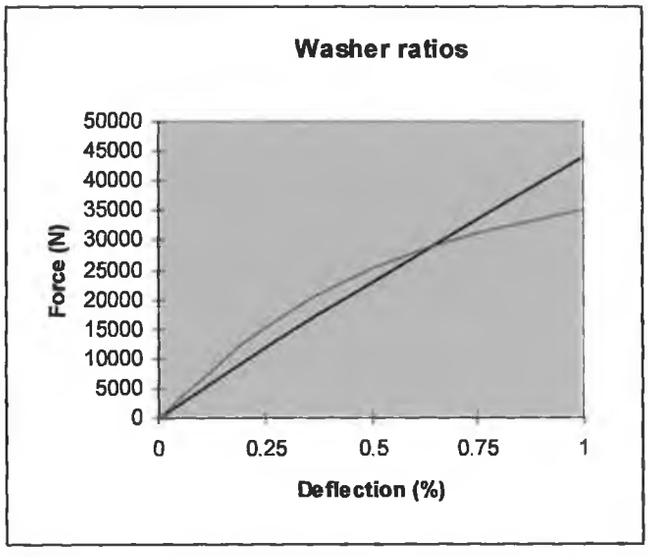

Figure V-5 Behaviour of a Belleville washer

Design with Belleville washers (figure V-6):

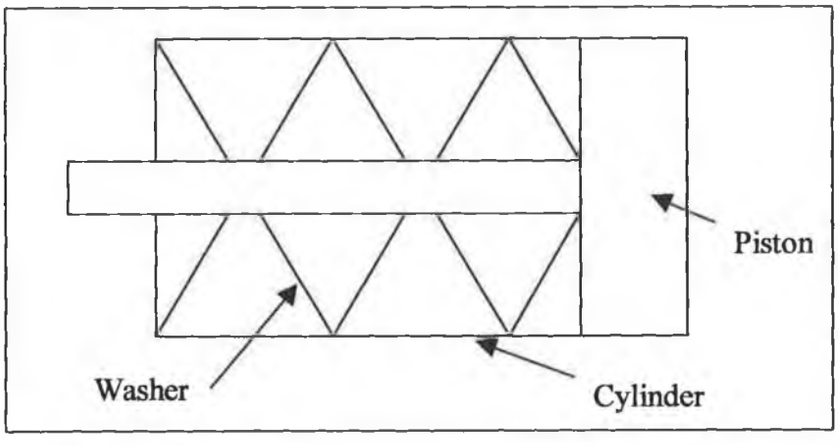

Figure V-6

Because Belleville washers are only suitable for very small displacements [25], this solution can not be favoured. Indeed because a capacity of three kilograms of water is required, the piston volume must be 2.93×10^{-3} m^3. Therefore to get this volume, a long piston is required in order to avoid a large piston diameter (avoiding a large torque). Indeed the larger the piston diameter is, the larger the torque is, leading to the impossibility to find an appropriate DC motor.

C-Heavy-duty spring

A spring configuration is more appropriate than Belleville washers are since these springs have a linear behaviour and larger displacements. However their stiffness is smaller than that of Belleville washers. As an example, a stiff spring has a stiffness of about $50N.mm^{-1}$ for a 100mm deflection and a free length of about 300mm.

Design with heavy duty spring (figure V-7):

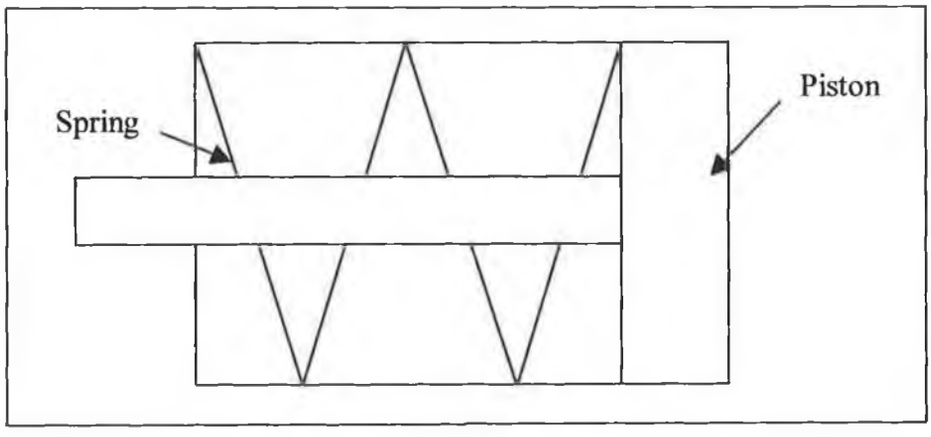

Figure V-7

However this solution is not appropriate because such springs are too cumbersome. As a matter of fact its external diameter is too large to provide a small piston diameter. Moreover, the ratio free length/ deflection is too large.

In summary, even if using a spring is the most appropriate solution, it can not be adopted since the high duty spring is too cumbersome and its deflection is not large enough.

D-Conclusion

A differential pump using a counter-force (springs, washers, etc.) will tend to reduce the power required but will unfortunately not reduce the torque. The only way to reduce the torque is to reduce the piston area (i.e. the piston diameter). But reducing the diameter leads to the impossibility to install these springs.
Finally the only potential solution is to design a very long piston with a small diameter. After several attempts to get a good compromise between the length of the piston and its radius, the following dimensions are selected:

$$\begin{cases} r = 0.028\text{m} \\ l_{piston} = 0.4\text{m} \end{cases}$$

Hence 3 pistons will be required:

$$\text{Capacity} = 3\times(\pi\times 0.028^2\times 0.4)\times 1020^* = 3.01\text{kg}$$

*Density taken in the worst case

These values will be confirmed in chapter VI where several attempts to minimise the energy requirement are performed.

Note: If springs had to be used, four of them (in series) would be necessary, involving an inappropriate total free length of 1.2m (4×0.3m)

4-BALL SCREW

A-Transformation of rotary motion into piston translation

Two different ways can be considered to transform the angular velocity of the motor into the piston translation. Some other ways will not be discussed here because they are not suitable. For example, a spur gear and rack would be too cumbersome, too heavy and not accurate enough. The efficiency is the main parameter selection. Both solutions will be further described. The first one is a lead screw while the second one is a ball screw as shown in table V-1.

	LEAD SCREW		BALL SCREW	
	Advantages	**Disadvantages**	**Advantages**	**Disadvantages**
Accuracy	Very accurate. Up to 0.0001mm per mm		Very accurate. Moreover, when mounted preloaded the backlash is eliminated	
Life	They can travel several hundreds million of centimetres		When well mounted, they have a very long life	
Maintenance	They are self-lubricated and the nuts are wear compensated. Hence no maintenance		They can be self-lubricated via felt wipers. Hence no maintenance	
Cost	Less expensive than comparable ball screws			They are more expensive than lead screws
Efficiency		About 50%	Higher than 90%.	70% if mounted preloaded

Table V-1 Comparison between lead screw and ball screw

The ball screws are chosen for their higher efficiency. When mounted preloaded, the ball screws are more accurate since the backlash is eliminated. However their efficiency is "only" 70%. But it must be kept in mind that a drop of 20% of the efficiency is harmful since more batteries or bigger ones will be required. Hence three ball screws (not preloaded and having an efficiency of 90%) are required.

B-Selection of the ball screw

The specifications of the ball screw will be achieved using *STEINMEYER* catalogue data [21]
STEPHEN WOLFRAM, The Mathematica Book, 3rd edition, Mathematica Version 3, Cambridge University Press
FIN CHAPT 04
[22][25]. Then its lifetime will be calculated. The 1416/4.20.013 type will be discussed due to its appropriate characteristics shown in table V-2:

Ball screw diameter (mm)	Lead screw (mm)	Dynamic axial load capacity Ca (N)
20	4	14400

Table V-2 Ball screw characteristics

During one cycle, 1.1kg of water will be pumped at the sea surface (1m deep). Then 1kg of water will also be pumped at 100m deep due to density variations (value taken as an average). Then 1.1kg of water will be released at 200m deep when resurfacing is required. Finally 1kg of water will be released at 100m deep. Table V-3 shows the characteristics for 1 cycle.

Step	Time in seconds	q_i Time of each duty in %	n_i (rev/min)	Depth (m)	Force (N) F_i
No. 1	56	16.3	117	1	25N
No. 2	72	21	83	100	2489N
No. 3	142	41.4	47	200	4978N
No. 4	73	21.3	82	100	2489N

(i= cycle number)

Table V-3 Duty cycle

For more information about the velocity and the time per duty (refer to appendix B). These values are found by simulating the motor.

The dynamic equivalent axial load F_m can be calculated using equation V-2. F_m will be compared to the dynamic axial load capacity Ca. To be suitable, F_m must be smaller than Ca [[22][23]]:

$$F_m = \sqrt[3]{\left(\frac{q1 \times n1 \times F1^3 + q2 \times n2 \times F2^3 + ... + q4 \times n4 \times F4^3}{q1 \times n1 + q2 \times n2 + ... + q4 \times n4} \right)}$$

Eqn. V - 2

$$F_m = \sqrt[3]{\left(\frac{16.3 \times 117 \times 25^3 + 21 \times 83 \times 2489^3 + ... + 21.3 \times 82 \times 2489^3}{16.3 \times 117 + 21 \times 83 + ... + 21.3 \times 82} \right)}$$

$$F_m = 3420.5N$$

Because F_m<Ca (3420.5N<14400N), the ball screw is suitable.

And the average speed n_m is:

$$n_m = \frac{q1 \times n1 + q2 \times n2 + q3 \times n3 + q4 \times n4}{q1 + q2 + q3 + q4}$$

Eqn. V - 3

$$n_m = \frac{16.3 \times 117 + 21 \times 83 + 41.4 \times 47 + 21.3 \times 82}{16.3 + 21 + 41.4 + 21.3}$$

$$n_m = 73.5rpm.$$

The ball screw is now specified. However, because the ball screw is long, thin and has one free end, both the critical load (F_{max}) and the critical speed (n_{max}) must be determined. For the ball screw to be reliable, both F_m and n_m must be smaller than F_{max} and n_{max} respectively:

Critical load:

$$F_{max} = 0.5 \times P_B$$

Eqn. V - 4

$$F_{max} = 0.5 \times \frac{\lambda \times d_N^4 \times 10^4}{l^2}$$

$$F_{max} = 0.5 \times \frac{1.4 \times 20^4 \times 10^4}{400^2}$$

$$F_{max} = 7000N$$

Where : | λ=1.4 (coefficient for a fixed-free screw)
d_N: nominal screw diameter (mm)
l: length of unsupported screw (mm)

Critical speed:

$$n_k = \frac{\alpha \times d_N \times 10^7}{l^2} \times 0.8 \qquad \text{Eqn. V - 5}$$

Where: α=3.9 (coefficient for a fixed-free screw)

$$n_k = \frac{3.9 \times 20 \times 10^7}{400^2} \times 0.8$$

$$n_k = 3900 \text{ rev.min}^{-1}$$

Finally the maximal force not to exceed is 7000N (F_{max}) and the speed not to exceed is 3900rev.min^{-1}. Because Fm and n_m are below these values, the ball screw is well chosen.

Then its nominal service life can be calculated.

Nominal service life:

$$L_{10} = \left(\frac{F_{max}}{Fm}\right)^3 \times 10^6 \qquad \text{Eqn. V - 6}$$

$$L_{10} = \left(\frac{7000}{3420.5}\right)^3 \times 10^6$$

L_{10}=8.5×10^6 revolutions

Knowing that a cycle is completed in 2×629 revolutions (pumping and releasing) and per ball screw:

$$\text{Number of cycles} = \frac{8.5 \times 10^6}{2 \times 629} = 6756$$

C-Conclusion

From the calculations, the ball screws are suitable and no problem of reliability will be encountered. Moreover this design will work for about 6756 cycles.

5-CONCLUSION

A differential piston has been discussed in order to reduce the power required. However in the present case, it is cumbersome and would involve a large piston diameter. This unfortunately leads to the impossibility to find an appropriate motor since the torque to overcome at 200m deep would be too large. Hence the solution must be a very long and thin piston. Another advantage of using a thin piston is that the projected area of the profiler can be reduced. Thus, the drag force has less effect on the dynamics of the profiler.

Concerning the ball screw, the most efficient one was selected, even if some accuracy was lost since backlash is not eliminated. However, the maximum backlash for this ball screw is 0.03 millimetre, which is equivalent to 0.076g. This amount leads to an error of 0.075% over a full pumping/releasing of the piston. Obviously the backlash in this case is not essential.

Subsequently the selection of the appropriate motor, the energy required and the selection of the battery can be considered. The main criteria are the weight and the dimensions of both the motor and the battery. Indeed they must not be too cumbersome to fit inside the profiler.

Finally, as explained in chapter VII, Teflon will be used for the coating of both the piston and the cylinder because of its very low coefficient of friction (about 0.04) [26]. Thus the friction between the piston and the cylinder will be neglected (η_p=1).

Moreover, metal seals coated with Teflon show improved sealing properties[27].

CHAPTER VI:

MOTOR SELECTION

1-INTRODUCTION

The first aim of this chapter is to determine the maximum torque that the motor must overcome. This maximum torque will occur at 200m deep where the pressure is the highest (about 20 bars). If the motor can create such a torque with margin for safety, the motor will be able to work at any depths between 0 and 200m deep.

Using Simulink, the simulation of the motor response can be accomplished for the operational depths (1, 100 and 200m deep) in order to determine both the amperage and the time required to pump (release) water. The product of the amperage by the time is commonly called capacity. Finally once this capacity is calculated, the appropriate battery can be selected.

2-TORQUE

From Steinmeyer catalogue [22], the torque formula is:

$$T = \frac{F \times l}{2 \times \pi \times \eta_t}$$

$$T = \frac{\left[(\rho \times g \times h) \times (\pi \times r^2)\right] \times l}{2 \times \pi \times \eta_t}$$

Eqn. VI-1

Where:

- F: Force
- ρ: Water density (1030 $kg.m^{-3}$)
- g: Acceleration of gravity (9.81 $m.s^{-2}$)
- h: Maximum depth (200m)
- r: Piston radius (0.028m)
- l: Lead screw (0.004m)
- η_t: Ball screw efficiency (0.9)

Therefore for $F=F_{max}=4977.4N$, the torque is equal to T=3.52 N.m.

The maximum torque that the motor has to overcome is 3.52N.m. For an operational margin, 1N.m is added to the torque. Thus the motor must be able to create a torque of 4.5N.m.

3-MOTOR SELECTION

A-Stepper motor

First of all, stepper motors seem interesting since they are easy to control. However their main drawback is that they can not handle high torques. Indeed a torque of 3.52N.m is very large for a stepper motor. An American company, API MOTION, creates such motors (ST-342). However they are very expensive, heavy (3.8kg), relatively cumbersome (□87.4mm×118.1mm) and above all the power required is too large (both high voltage and amperage required), about 200W. This is why this solution will not be studied any further.

B-High torque motor

These motors are more suitable for our design. Indeed they are less cumbersome (Ø103mm×45.4mm) and very light (1.8kg). They have a permanent magnet field and a wound armature which act together to convert electrical power to torque. Depending on the voltage and the desired motor speed, both the developed torque by the motor and the required amperage can be determined. These parameters are obtained as follows [[28]; [29]; [30]]:

$$I = \frac{Vs - K_B \times \omega}{(R_S + R_M)}$$

$$T = \frac{K_T \times (Vs - K_B \times \omega)}{(R_S + R_M)}$$

$$V_{EMF} = K_B \times \omega \qquad \text{Eqn.VI - 2}$$

Where:
- I: Current (Amp)
- V_S: Applied voltage (V)
- K_B: Back EMF constant (V per rad/s)
- ω: Angular velocity (rad/s)
- R_M: DC resistance (Ω)
- R_S: Power source resistance (Ω)
- K_T: Torque sensitivity (N.m/Amp)
- L_M: Inductance (H)

The motor QT-3403-A from KOLLMORGEN HIGHTECH Ltd will be studied. This motor can create a peak torque of 5.3N.m at very low velocities. The source voltage is 24V and a peak current of 5.71A (i.e. 137W). Depending on the depth, the appropriate angular velocity will be chosen. The motor characteristics are shown in table VI-1:

Lm **H**	**Kt** **N.m/A**	**Rm** **Ω**	**Kb** **V per rad/s**	**Inertia** **N.m.s^2**	**Friction N.m** **per rad/s**	**Rs** **Ω**
8.2×10^{-3}	0.9485	3.85	0.949	0.00133	0.2385	negligible

Table VI-1 Motor characteristics

The motor response is then simulated using Simulink. This is performed assuming no feedback (refer to chapter VIII p97 for more information about figure VI-1) and an input voltage of 24 Volts. In this first block diagram, no "external torque" (external torque=0) is applied since this simulation takes place at the sea surface. This "external load" is also known as the torque disturbance. As shown in figure VI-2, the motor velocity is 12.519 rad.s^{-1}, the torque created by the motor is 2.986N.m and the amperage required is 3.1482A. The exact values are found from the "ampere.mat" and the "velocity.mat" files. These simulations last only 0.05 seconds since all the outcomes have reached their final state.

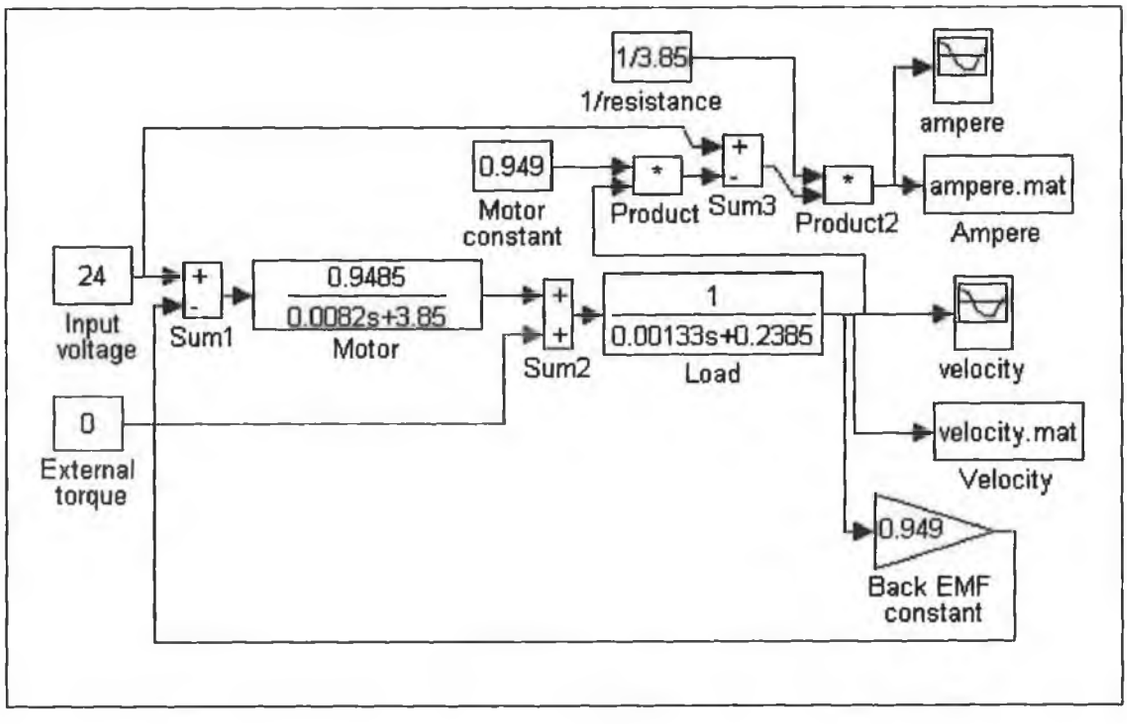

Figure VI-1 Block diagram of the motor at the sea surface

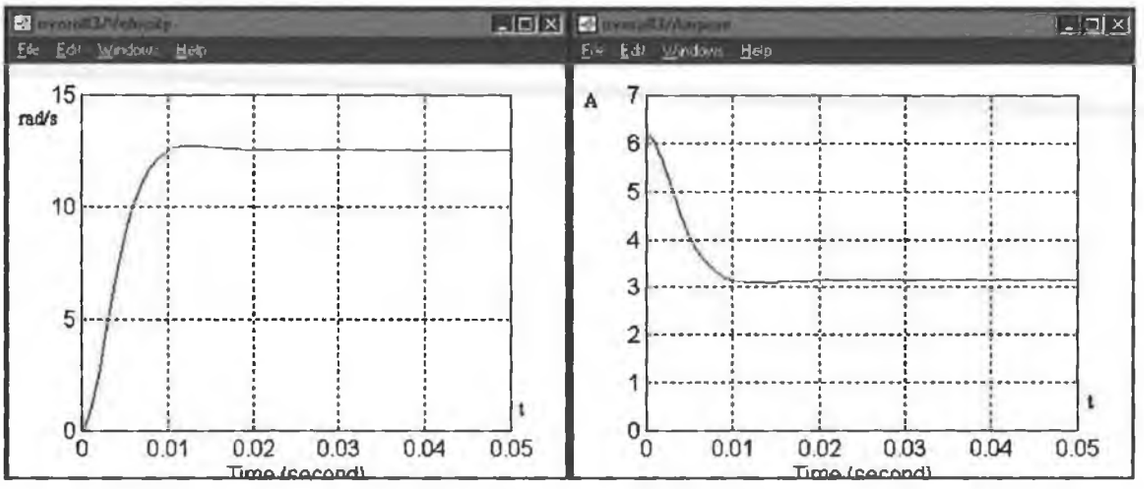

Figure VI-2 Response of the motor at the sea surface

Figure VI-3 illustrates the block diagram of the motor at a depth of 200m ("external torque"=-3.52N.m) and figure VI-4 represents the response of the motor. In this case, the motor runs at a velocity of 5.0661 rad.s^{-1}, the amperage is 4.985A and the torque created is 4.73N.m.

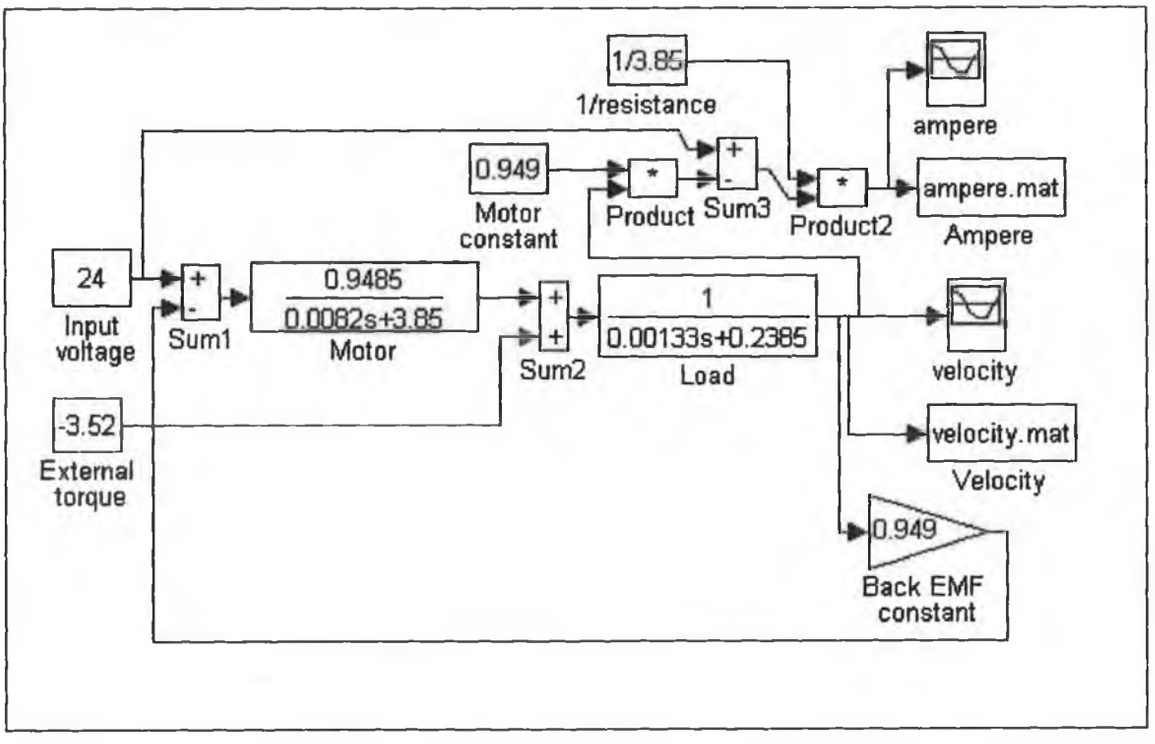

Figure VI-3 Block diagram of the motor at 200m deep

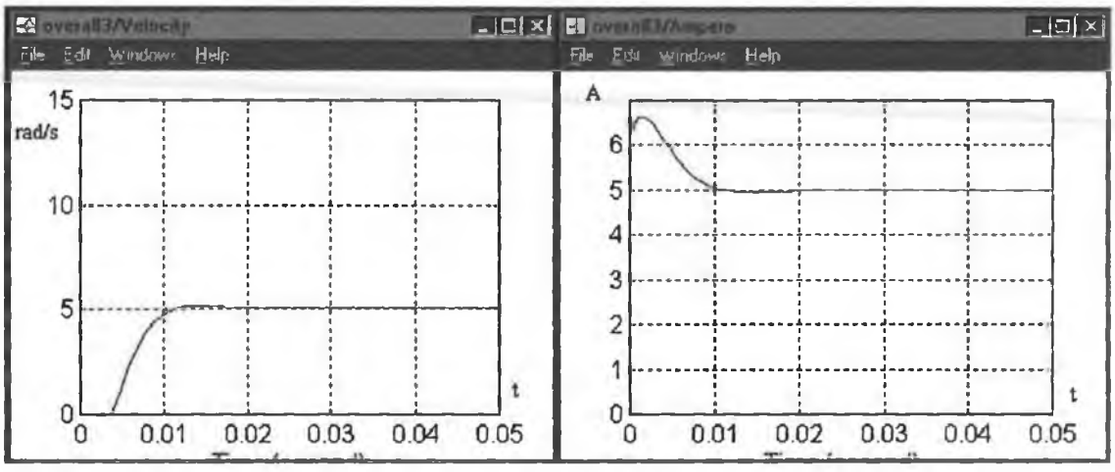

Figure VI-4 Motor response at 200m deep

From these results, it can be concluded that even at the sea surface, the motor creates a high torque, which requires high amperage. This is unfortunate because a large amount of power will be required even if the external force is small. In fact it is because such a motor is more suitable where high torques have to be overcome.

In order to reduce the power required when pumping water at the vicinity of the sea surface, a less powerful motor could be connected. Unfortunately it would become useless and unable to work deeper where the water must be discharged. Consequently the profiler could not resurface.

Therefore, even if the chosen motor requires a lot of power regardless of the depth, it is suitable since it can activate the piston at 200m deep.

Several other motors have been tested but all of them require more power or could not create such a high torque.

It must be stated that these exact values are determined assuming no feedback. The use of feedback reduces the input voltage by few millivolts (this is proven in chapter VIII). Thus the motor velocity and the amperage are consequently reduced.

Therefore for the battery capacity calculation, the feedback must be taken into consideration even if the control is studied in chapter VIII.

C-Sketch of the internal device

As shown in figure VI-5 (Refer to Appendix E), the solution using three identical ball screws, pistons and motors has been chosen. The sensors (⌀90mm⌀515mm) will be placed in the middle of the device (not shown in the figure). Three bearing supports are set to withstand the axial forces since these motors can not handle high axial forces (about 500N). Finally, three couplers will be set between the motor and the ball screw end.

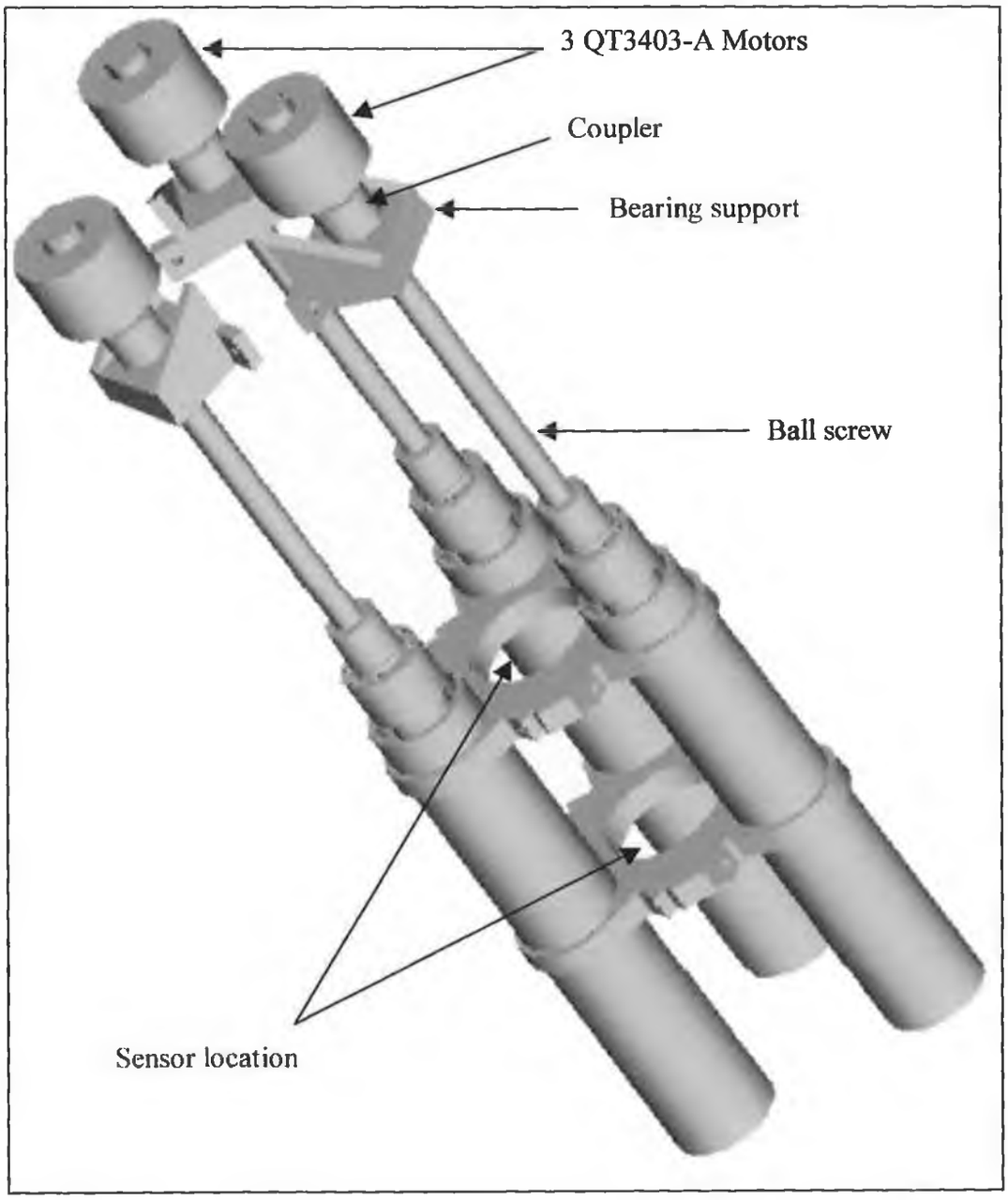

Figure VI-5 Internal system

4-BATTERY SELECTION

Because the profiler is disposable, a non-rechargeable and disposable battery is more suitable. This type of battery has a lower internal resistance (previously neglected), a higher weight/energy density and more importantly a higher volume/energy density than a rechargeable battery. Table VI-2 summarises the differences between both kinds of batteries [[31]; [32]; [33]]:

	Non-rechargeable	**Rechargeable**
Self discharge	About 2% a year	15 to 25% a month
Internal resistance R_S	Low	High
Weight related energy density	High	Low
Volume related energy density	High	Low
Environment protection	less harmful than a secondary battery	Harmful

Table VI-2

Computation of the capacity of the batteries (A.h):

-Assumptions:

The battery must deliver 24 volts to the motor

Quantities of water assumed in the worst case

-Capacity calculation:

Four different steps must be analysed per cycle:

1-Pumping 1.1kg of water at the sea surface

2-Pumping 1kg of water at 100m deep (average of the density variation)

3-Releasing 1.1kg of water at 200m deep

4-Releasing 1 kg of water at 100m deep

1-When a quantity of 1.1 kg of water has to be pumped, 3.0559A are required for 55.9seconds. These values are shown in figure VI-6 where the simulation stops automatically when 1.1kg of water has been pumped.

Note that including the error due to the feedback from the tachometer, the input voltage is not 24V but 23.3684V.

Therefore the capacity is **C1**=3.0559◈55.9=**170.82A.s**.

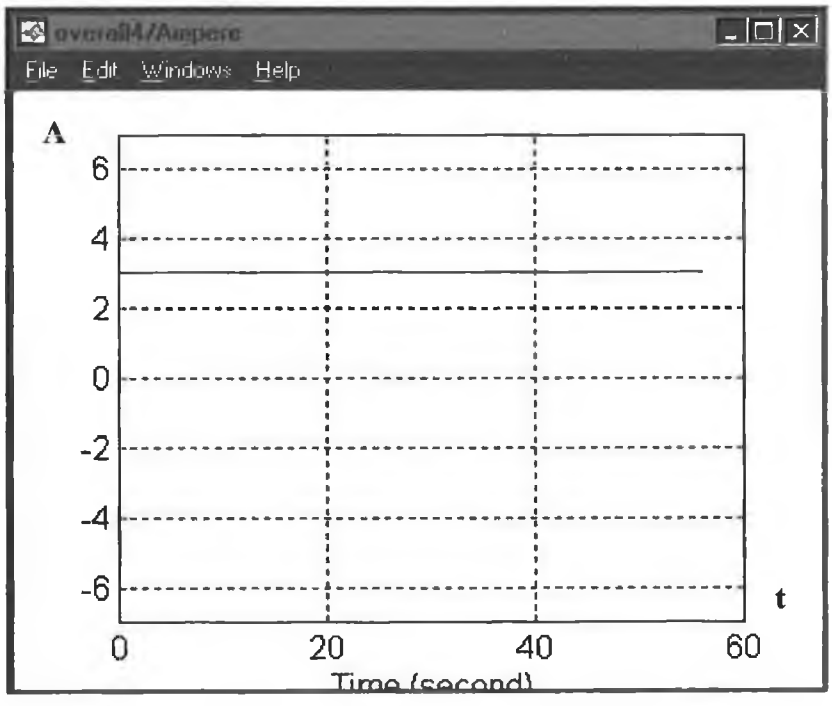

Figure VI-6 Capacity required at the sea surface

2-When pumping 1 kg of water at 100m deep is required, the motor necessitates 0.3314A for 71.5s. Therefore the capacity is: **C2**=0.3314◈71.5=**23.7A.s**.

3-This is the part requiring the largest quantity of energy (releasing 1.1kg of water at 200m deep): 4.92A for 141.7s. In this case, the capacity is:

C3=4.92◈141.7=**697.2A.s**.

4-When releasing 1kg of water at 100m deep, the motor requires 4A for 72.72s, therefore the capacity is: **C4**=4◈72.72=**290.9A.s**.

Note that in this case, the quantity of energy is much larger than in part 2. This is because the external pressure acts as a counter-force.

Refer to appendix C to get more information about these calculations.

In order to determine the overall capacity required, the sum of C1, C2, C3 and C4 (in A.s) must be multiplied by 200 (cycles) and divided by 3600 to convert the capacity into ampere.hour (A.h):

$$\text{Capacity required} = \left(\frac{C1 + C2 + C3 + C4}{3600}\right) \times 200 \qquad \text{Eqn. VI - 3}$$

$$\text{Capacity required} = \left(\frac{170.82 + 23.7 + 697.2 + 290.9}{3600}\right) \times 200$$

$$\text{Capacity required} = 65.7\text{A.h}$$

Where: 200 for the number of cycles

3600 to convert from seconds to hours

Hence, the motor requires 65.7 A.h to work 200 cycles.

In order to reduce the capacity, different lead screws and different piston radii are tested. For example a reduction of both the lead screw and the piston radius reduces the external torque but increases the pumping (discharging) time. The same simulation procedure being used than above, the different capacities are shown in table VI-3:

Lead screw l (m)	0.002		0.004		0.005	
Piston radius r (m)	0.028	0.03	0.028	0.03	0.028	0.03
Capacity A.h	89.2	80.9	**65.7**	70	79.3	120.3

Table VI-3

It can be seen that both a large radius and a large lead-screw lead to a huge capacity requirement (120.3A.h). Indeed because of the large radius, the external torque leads the motor to its "limits". The motor velocity is therefore very low leading to a long pumping (releasing time).

Our choice, a lead screw of 0.004m and a piston radius of 0.028m, is the configuration requiring the less capacity.

Note: The maximal force that the ball screw having a 0.004m lead must not to exceed is 7000N (refer to chapter V), which is equivalent to a torque of 4.95N.m.

Therefore both the motor and the ball screw can withstand the required 4.5N.m.

Various batteries can be used in order to provide the required capacity. However the battery selection is limited by important criteria such as weight and volume. Three different types of batteries from the company Energizer will be compared: the characteristics of the ANSI-918A, ANSI/NEDA-915A and ANSI-13A (LR20) are shown in table VI-4. Used in series, the voltage becomes the number of batteries multiplied by the voltage of one battery. The capacity of a parallel stack is equal to the capacity of one battery multiplied by the number of batteries.

A safety coefficient must be added since the battery efficiency drops with respect to time and external temperature changes (the voltage will not remain constant). The minimum capacity requirement will be assumed to be 80A.h.

	ANSI-918A	ANSI/NEDA-915A	**ANSI-13A(LR20)**
Capacity (A.h)	52	26	18
Voltage (V)	6	6	1.5
Weight (kg)	1.9	0.885	0.1419
Dimensions (mm)	125.4◈136.5◈73	109.5◈66.7◈66.7	61.5; ⌀34.2
Quantity required	8	16	80
Actual capacity (A.h)	104	104	90
Total weight (kg)	15.2	14.16	11.352
Total volume (m^3)	$9.99◈10^{-3}$	$7.79◈10^{-3}$	$4◈10^{-3}$

Table VI-4 Battery specifications

The ANSI-13A (LR20) configuration is the most appropriate since both its weight and its volume required are the smallest. Because the voltage is only 1.5 volts, 16 of them are required in series in order to get 24 volts and this, five times to reach a capacity of 90 A.h. Thus 80 batteries are required. The capacity requirement was 65.7A.h but a capacity of 90A.h will be available.

5-CONCLUSION

Although these high torque motors are very expensive since they use rare earth magnets, better motors at lower prices could not be found. Indeed the torque that the motor must achieve is important for D.C motors. Only a few companies manufacture such motors. Reducing the piston diameter could reduce the torque but a longer piston would be required. It would lead to a larger profiler volume, hence more density variation effects. Moreover the longer the piston is, the more damaging it is to the ball screw. Another consequence would be a longer pumping (releasing) time. Therefore, more energy would be required.
The motor selection was difficult to achieve. Indeed, many parameters had to be taken into consideration.

Concerning the battery, a theoretical amount of 65.7A.h is required for our configuration. In all the simulations, a constant voltage (also called time invariant systems) was applied in order to simplify the calculations. However, it is very important to add some capacity as a safety factor since the voltage will not remain constant but will decrease with time and external temperature variations.
From the ANSI-13A (LR20) batteries a capacity of 90A.h will be available. Hence a capacity of about 25A.h is added to the theoretical capacity (65.7A.h).

All the internal components have been selected. These different components can be designed and drawn (Refer to appendix E). They represent the internal pump system including the motors fixing, screws and other components. Then the external volume can be chosen with the appropriate shape and material. This is achieved in the following chapter.

CHAPTER VII:

MATERIAL AND SHAPE OF THE PROFILER

1-INTRODUCTION

This chapter deals with the selection of suitable materials for the profiler external shape and the pump system. The mechanical behaviour of the external shape will be analysed. A pressure of 2×10^6 Pa, occurring at 200m deep, will be applied.
In a second time the use of a web for the bearing support will be highlighted. Indeed it is of particular importance that the axial force resulting from the external pressure is absorbed before reaching the motor since this motor can not withstand large axial forces. Moreover this bearing support holds the ball screw which needs high accuracy. Hence the bearing support deflection must be as small as possible.
The most appropriate external shape will be inferred from the previous results, then the necessity of a web for the bearing support will be demonstrated.

2-MATERIAL

A-External shape

In recent years there has been a rapid growth in the use of fibre-reinforced composites. This material is widely used for deep-sea floats, buoys and submersibles. Some advantages will lead to use fibreglass-Epoxy for the external shape. Its main advantages are that high strength and stiffness can be achieved at low weight. Moreover, this material is cheap and not corrosive. Steel is not suitable for such an application [34] since it is not corrosive resistant and above all its density is too high (about 7800 $kg.m^{-3}$). Aluminium is more appropriate than steel but is more expensive than fibreglass-Epoxy.

B-Mechanical characteristics of Epoxy and fibreglass [35]

Assumptions:

- Young's modulus E=50 $GN.m^{-2}$
- Poisson's ratio ν=0.25
- Density ρ=2100 $kg.m^{-3}$
- Thickness of the profiler: 0.005m

-Yield strength σ =100MN.m^{-2}. σ is assumed in the worst case. Indeed its magnitude widely varies depending on the percentage of fibreglass and its orientation.

C-Pump

Steel will be used for the piston since it is cheap to manufacture such shapes. However, it has been stated some years ago that seawater is one of the most insidious corrosive environments for immersed metal structures. Hence, emphasis shall be laid on the use of compatible materials. This problem is not fully resolved since oceanographic companies such as IFREMER currently study new coatings (ARCOR). Furthermore, a low coefficient of friction is required between the piston and the cylinder in order to avoid loss of energy.

Thus the coefficient of friction and the corrosion resistance along with cost are the main criteria of selection.

D-Corrosion prevention [[36]; [37]]

Corrosion may be regarded as the destruction of a material by chemical or electro-chemical reaction with seawater, while the erosion is used for similar destruction arising from abrasive physical action. A third related problem is that of fouling of materials by the attachment of marine organisms to their surface. Not all corrosion is to be regarded as detrimental. In many cases, the initial corrosion consists of chemical oxidation and a film of unreactive oxide is deposited over the surface of metal rendering it immune to further corrosive attack

The use of more than one material increases the likelihood of corrosion. This is because two dissimilar metals separated by a conductor, i.e. seawater, will act as a simple battery if they are connected to each other, and one will suffer rapid electo-chemical corrosion. The relative rapidity of corrosion under these conditions depends on which materials are used.

The effects of corrosion may be uniform over the surface of the material or restricted to certain areas, as occurs in pitting and stress corrosion. Prevention of corrosion is

vital and is generally achieved either by modifying the metals' properties or by applying a protective coating. Modification of the metals' properties is most simply achieved by alloying. Protective coatings may be metallic, generally provided by cladding (sandwiching of one metal between two sheets of another) which will not be discussed, galvanising or non-metallic materials.

In galvanising, electrolytic deposition of very thin layers of protective metals occurs on the surface of the material, as in the deposition of zinc on iron. The deposition of very thin layers allows the use of very expensive noble metals. But if noble metals are to be used, the deposited layer must be completely gap-free, as very rapid corrosion will occur in any exposed underlying base metal due to the separation in the galvanic series of the two metals.

Non-metallic coatings are of many types. Chemical protection occurs by the formation of films of reaction products such as the unreactive oxide layers already mentioned. To be effective, it is essential that the oxide film has a very low electrical conductivity and thus acts also as an insulator for the underlying metal. Not only does painting provide mechanical protection but by suitable choice of paint also forms corrosion inhibitors and is probably the most widely used type of corrosion protection.

Biological fouling does not usually affect the mechanical properties of materials except for those subject to attack by boring organisms. It may, however, provide much more favourable microenvironments on the surface of the material for the initiation of corrosion, especially crevice corrosion. It may also destroy any protective coating already present. The provision of poisons in the paint to kill settled animals, or vibration, gentle heating or rapid water flow to prevent the initial settlement, will usually control the problem. It should be noted, however, that the presence of some fouling might help to prevent corrosion by the reduction of water velocity at the surface of the material covered by a thin film of bacterial slime or algae.

The exact location of the profiler greatly affects the corrosion that is likely to occur. Deep waters are generally lower in oxygen than well-aerated surface waters and pitting may be more prevalent. On the other hand, the lower the temperature in deep water is, the more the rate of corrosion decreases. Differential aeration resulting in the rapid alternation of oxide film breakdown and formation also accelerates corrosion. A

further important environmental effect is that of water speed because the higher the water velocity is, the greater the chances of damaging the protective film increases. Titanium is often used. Indeed its oxide film is more resistant than that of aluminium.

The choice of materials to be used for the piston is not easy. Many conflicting factors are to be taken into account. However, in our configuration the main criteria are the cost and the coefficient of friction. Indeed it is fundamental to have a low coefficient of friction in order to reduce the losses due to friction.

Table VII-1 shows the corrosion penetration and the coefficient of friction of relevant coating materials [[26]; [38]]:

COATING MATERIAL	**CORROSION PENETRATION (mm/year)**	**COEFFICIENT OF FRICTION**	
		Dry	Greasy
Steel/Steel	0.004	0.58	0.15
Copper/mild steel	0.0038 (copper)	0.36	0.18
Aluminium /Aluminium	0.00038	1.4	
Nickel/mild steel	0.0025 (nickel)	0.64	0.178
Titanium/Titanium	Nil	0.5	0.2
Teflon/ teflon	Nil	0.08	0.04

Table VII-1 Coating selection

Teflon is a "noble metal" of the plastics in that it is corrosion resistant to practically all environments up to 300°C [39]. It is used for their low coefficient of friction in coating.

From table VII-1, Teflon is the most appropriate coating. Indeed, over four months there will not be any corrosion problems and due to the very low coefficient of friction, losses will be neglected.

The internal surface of the cylinders (in steel) will be coated with Teflon. Corrosion resistant paint will be applied on their external surfaces since these areas do not need a low coefficient of friction.

3-SHAPE

In order to reduce the energy required, the external shape must be optimised as much as possible. Indeed the seawater density variations will have less influence on an optimised shape as explained below.

A-Influence of the profiler volume

Assumption: Seawater density varies from 1020kg.m^{-3} to 1030kg.m^{-3} depending on its salinity, pressure and temperature (Refer to appendix A).

Explanation: Depending on the profiler velocity, a certain amount of water has to be pumped or released. In order to reduce the energy required, it is important to pump as few water as possible.

Example:

A-Assuming for instance a profiler volume equal to 1m^3, the buoyancy is, taking into account the density variation (in kg):

Buoyancy1A=volume×density1 =1×1020 =1020kg

Buoyancy2A=volume×density2 =1×1030 =1030kg

Therefore the profiler should have an initial mass of say 1019.9kg (to remain at the sea surface) and capable of pumping 10.2kg to sink.

B-Now assuming a volume of the profiler twice smaller (0.5m^3), the buoyancy is therefore:

Buoyancy1B= volume×density1 =0.5×1020 =510kg

Buoyancy2B= volume×density2 =0.5×1030 =515kg

Therefore an initial mass of 509.9kg is necessary in order to be positively buoyant. And a capacity of 5.2kg is required, allowing the profiler to sink. Hence, to have a smaller effect on the profiler, the range of buoyancy can be reduced by decreasing the profiler volume. Obviously, the two volumes mentioned above are just used as an example. Indeed such profilers would be too heavy and their mass variations would be

too large (10.2kg or 5.2kg). This example only demonstrates that it is primordial to optimise the volume of the profiler as much as possible.

B-Shamrock shape

The first solution under study is optimised as shown in figure VII-1. As explained previously, the volume of the profiler should be as small as possible. Moreover, by reducing the projected area, the drag force will also be reduced. In each protuberance of the following external shape is mounted a piston, the sensors being in the middle (not shown).

The exact profiler volume (calculated with Pro-Engineering) is: 5.63×10^{-2} m^3.

Hence the buoyancy force will vary from (in kilograms):

$mass_{(\rho=1020)}=5.63\times10^{-2}\times1020=57.4kg$

$mass_{(\rho=1030)}=5.63\times10^{-2}\times1030=57.9kg$

The difference between these two values is equal to 0.5kg. Including the 1.1 kilograms required from the dynamics of the profiler (1.6kg) and having a pumping capacity of about 3kg, the profiler will be able to sink or rise.

An initial mass of the profiler of 57.3kg can be assumed. Once it is filled up with water, its mass is 60.3kg.

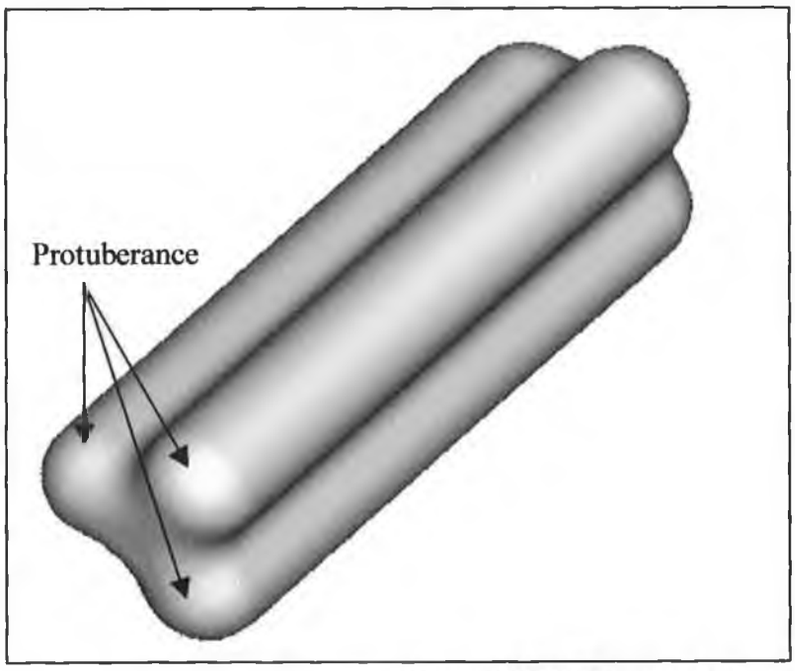

Figure VII-1 Shamrock shape

C-Cylindrical shape

In this case, figure VII-2, the volume is: 9.94×10^{-2} m^3. Hence the buoyancy force will vary from:

$mass_{(\rho=1020)}= 9.94\times10^{-2} \times1020=101.4kg$

$mass_{(\rho=1030)}=9.94\times10^{-2} \times1030=102.4kg$

Note that the volume used (9.94×10^{-2} m^3) is used for the dynamics page 41.

The difference between the two values is equal to 1kg. So the initial mass of the profiler can be 101.3kg. When full of water, its mass becomes 104.3kg. It can be seen that because the volume in this case is twice larger, twice more water is required.

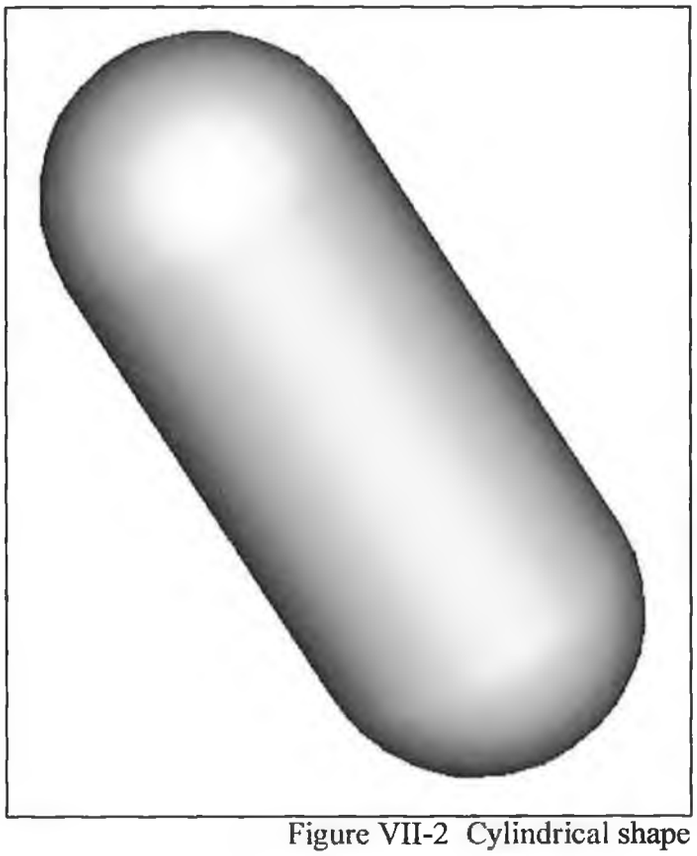

Figure VII-2 Cylindrical shape

In order to reduce the energy required, it is easy to imagine that the first solution is more appropriate since the seawater density variation has less effect on the profiler. Moreover it also has a smaller projected area, hence smaller drag force. Therefore less water needs to be pumped than for the second solution.

4-STRESS ANALYSIS OF THE EXTERNAL SHAPE

In order to analyse the stress (and deformation) acting on both external shapes under pressure at 200m deep, a Finite Element Analysis will be performed using Ansys software[40][41][42][43]. The mechanical characteristics of Epoxy+fibreglass are given page 77. The pressure is applied perpendicularly to the surface of the body.

A-Shamrock shape

Because of the two symmetries of the profiler volume, only $1/6^{th}$ of the volume needs to be considered (figure VII-3).

Stress:

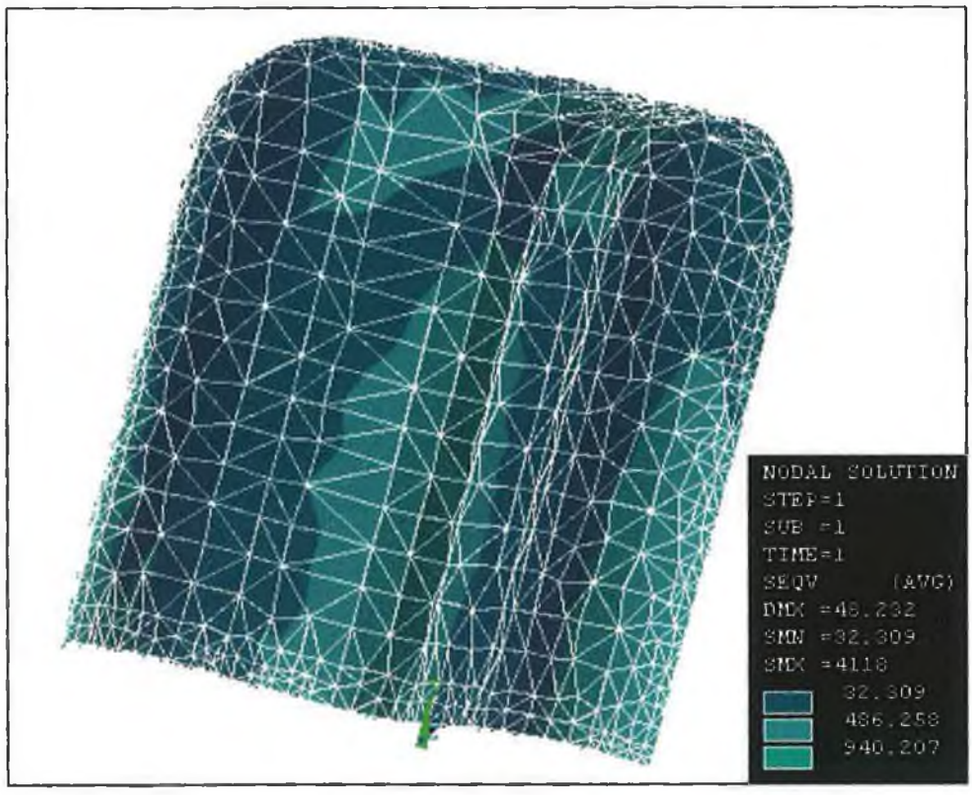

Figure VII-3

The maximum stress acting on the profiler is 940 $MN.m^{-2}$. Because this value is beyond the Yield stress (σ=100 $MN.m^{-2}$), the composite material will not be able to withstand such a pressure. This means that the profiler is operating in the plastic range. After being deflected once, this external shape will not come back to its initial shape. Hence this shape can not be used.

Deflection:

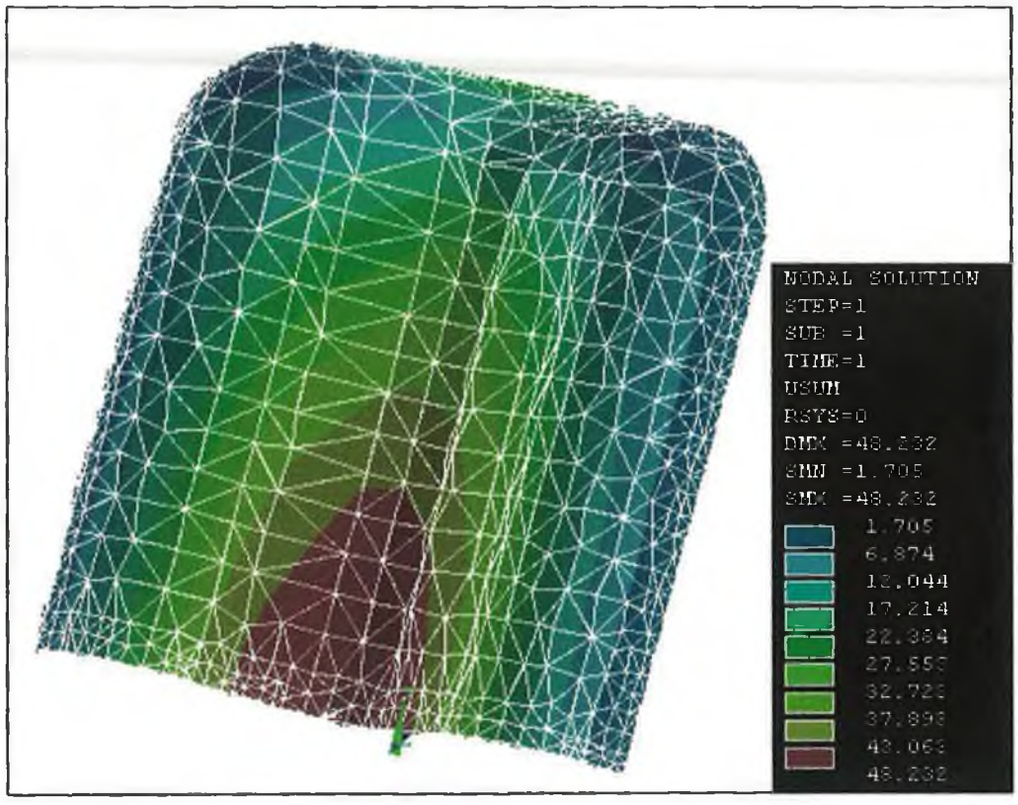

Figure VII-4

This would lead, as shown in figure VII-4, to a deflection of 48.2 millimetres. Obviously, this value is far much too large and unrealistic since the profiler would implode before reaching this deflection.

In order to reduce the deflection, six ribs could be used as shown in figure VII-5.

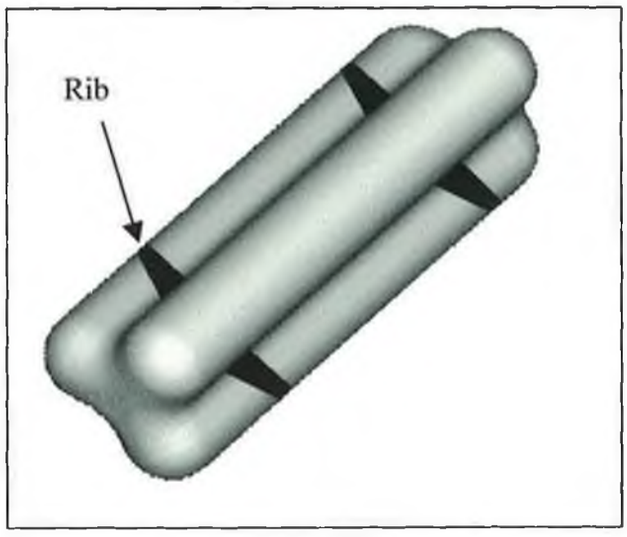

Figure VII-5

However, even if the profiler deflection could be significantly reduced with these ribs, the drag coefficient (i.e. drag force) would be much larger. This would lead to a reduction of the profiler velocity or more energy being required. This shape will not be retained.

B-Cylindrical shape

Because the previous external shape is not appropriate, the cylindrical shape (hollow cylinder with two hemispherical ends) will be studied. As shown in figure VII-6 and figure VII-7, the stress and the deflection at 200m deep. The profiler dimensions are:

- External radius=175mm
- Length=400mm

Because of the symmetries of the profiler volume, only $1/8^{th}$ of the shape needs to be considered.

Using this shape, the stress is significantly reduced. Moreover the maximum stress is below σ ($66.024MN.m^{-2}<100MN.m^{-2}$). Consequently the following shape will be used even if seawater density variations have more influence on the profiler.

Stress:

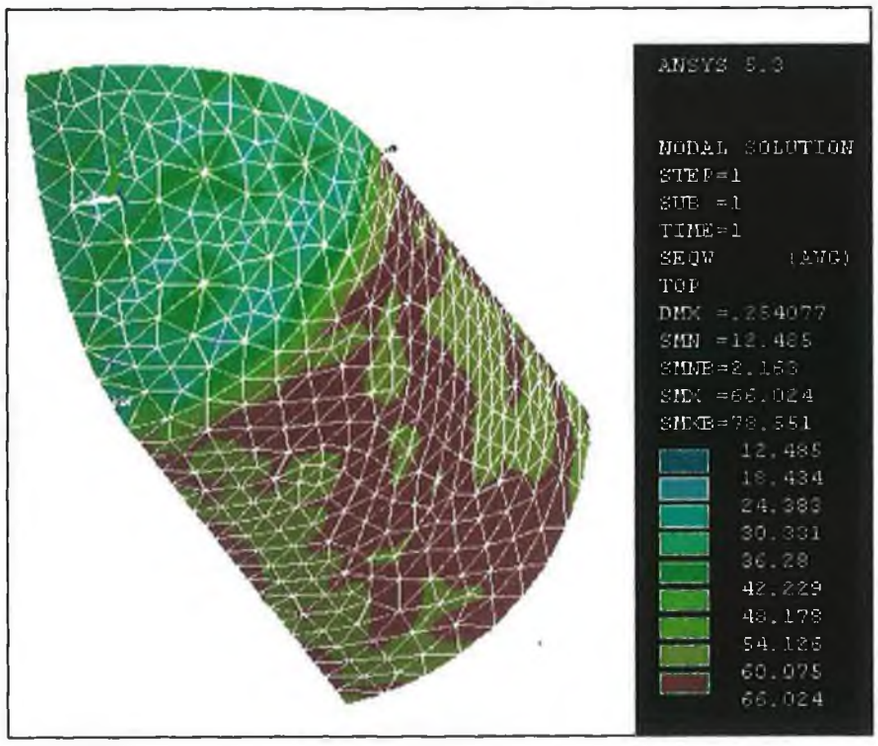

Figure VII-6

Deflection:

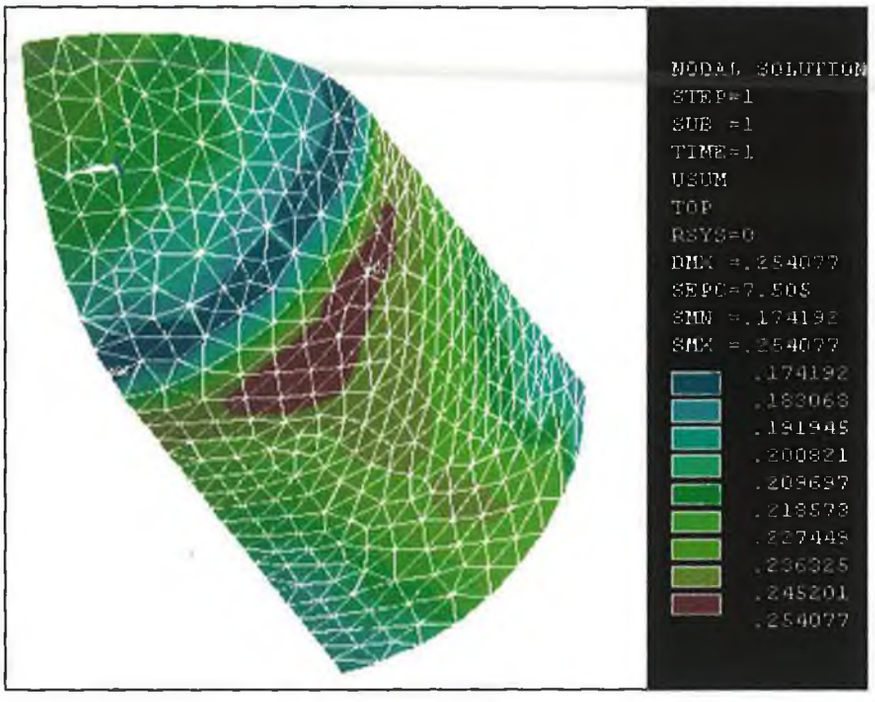

Figure VII-7

5-BEARING SUPPORT

An appropriate shape for the bearing support is essential since it has two different purposes. The first one is to maintain the ball screw in its initial position. Indeed because the guide has to be very accurate, the bearing support has to be robust. Its second aim is to withstand the high axial force due to the external pressure exerted on the piston. Indeed the selected motor can only withstand small axial forces (few hundreds of Newtons). The magnitude of the maximal force is 4978N (occurring at 200m deep). Hence, the deformation of this element must be calculated to make sure that it is insignificant and not annoying for the system. Two different configurations, without and with web, will be studied (figure VII-8). As shown in figure VII-9, the first design for this element was only a prismatic shape manufactured in steel.

Mechanical properties and results:

- Young's modulus E=210 $GN.m^{-2}$
- Poisson's ratio ν=0.3
- Volume: height=0.07m, thickness=0.03m, breadth=0.08m

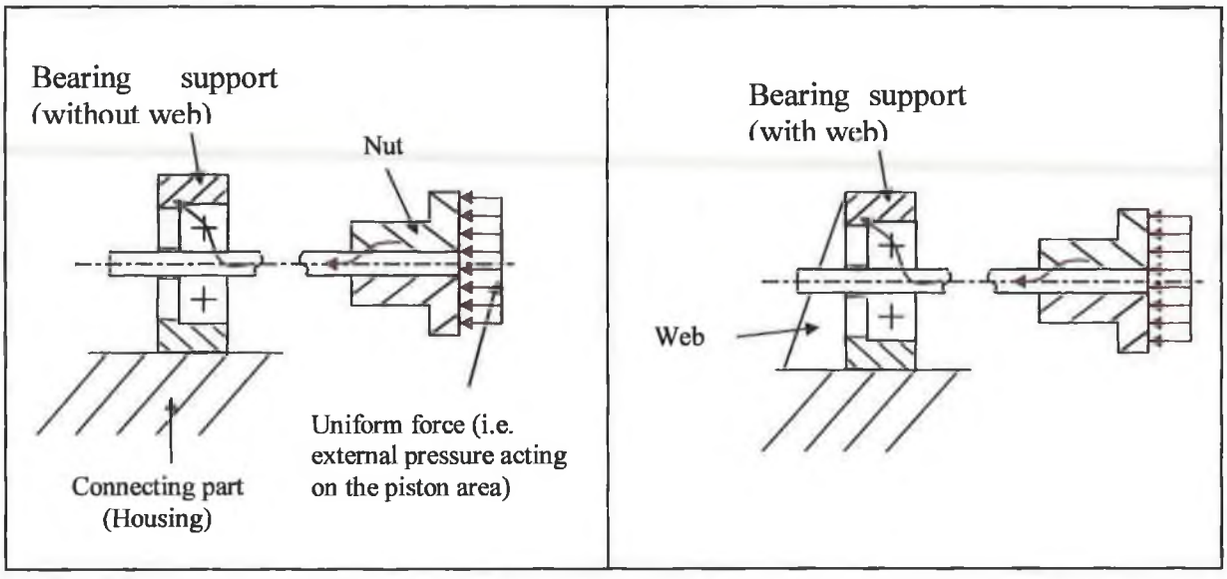

Figure VII-8: Action of the force on the two different configurations

A-Without web

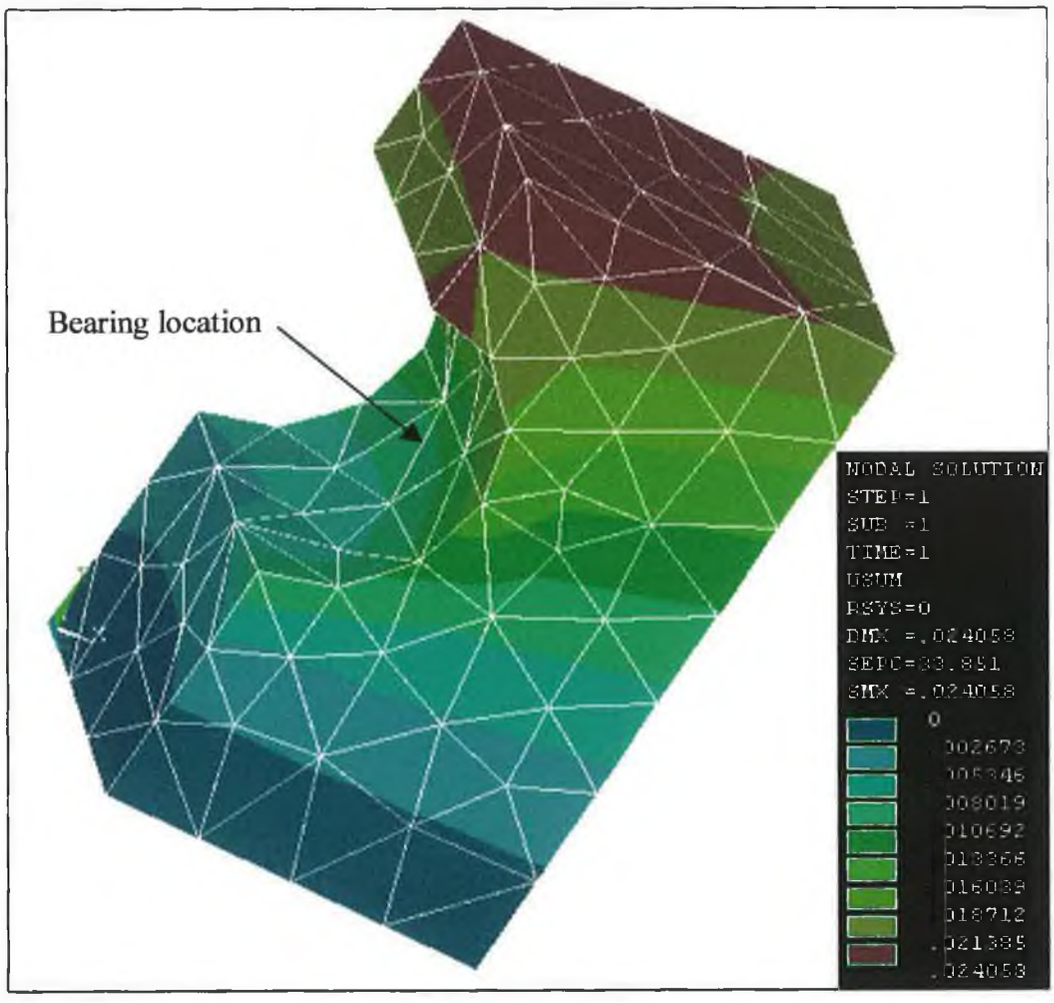

Figure VII-9 Deflection of the bearing support without web

B-With web

Even if the deflection is very small without web, the deflection is much smaller when a web is used (figure VII-10). In this configuration, the maximum deflection is only 0.014506mm.

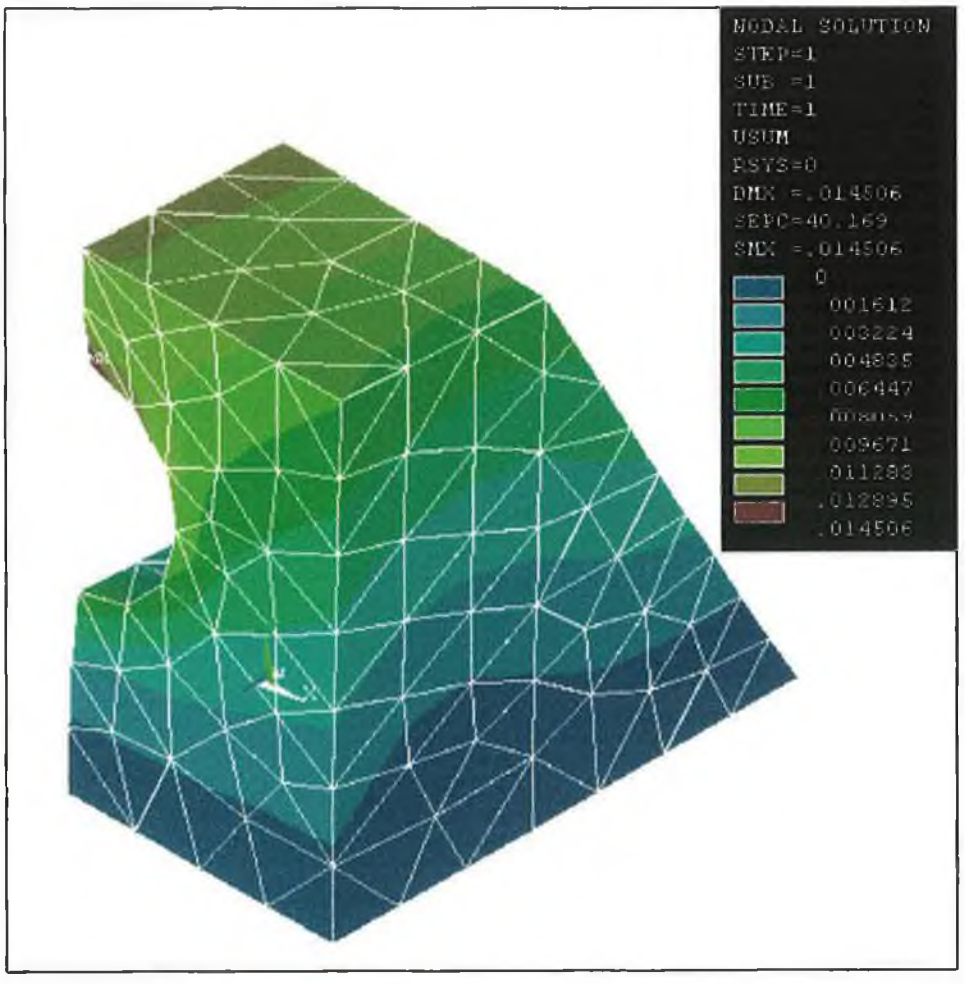

Figure VII-10 Deflection of "bearing support" with web

This represents a reduction by 40% of the previous deflection. Because high accuracy and strength are required, the use of reinforcement is necessary.

6-STRESS ANALYSIS OF THE CYLINDER FIXATION:

The aim of this analysis is to evaluate the stress and the deformation of the profiler near the fixation points. The interest of this study is to attest the reliability of the profiler design.

- **Theoretical analysis**

Figure VII-11 shows the simplified external shape, divided into 3 parts: Upper part, cylinder and lower part). The fixation is also shown between these different parts.

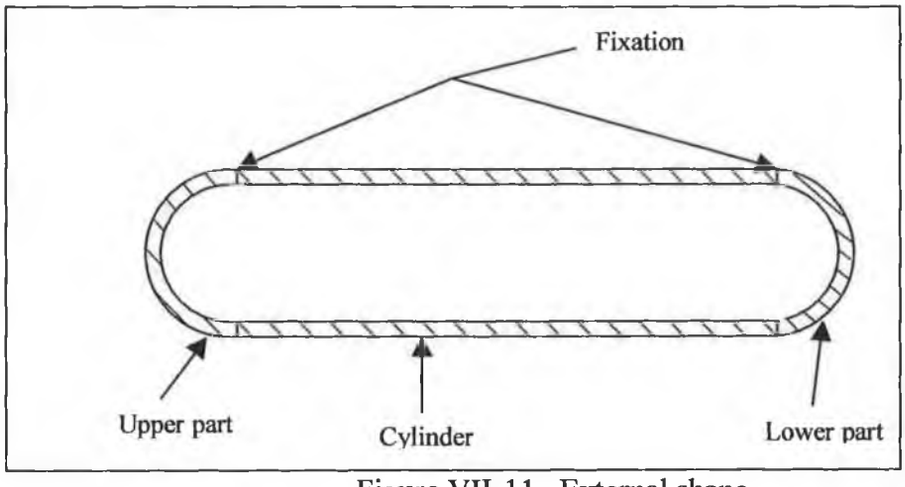

Figure VII-11 External shape

Assumptions: the bell's movement is imposed as null and the cylinder's deformation is studied. In this case the deformation of the fixation, between the part (lower or upper) and the cylinder, is maximum (figure VII-12).

Where,[44]:

ΔR= Radius' variation
a=external radius(175mm)
p_e= external pressure (2MPa)
E= Modulus of Young ($210x10^3$MPa)
t= thickness (5mm)

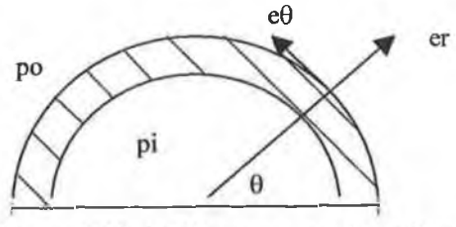

Figure VII-12 Pressure on the allow cylinder

$$\Delta D = \frac{p_e \times a^2}{E \times t} = 0.058mm = 58\mu m$$

The maximum diameter's variation between the part and the cylinder is 58μm.

This result, based on a simplified design using a basic equation, proves that only a small displacement between the bell and the cylinder is present.

- **Finite element analysis :**

The simulation with Ansys, figure VII-13, is achieved using the same data (where only a quarter is studied since the external shape is symmetrical). [[40][41][42] [43]]

Using axisymmetrical quadratic elements (Plane42) with the following Conditions:

-A: no displacement /x, continuity condition

-B: no displacement /x, block the plate to get a maximum displacement between the different parts at the fixation

-C: no displacement /y, continuity condition

Applied pressure: 2Mpa

Modulus of Young: $210x10^3$MPa

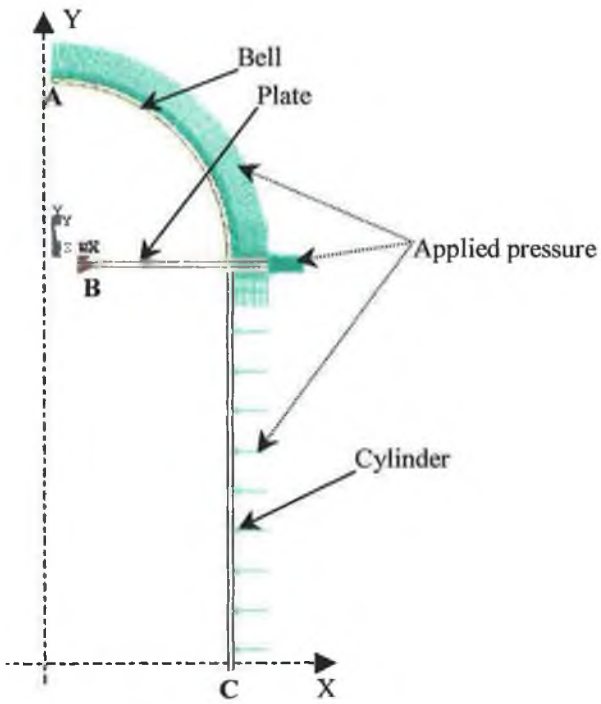

Figure VII-13 Simulation

Ansys solution shows than the Maximum Stress (67.2 MPa) is small compared with the elastic limit of 250MPa for classical steel.

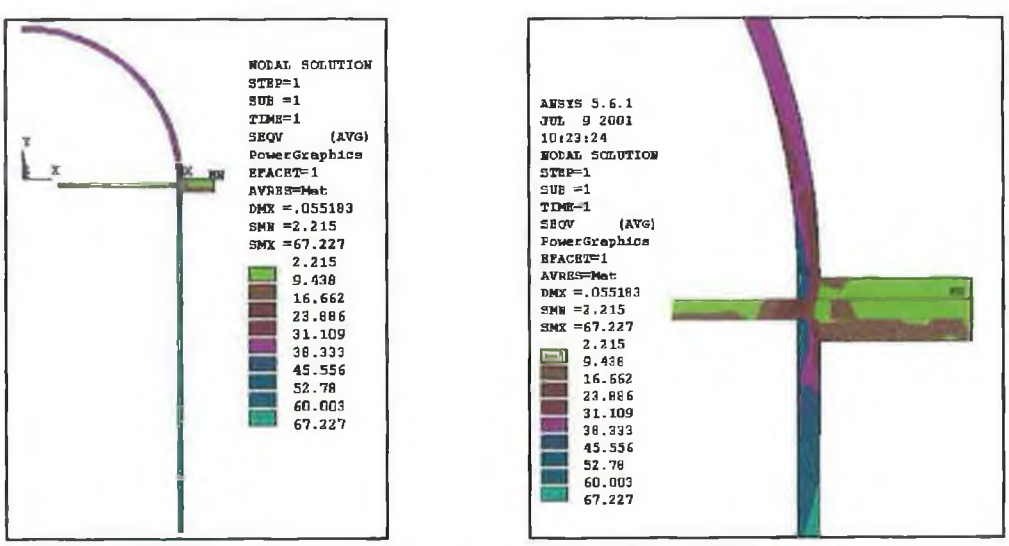

Figure VII-14 Von Mises stress result

The displacement is less than 49μm, near the fixation. This is small compared with the dimension of the profiler. This deformation will not modify the quality of the assembly.

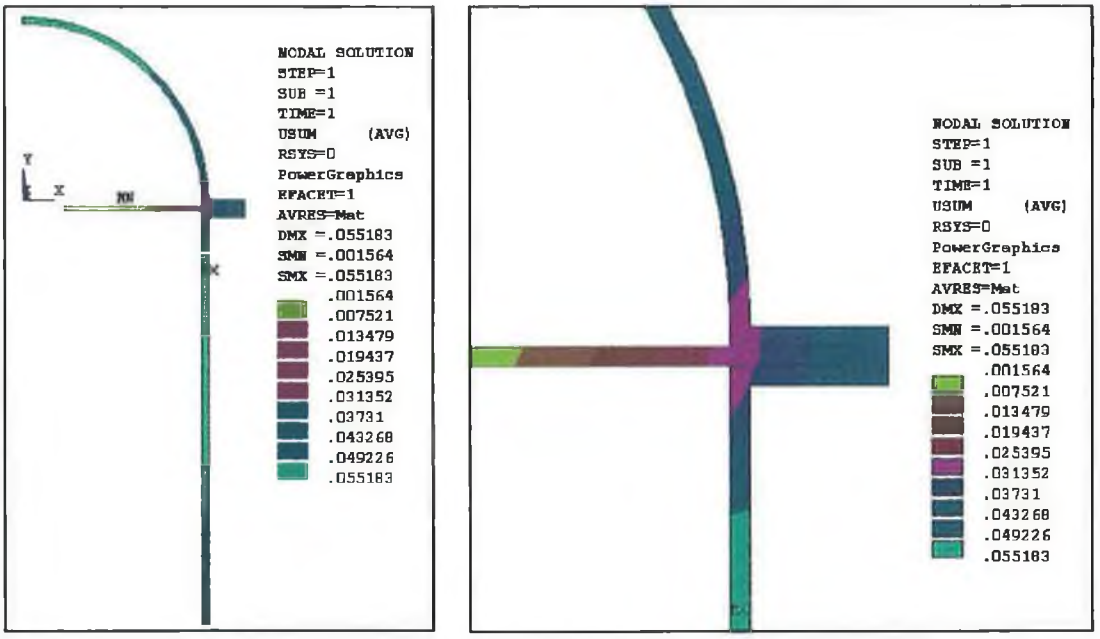

Figure VII-15, Total Displacement (usum) Result

Furthermore, the result of the magnified deflection shows no discontinuity in the assembly deformation near the fixation.

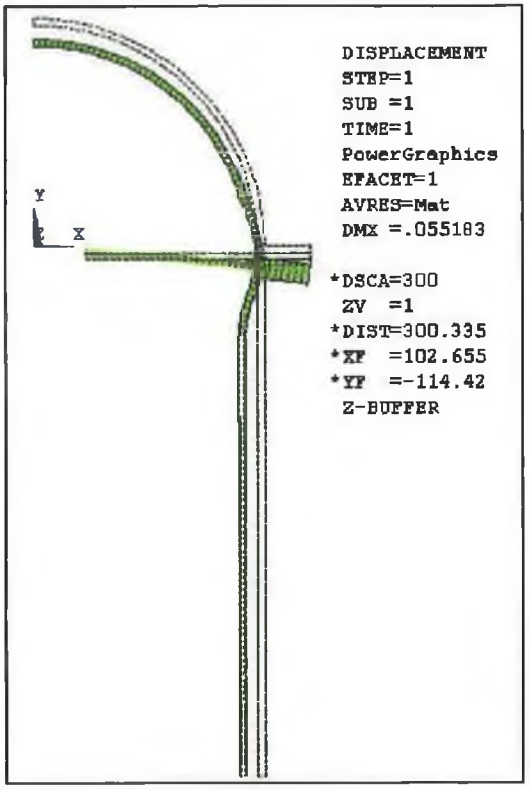

Figure VII-16 Magnified Deflection (Amplified scale 300:1)

7-CONCLUSION

Several conclusions can be stated. First of all, fibreglass and Epoxy composite will be used for the external shape due to its several mechanical advantages such as corrosion resistance, low weight, high strength and low cost. All these advantages make it very popular in oceanographic explorations.

Using Teflon as the coating over steel for the piston is the best configuration. Concerning the part made of steel in contact with seawater that does not require a low coefficient of friction, paint will be used since it is reliable and very cheap.

Concerning the mechanical behaviour of the external shape, the first one having three protuberances was attractive in order to reduce the energy requirement. However it can not be used due to the huge stress acting on it even if ribs are used.

As a comparison the stress acting on the second shape (cylinder + hemispheric ends) is about fourteen times smaller. This is because there is no shearing stress due to the axysymmetry of the profiler. It can be noticed that the maximal stress occurs in the cylindrical part; the stress magnitude is twice bigger than in the hemispheric parts. This is because in thin pressure vessel, the hoop stress in cylinders is twice bigger than in spheres [45][46].

However, from an energy point of view, the chosen shape is less appropriate since one more kilogram needs to be pumped (released) per cycle.

Finally even without the web, the deflection of the bearing support is very small, its use enables a reduction in the bearing support deflection by 40%. This is important for the ball screw to work properly. Indeed, high accuracy is required since one of its ends is free.

Now that all the components have been designed and dimensioned, the remaining drawings can be drawn (refer to appendix E). The full profiler system can be seen on the very last page of Appendix E.

CHAPTER VIII:
CONTROL DESIGN OF THE PROFILER

1-INTRODUCTION

The first purpose of this chapter will be to discuss the way of controlling the profiler velocity ($0.05 m.s^{-1}$). In order to get an accurate profiler velocity, the motor must be controlled using the most appropriate method. Thus to increase the accuracy [[47];[48]], a closed loop system using an angular motor velocity feedback will be studied. Indeed in such a system, the actuating error (which is the difference between the input signal and the output signal) is fed to the controller (by the tachometer which converts the angular velocity into a voltage) so as to reduce the error and bring the output signal of the overall system to the desired value.

The stability of the control system will be studied afterwards. Indeed it is primordial for the system to be stable or in other words that the output signal is bounded.

Finally the simulations will be undertaken in order to determine the settling time and percentage overshoot of the piston at the previously studied depths. One shall underline that controlling a underwater vehicle is highly complex [[49];[50]].

2-SELECTION OF THE CONTROL METHOD

A-Mathematical method

The mathematical method to control the profiler velocity is shown in figure VIII-1. Once the pressure determined by the sensor, the appropriate motor speed can be selected. Once the salinity and temperature are found out, the actual water density can be calculated. Finally, once the vertical water current (v_c) determined by the sensor, the quantity of water required to dive or resurface can be calculated. This is achieved by using the second order differential equation derived in chapter IV.

The main disadvantage of this method is that it is completely dependent on the simplified differential equation. Hence the error induced will lead to an inaccurate actual velocity.

This way of controlling the motor is rather complicated and is not suitable for such an application. A less complex and more accurate solution must be found in order to get a fast and efficient response from the motor.

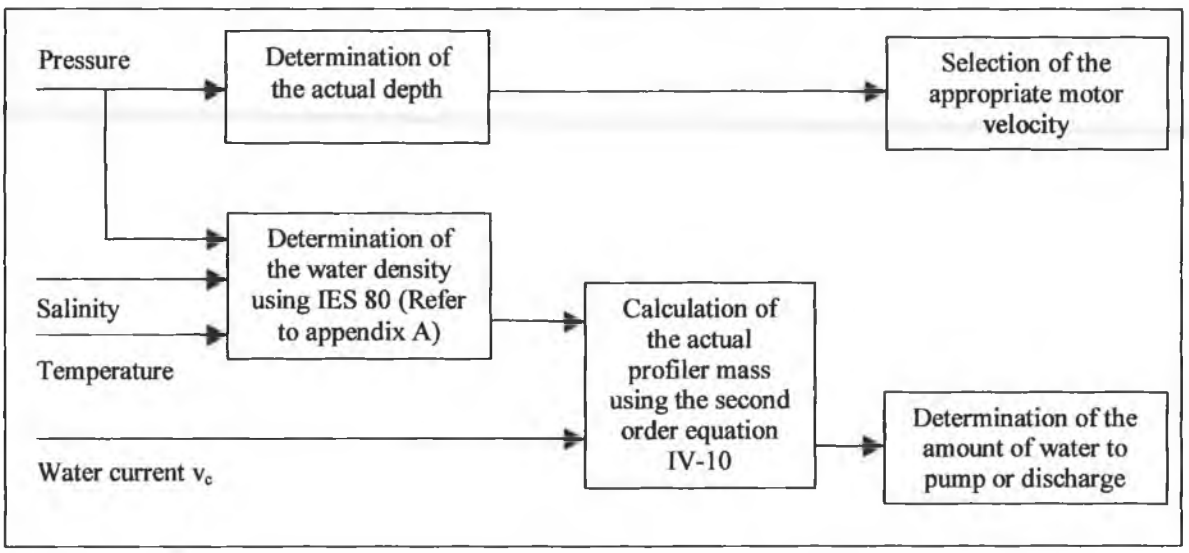

Figure VIII-1 Mathematical method

B-Pressure difference method

The velocity of the profiler is controlled by the pressure difference between two consecutive collected data. Considering an incremental mass of water, when water has to be pumped or released, this amount is divided into quantities of 0.05 kilogram. This corresponds to a piston displacement of 1.98 centimetres assuming a water density of 1025 $kg.m^{-3}$ (a variation of ±5 $kg.m^{-3}$ of this density leads to an error of ±0.49%). Whenever, the pressure difference is not in the predefined range, (figure VIII-2), the piston will pump or release an amount of times 0.05 kilogram to get into this range.

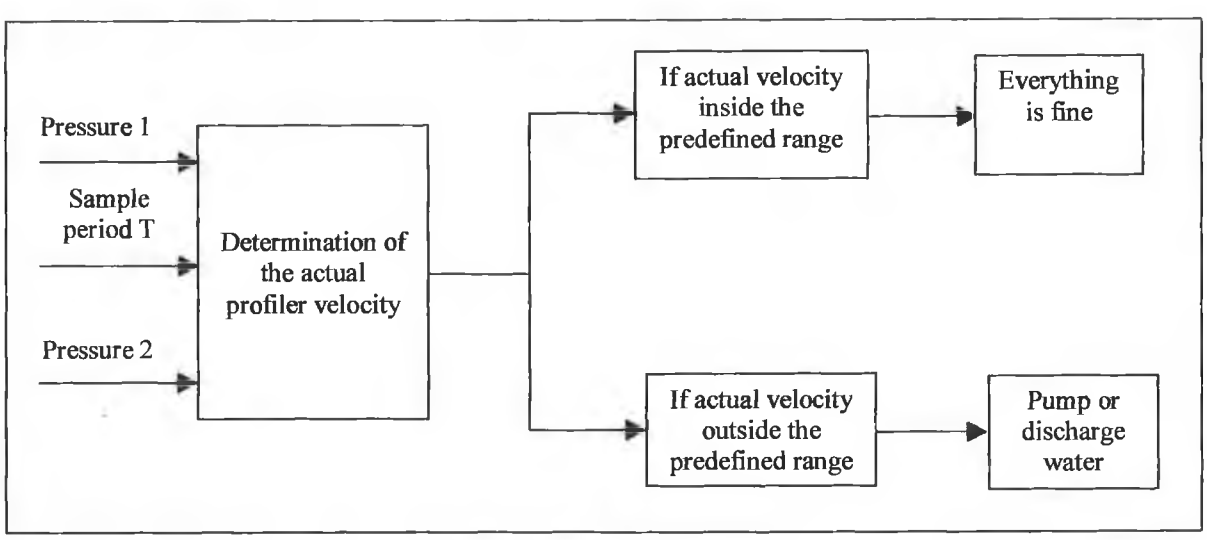

Figure VIII-2 Pressure difference method

Assumptions:

-Considering two consecutive pressure measurements:

-Pressure1 at time 1

-Pressure2 at time 2

Hence the pressure difference is: ΔP=Pressure2-Pressure1

-The sample period T (time between the two successive measurements): 10 seconds

It is not necessary to use a faster sample period since the velocity profiler is very slow.

-The aim is to accept velocities in the range 0.04 $m.s^{-1}$ (80% of 0.05 $m.s^{-1}$) to infinity (say 1 $m.s^{-1}$ since this velocity is unreachable for such profilers). This means that the velocity is acceptable if the profiler dives (rises) between (figure VIII-3):

$$0.04 \leq v \leq 1 (\equiv \infty)$$

Method:

The distance travelled during one period is equal to $\frac{\Delta P}{\rho \times g}$

Therefore, the actual profiler velocity v is:

$$v = \frac{\Delta P}{\rho \times g} \times \frac{1}{T} \qquad \text{Eqn. VIII-1}$$

Hence,

$$v_1 \times \rho \times g \times T \leq \Delta P \leq v_2 \times \rho \times g \times T$$

$$0.04 \times 1025 \times 9.81 \times 10 \leq \Delta P \leq 1 \times 1025 \times 9.81 \times 10$$

$$4022.1\ N.m^{-2} \leq \Delta P \leq 1005552.5\ N.m^{-2}$$

Note: The large difference between these two values exists because the second pressure ($1005552.5 N.m^{-2}$) represents infinity.

Finally, if the pressure difference is inside this range for the diving motion, there is no need to pump or release water. However, if the velocity is not in this range, water must be pumped (released):

-The profiler is going too slowly when sinking ⇨ Pump water

-The profiler is going too slowly when resurfacing ⇨ Discharge water

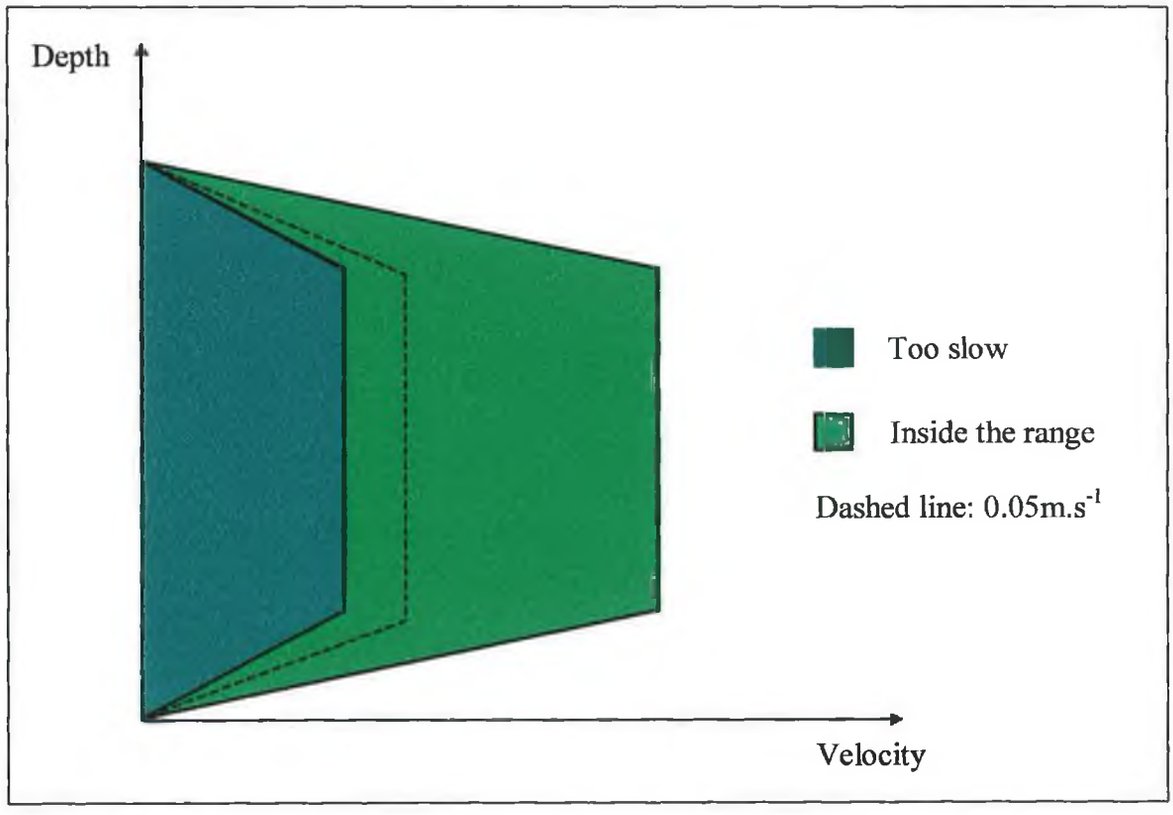

Figure VIII-3 Acceptable range

C-Selection

Because of its greater accuracy, the pressure difference method will be chosen. Indeed with this method, the simplified second order differential equation is not used. Only actual data are collected and used in "real time". Moreover it is easier to handle two consecutive variables than four different ones. This leads to an easier control design and a faster response.

The way of controlling the motor can, now, be developed.

3-ARMATURE CONTROL VERSUS FIELD CONTROL

In a permanent magnet DC servomotor, the magnetic fields produced by a permanent magnet and, therefore the magnetic flux, is constant. Such servomotors can be controlled by the armature current. Such a scheme to control the output of this motor by the armature current is called armature control.

In the case where the armature current is maintained constant and the speed is controlled by the field voltage, the DC motor is called a field-controlled DC motor. However, the requirement of constant armature current is a serious disadvantage. It is much more difficult to provide a constant current source than a constant voltage source [51]. Moreover, the time constants of a field-controlled DC motor are generally large compared with the time constants of a comparable armature-controlled DC motor.

4-SIGNAL CONDITIONING (From sensors) [52]

A-Amplifier [53]

Since the electrical signals produced by most transducers (i.e. the tachometer) are at low voltage, it is necessary to amplify this voltage before it is suitable for transmission to the motor. Moreover, the amplifier must have very high input impedance because transducers are high impedance and do not tolerate current drain. At the same time, the amplifier must have low output impedance since it feeds into the armature circuit of the motor.

B-Filter [53]

A filter might be required to alter the amplitude with respect to frequency of the tachometer. Ideally, a filter will not add new frequencies to the input signal, nor will it change the component frequencies of that signal, but it will change the relative amplitudes of the various frequencies of the tachometer. Filters are often used in electronics systems to emphasise signals in certain frequency ranges and reject signals in other frequency ranges. A Low-Pass filter might be necessary since it passes low frequency signals and rejects signal at frequencies above the filter's cut-off frequency.

5-TACHOMETER [52]

It is a transducer that converts an angular velocity magnitude into a voltage:

$V=\omega \times K_{ta}$ Eqn. VIII-2

Where K_{ta} : Tachometer constant (1Volt per 1000 revolutions=0.0095 volt per radian)

6-BLOCK DIAGRAM (Assuming no saturation)

Before simulating the armature controlled motor (using Simulink), the stability of the overall system must be checked. Indeed an unstable closed-loop system is of no practical value.

In order to study theoretically the stability of the system, the saturation can not be taken into consideration. Although this saturation represents the amplifier limitation (the system works in the range ±24 volts and not from $-\infty$ to $+\infty$), its implementation adds to the system a non-linear term. This is unfortunate since it is very difficult to solve. Therefore, the stability will first be studied assuming no saturation before simulations are achieved including the saturation.

Figure VIII-4 represents the block diagram of the system without saturation:

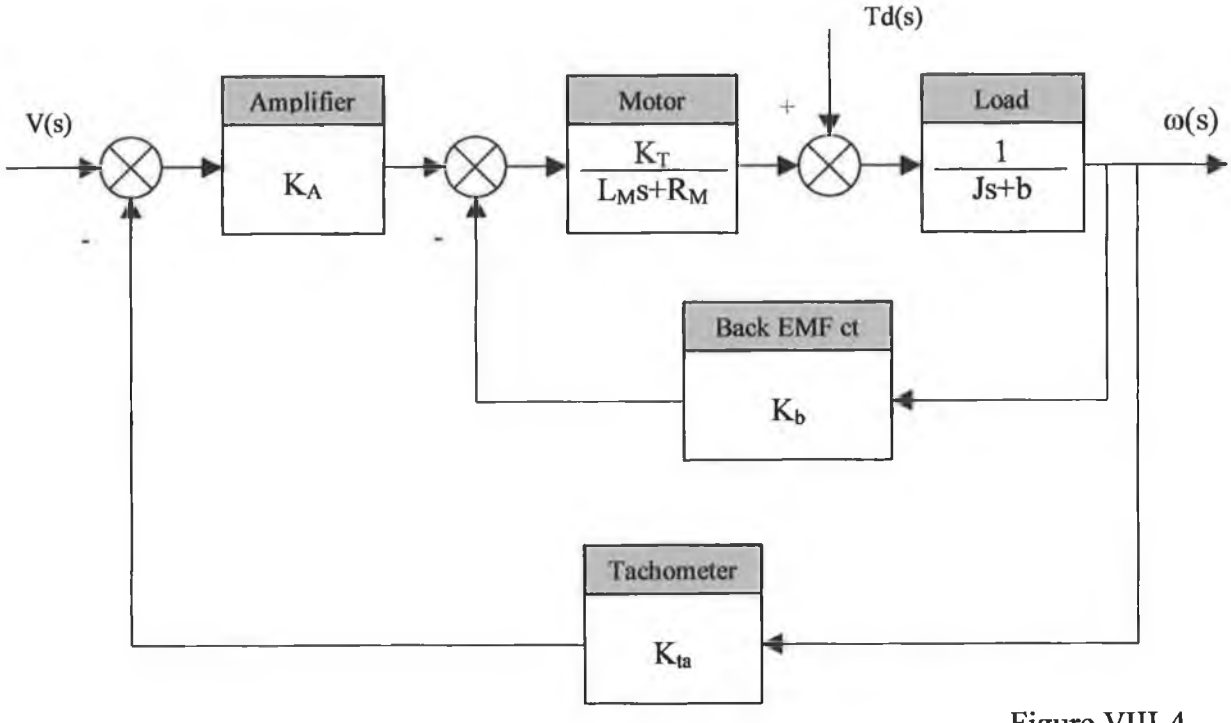

Figure VIII-4

Where:

- v(s): Source voltage
- K_T: Motor constant=0.9485N.m.A^{-1}
- R_M: Armature resistance=3.85Ω
- L_M: Armature inductance=0.0082H
- J: Inertia=13.3×10^{-4}N.m.s^2
- b: Friction=0.2385N.m per rad.s^{-1}
- K_b: Back EMF constant=0.949Volt per rad.s^{-1}
- K_{ta}: Tachometer constant=0.0095
- K_A: Amplifier=10^4
- Td: Torque disturbance (depends on the depth)
- ω(s): Angular velocity
- s: Laplace transform

7-STABILITY

A-Assumptions

-The system is assumed "linear time invariant"[51]:

Linear: Strictly speaking, linear systems do not exist in practice, since all physical systems are non-linear to some extent. Linear feedback control systems are idealised models that are fabricated by the analyst purely for the simplicity of analysis and design. For linear systems there exists a wealth of analytical and graphical techniques for design and analysis purposes. However, non-linear systems are very difficult to treat mathematically, and there are no general methods that may be used to solve a wide class of non-linear systems.

Time invariant: When the parameters of a control system are stationary with respect to time during the operation of the system, the system is called a time invariant system. In practice, most physical systems contain elements that vary with time. For example, the winding resistance of the electric motor will vary when the motor is being first excited and its temperature is rising, the efficiency of the battery depends upon the

external temperature. Although a time varying system without non-linearity is still a linear system, the analysis and design of this class of systems are much more complex than that of the time invariant systems.

B-Definition

Stability is used to distinguish if a system is useful or not. A system is defined as stable when the response is bounded [54]. That is, if the system is subjected to a bounded input or disturbance and the response is bounded in magnitude when time tends to infinity, the system is stable (figure VIII-5):

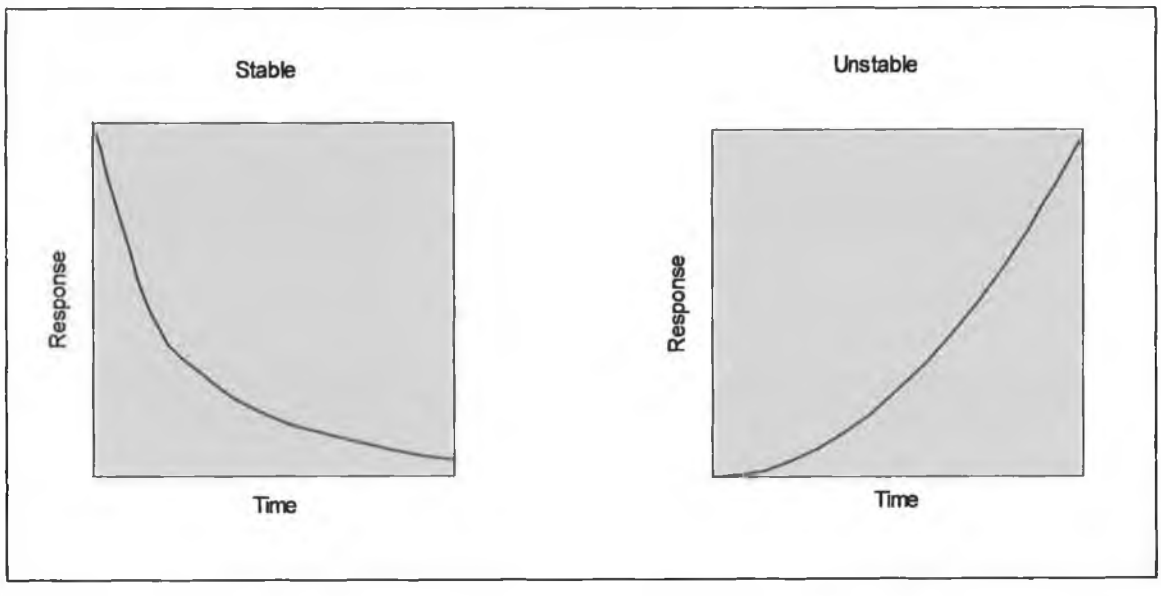

Figure VIII-5 Definition of a stable and unstable system

C-Condition of a stable system

To be stable, the poles (values for which the denominator of the transfer function are equal to zero) have to be located of the left-hand of the s-plane i.e. the real parts of the roots of the denominator must be negative.

On the following figures (VIII-6 to VIII-9), different configurations of response according to the location of the poles on the s-plane are shown:

Note: -Re: horizontal axis (real part)

-Im: vertical axis (imaginary part)

Overdamped:

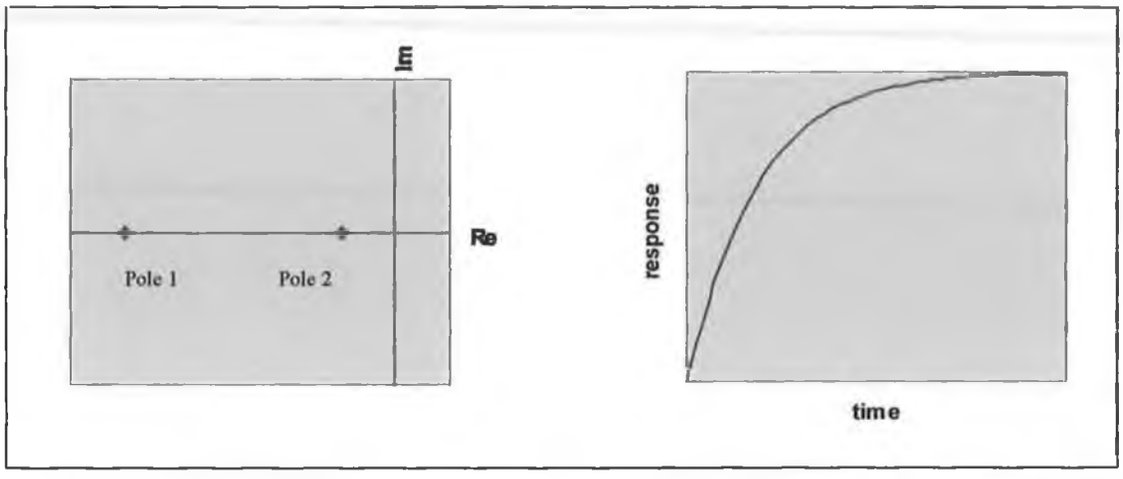

Figure VIII-6

Critically damped:

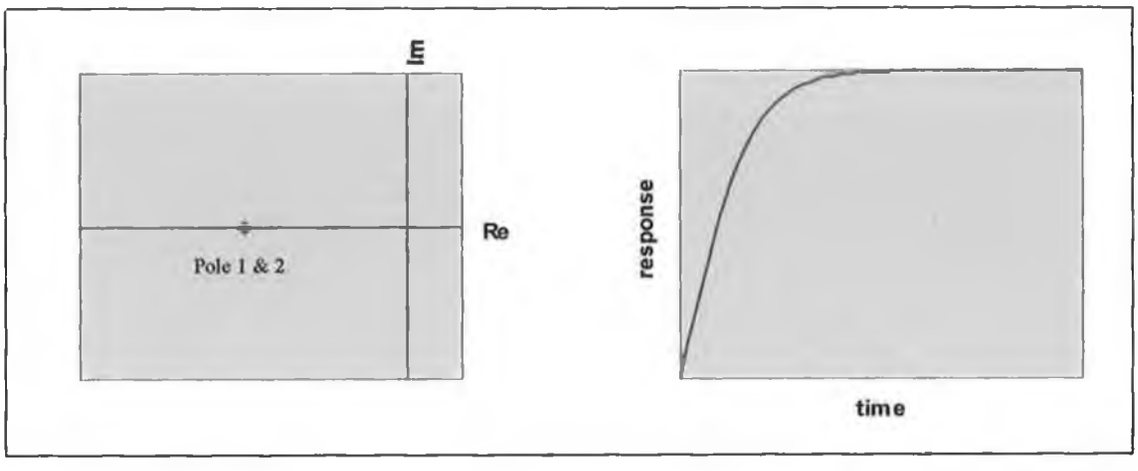

Figure VIII-7

Undamped:

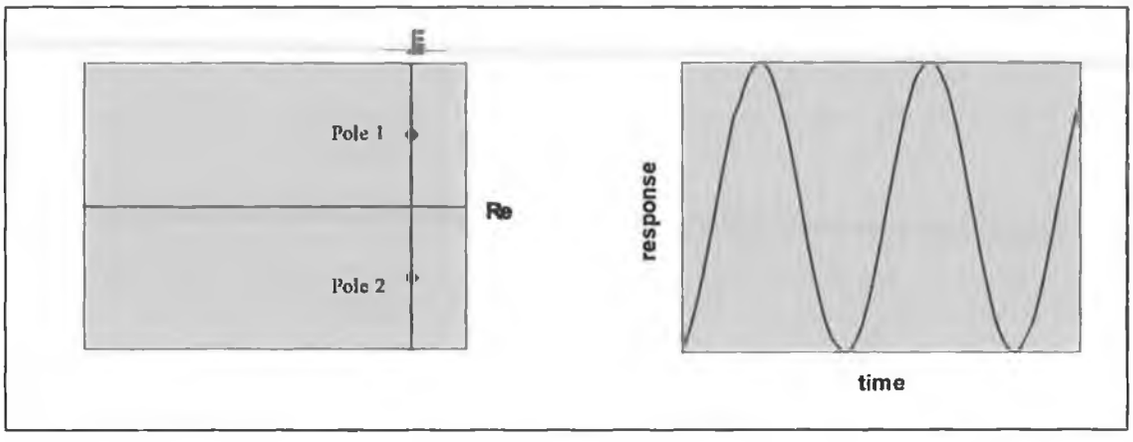

Figure VIII-8

Underdamped:

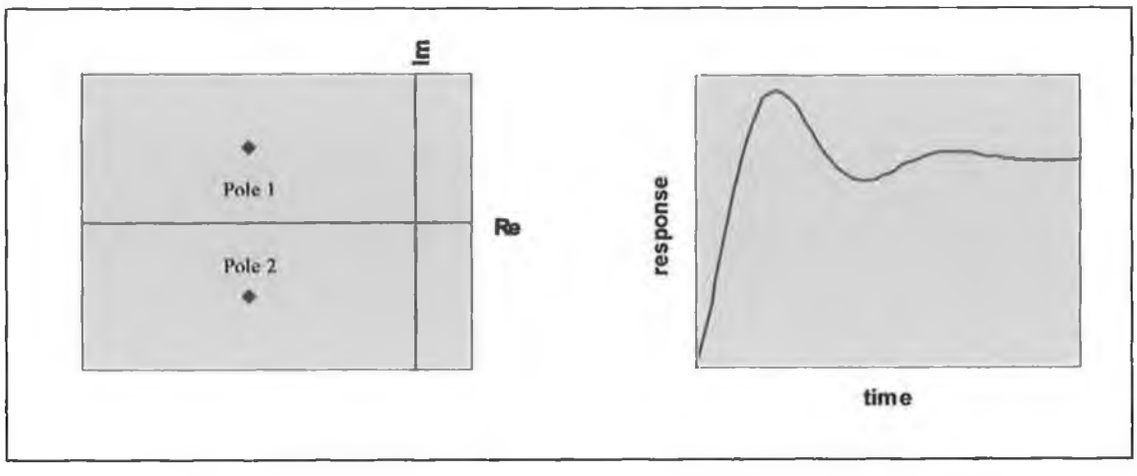

Figure VIII-9

The previous graphs indicate that to get a fast response from the motor, the undamped configuration must be avoided since it is not stable (the real part of the poles are equal to 0 and not negative).

The most appropriate configuration is the "idealised" critically damped system. However such a "theoretical" system is unlikely to occur. Thus an underdamped or overdamped system having a quick settling time is the most suitable.

Note: The imaginary values represent the damped frequency.

D-Determination of the system stability

The aim of this paragraph is to demonstrate the stability of the system shown in figure VIII-10. If the poles of this overall block diagram are negative, the stability will be proven.

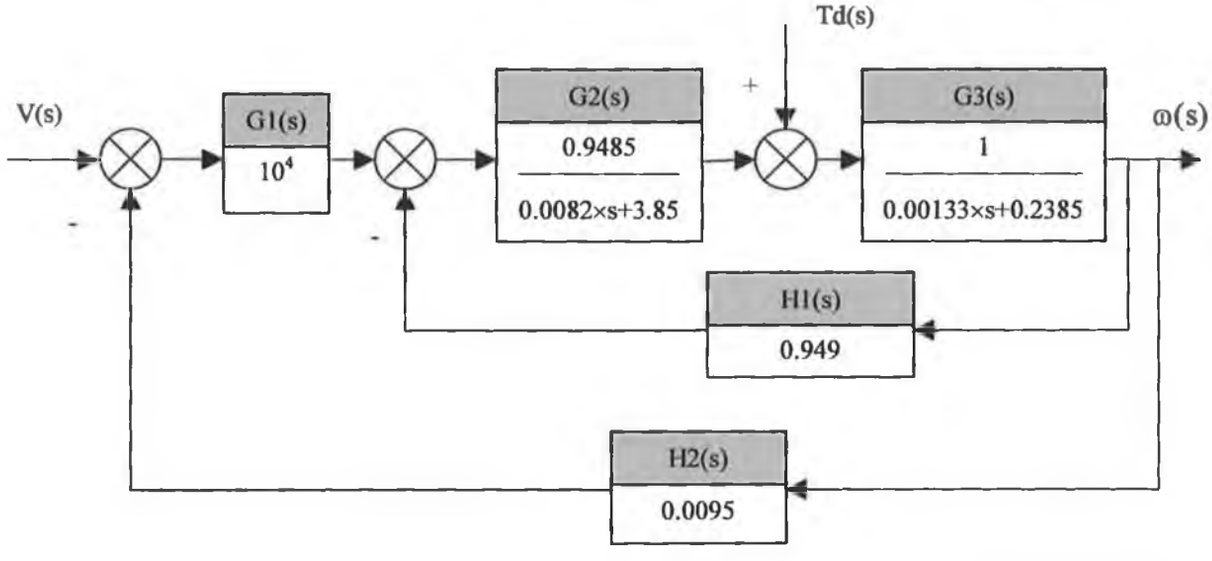

Figure VIII-10

Where: G1(s) represents the amplifier
G2(s) represents the motor
G3(s) represents the load (Inertia and friction)
H1(s) represents the back EMF constant
H2(s) represents the tachometer conversion

Because there are two inputs: the input voltage V(s) and the torque disturbance Td(s), two stability tests must be achieved [54]:

$$1:\ \frac{\omega(s)}{V(s)} \text{ assuming } Td(s)=0 \qquad \text{Eqn. VIII-3}$$

$$2:\ \frac{\omega(s)}{Td(s)} \text{ assuming } V(s)=0$$

If both calculations lead to a stable system, then the overall system is stable.

1: $\frac{\omega(s)}{V(s)}$, Note that for simplicity letters will be used instead of numbers.

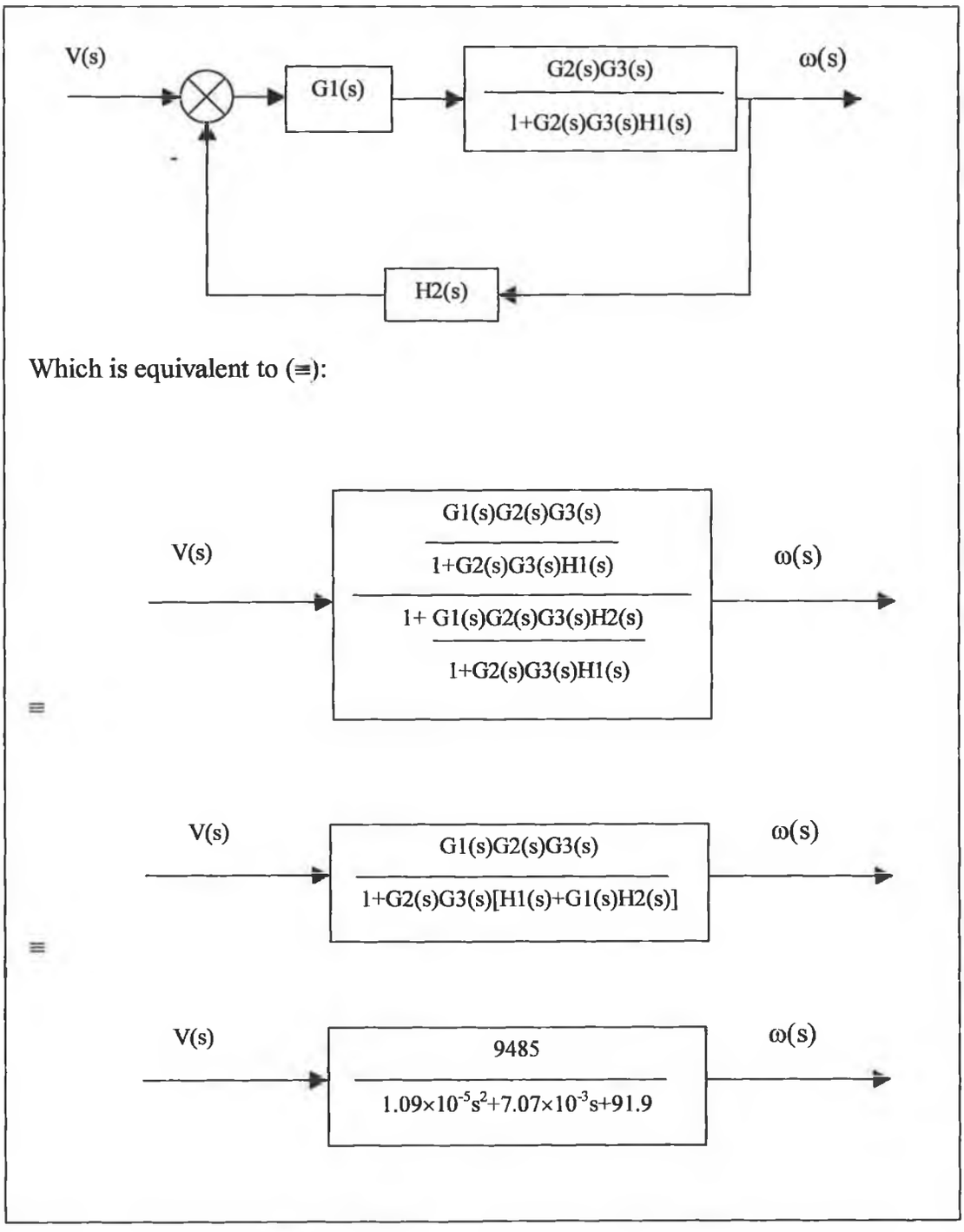

Figure VIII-11 First stability determination

The denominator is a second order polynomial equation, it can be easily solved. The roots of this equation are: s_1=-324.3+2885.48i

s_2=-324.3-2885.48i

So from the first test, the system is stable since the real parts are negative (-324.3).

2: $\frac{\omega(s)}{Td(s)}$

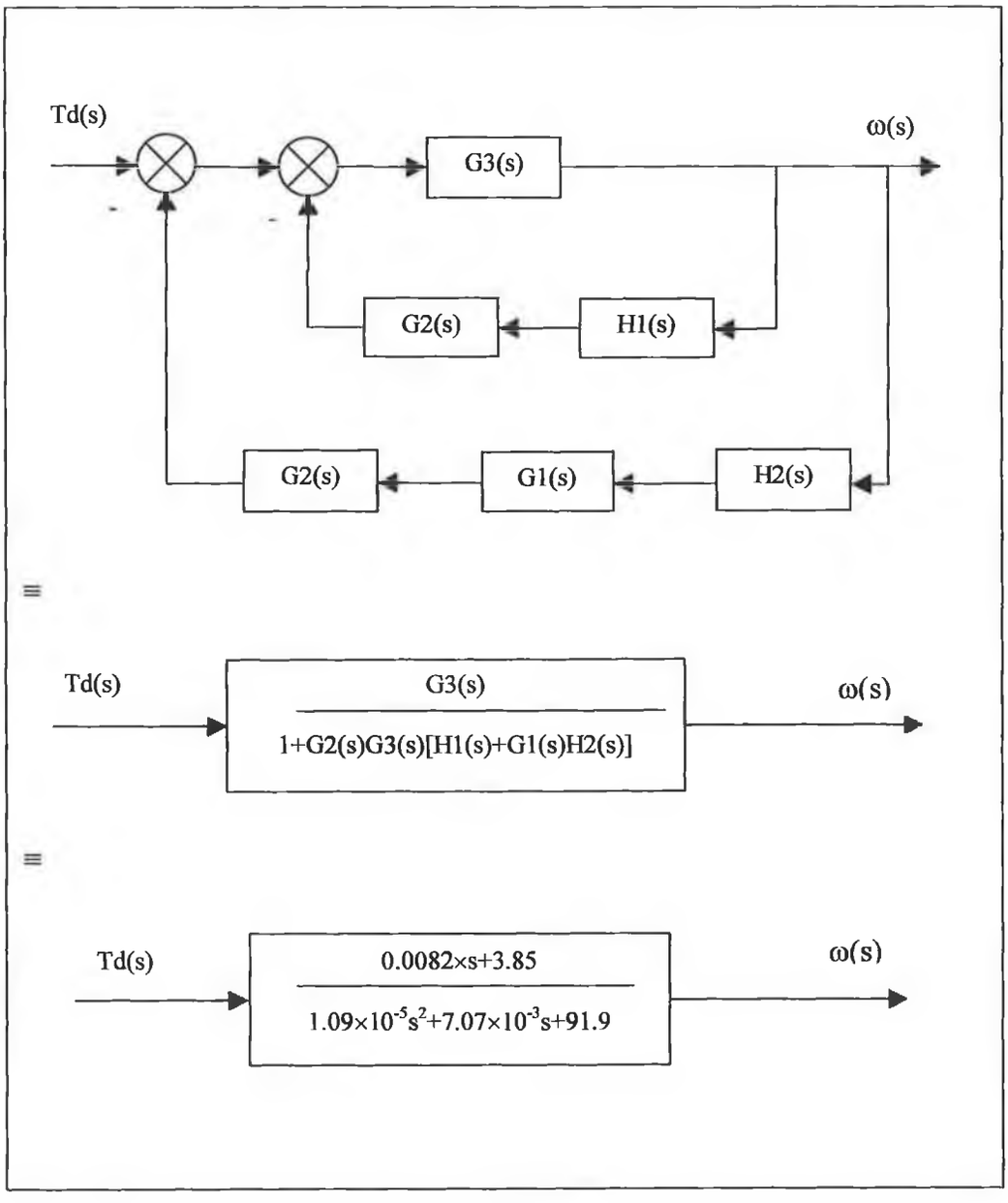

Figure VIII-12 Second stability determination

As excepted [54], the same denominator is found. Hence the roots are:

$$s_1=-324.3+2885.48i$$

$$s_2=-324.3-2885.48i$$

The second test is also stable. Therefore, because both tests are stable, the overall system is stable assuming no saturation (hence no non-linear equation).

Graph on the s-plane (figure VIII-13):

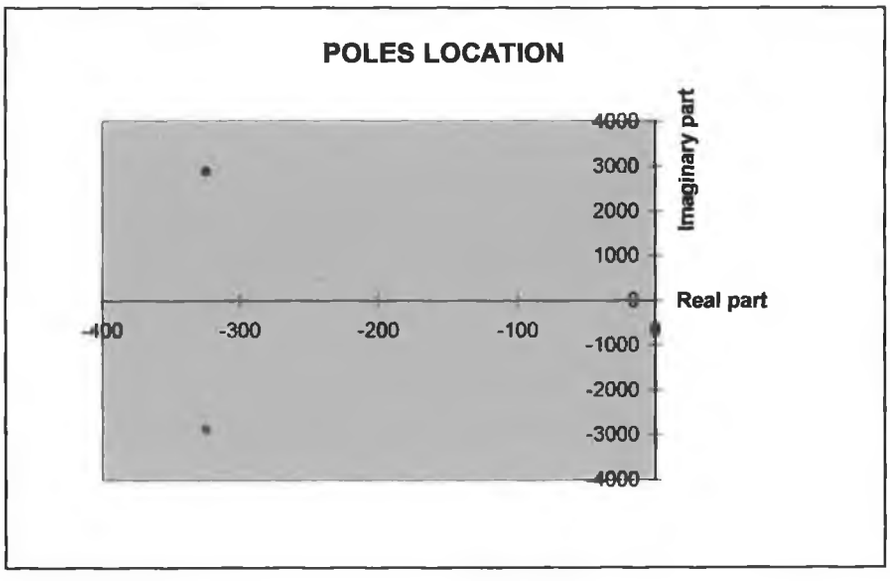

Figure VIII-13

E-Conclusion

Finally because the poles are negative, the system is stable. However, the saturation of the amplifier was not taken into consideration. Thus, a test (using Simulink) will be carried out to simulate the actual stability of the motor. The determination of the time response and the percentage overshoot will also be achieved to ensure a fast response of the system at any depths.

8-SIMULATION

Because the overall system is complex, it is subdivided into four different block diagrams: the motor, the "motor + amplifier + tachometer", the "direction of rotation of the motor" and the overall one. A more explicit graph is shown in figure VIII-14. From figure VIII-10, the block diagrams are shown crescendo.

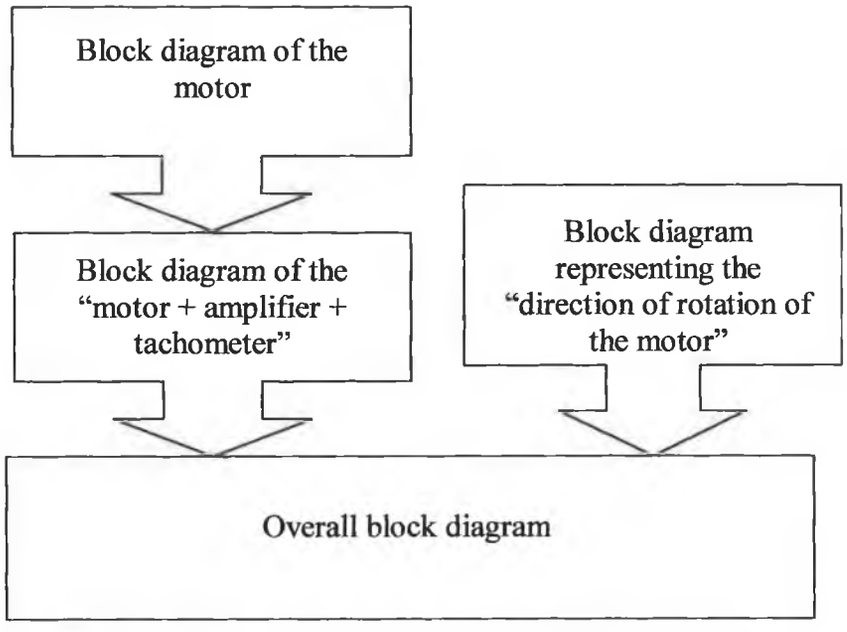

Figure VIII-14

Several inputs/outputs from a block diagram match the outputs/inputs of the following block diagram. To be more understandable, a key is given below:

1	Pressure 1
2	Pressure 2
3	Direction of rotation of the motor
4	Input voltage
5	Armature voltage
6	Motor velocity
7	External torque

Figure VIII-15 represents the motor block diagram and its characteristics [55]. While Figure VIII-16 represents the block diagram of the "Motor + Amplifier +Tachometer", the saturation block being included.

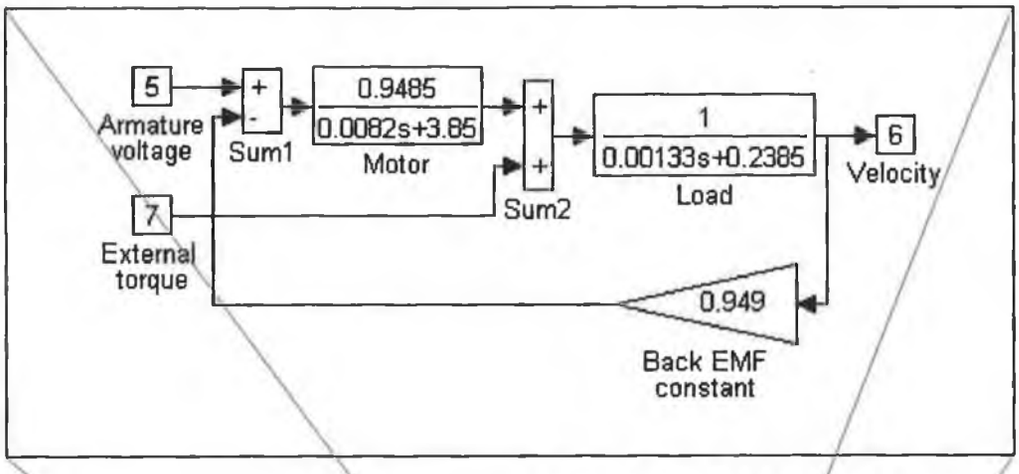

Figure VIII-15 Motor block diagram

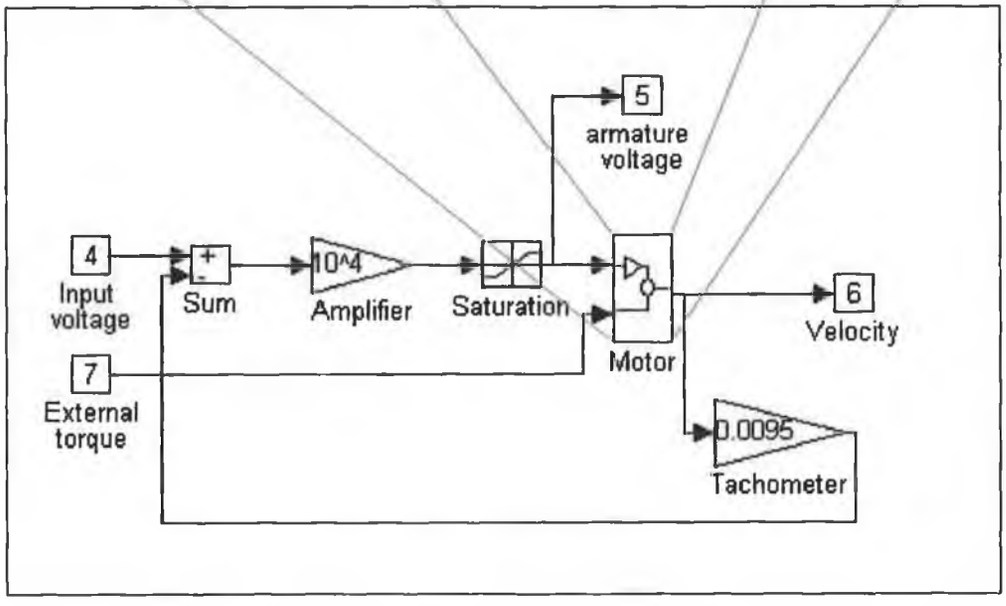

Figure VIII-16 "Motor + Amplifier + Tachometer" block diagram

Figure VIII-17 represents the "direction of rotation of the motor". This block diagram has been achieved using Boolean algebra. From the output 3, a signal carrying the information 1, 0 or –1 (depending on if the motor pumps, is at rest or releases water) comes out. This output signal is transformed and generates input 4 (input voltage) of figure VIII-16. This is realised via the switch 1 of figure VIII-18.

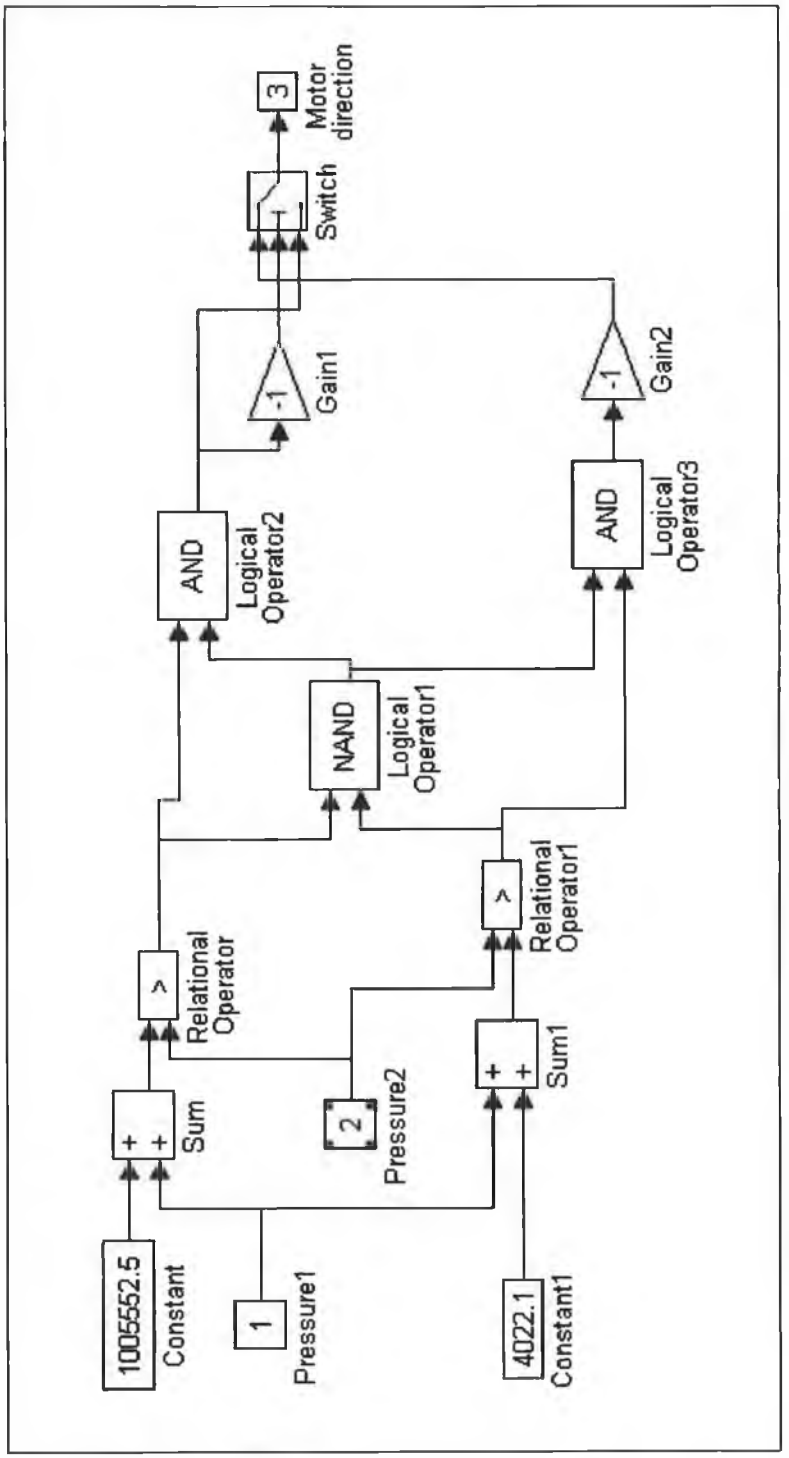

Figure VIII-17 Direction of rotation of the motor

Figure VIII-18 represents the overall control system, including the three previous block diagrams, where 0.05 kg is pumped or released if necessary. If this motor is at rest because the profiler velocity is in the predefined range, another measurement is executed 10 seconds later and so on until the profiler velocity goes out of the range or the desired depth has been reached.

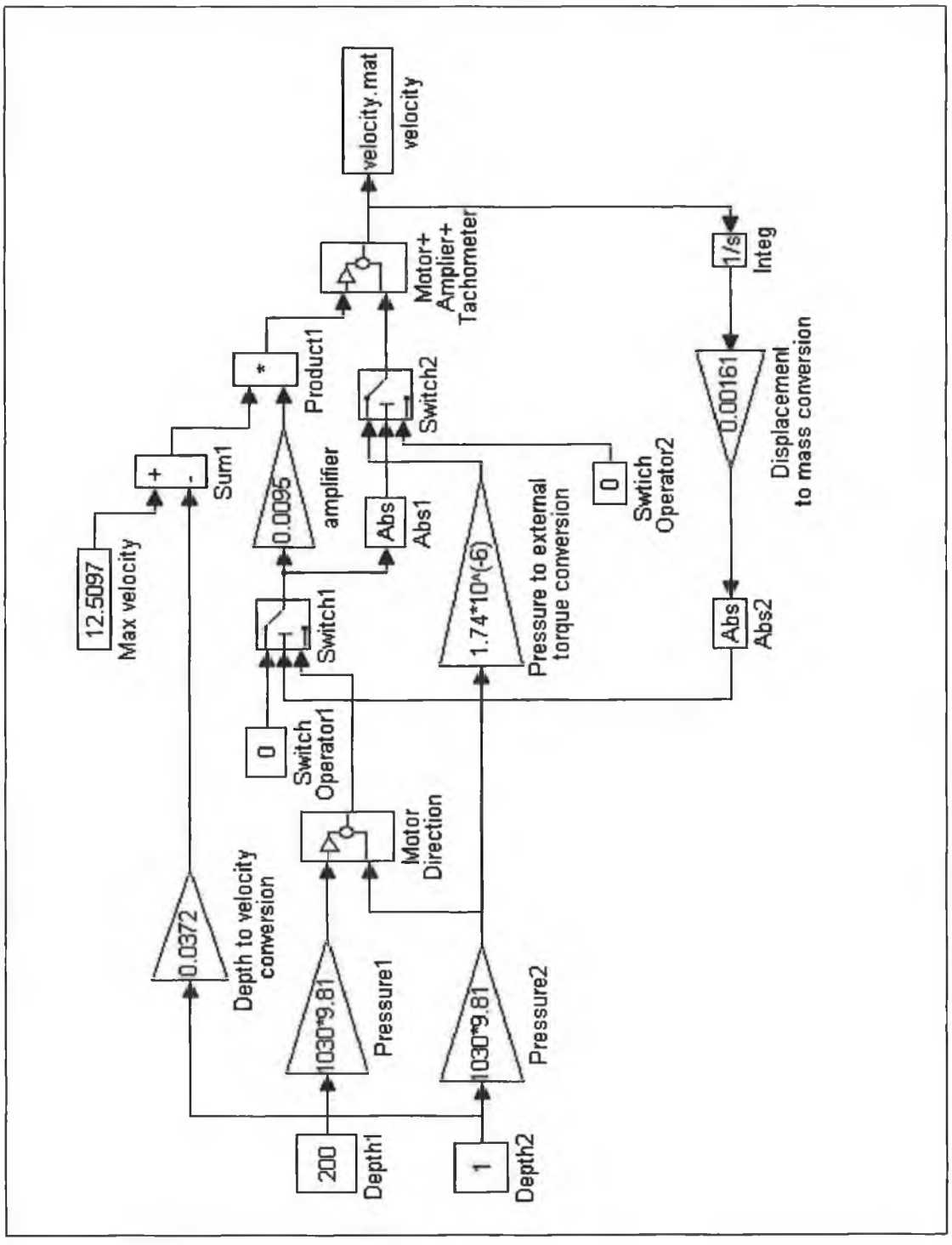

Figure VIII-18 Overall block diagram

Stability:

As can be seen in the different appendixes and in figure VIII-19 (A to C), at any depth the velocity always converges after a certain amount of time.

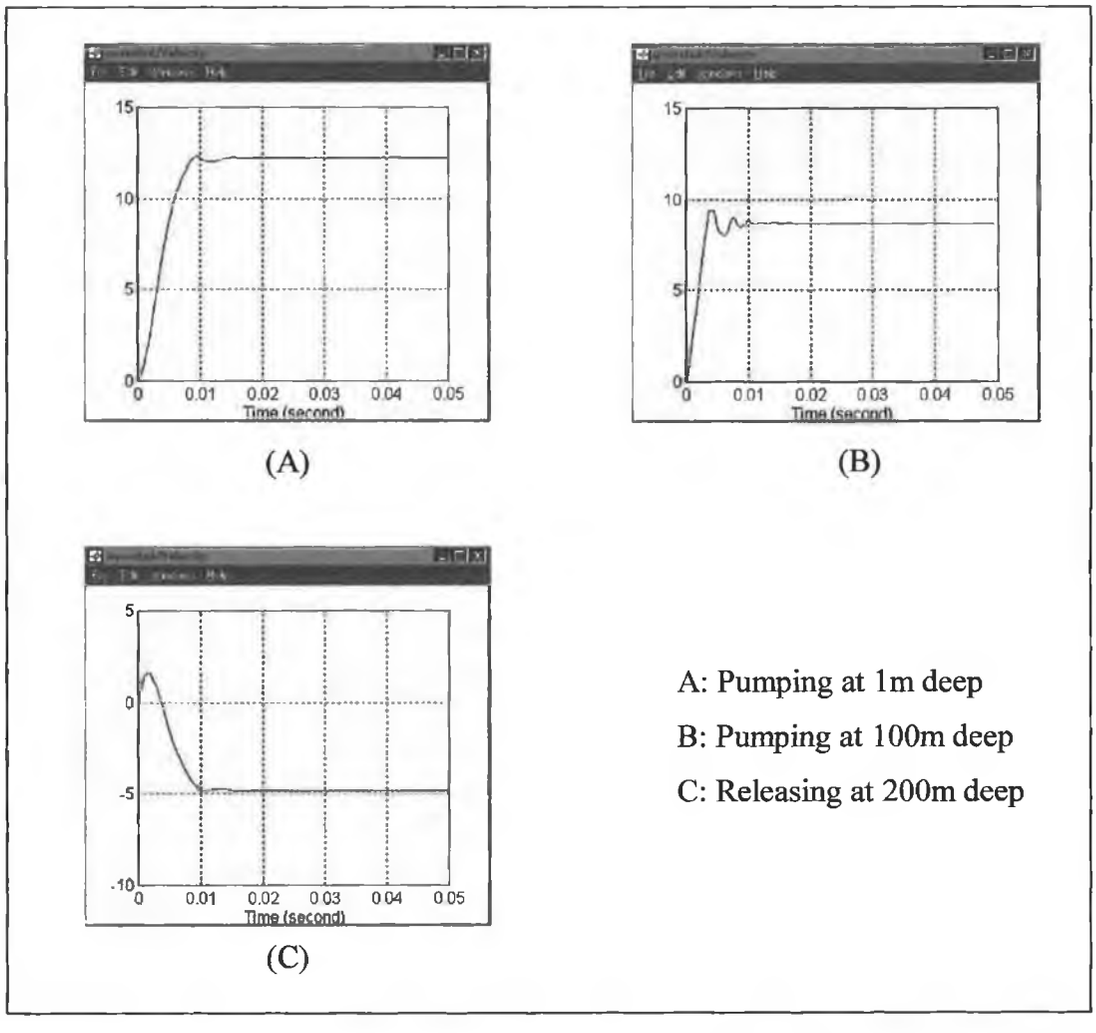

Figure VIII-19 Motor stability

Many more tests have been achieved and in every case the output velocity converges after a certain amount of time. So even if the stability using a saturation block could not be proven theoretically, the different simulations show that the motor is stable.

Settling time and percentage overshoot [56]:

Settling time: It is the time required for the system to settle within 2% of the input amplitude. From simulations, the settling times at: 1m deep (pumping), 100m deep (pumping), 200m (releasing) and finally 100m deep (releasing) will be achieved.

Percentage overshoot: The amount that the waveform overshoots the steady state, or final, value at the peak time, expressed as a percentage of the steady state value.

The results are summarised in table VIII-1. For more information, refer to appendix D.

Depth / Results	Pump at 1m	Pump at 100m	Release at 200m	Release at 100m
Settling time(s)	0.0086	0.0091	0.0144	0.0098
Final velocity ($rad.s^{-1}$)	12.2268	8.6898	4.8224	8.5425
Maximum velocity($rad.s^{-1}$)	12.3378	9.3695	4.893	8.6095
Percentage overshoot(%)	0.91%	7.82%	1.46%	0.784%

Table VIII-1

Note that the maximum overshoot occurs when water is pumped at high depth.

9-CONCLUSION

The chosen way of controlling the motor seems to be the best. Indeed, a large range of velocities (from $0.04 m.s^{-1}$ to ∞) will obviously reduce the power required. Moreover it is more accurate to control the motor via two consecutive pressure data than using an approximated equation.

It can also be stated that the motor response is very fast and the maximum overshoot is low. As a comparison, a long time response would be annoying for accurate measurement of the thermocline. However, a long transient response could be improved and the steady-state error reduced by implementing a proportional + derivative + integrator controller (PID) which would unfortunately increase both the complexity and the cost of the system.

It is also very important to reduce as much as possible the error due to the feedback (being later the armature voltage). Indeed a large error would lead to an inaccurate output velocity which, leads to a higher energy consumption.

Concerning the stability, even if it could not be proven theoretically because of the non-linear term, which simulates the amplifier saturation (i.e. ±24 Volts), all the simulations achieved lead to a bounded response. This tends to prove that the motor is stable in any circumstance.

Hence the motor can be controlled without any problem.

CHAPTER IX:
STABILITY OF THE SUBMERGED AND FLOATING PROFILER

1-INTRODUCTION

This chapter deals with the study of the final parameter. It is essential to know if the profiler is stable even if strong seawater currents occur. The study of the stability can only be accomplished at the end of this thesis since all the components (ball screw, motor, etc) had to be chosen first in order to know their volume and weight (i.e. their centre of gravity).

Both centres of buoyancy and gravity of the profiler must be determined. Comparing them will enable to justify if the profiler is stable or not. Obviously it is primordial for the profiler to be stable. Indeed an unstable device would capsize and would lead to the impossibility of working properly.

2-STABILITY

To be stable in any circumstance, the centre of buoyancy, which is the centre of mass of the displaced water, must be above the centre of mass of the body (centre of gravity) [11]. The centre of buoyancy changes depending on if the profiler is either floating or fully immersed. When immersed (figure IX-1), the centre of buoyancy (O) is the centre of the profiler due to its symmetrical shape (axial and planar).

However, when the profiler is floating at the sea surface, its centre of buoyancy (O) goes down to (G) as shown in figure IX-2. In fact this happens because the immersed volume has decreased.

Firstly, the centre of buoyancy when fully immersed (O) will be calculated. Secondly its location will be determined when the profiler floats (G). The lower of these two locations will be compared with the centre of gravity of the profiler.

The determination of the centre of gravity (evaluated with SolidWorks) is achieved excluding the mass of both the batteries (location not known) and the electronic components (not known). However, these elements, having an influence on the centre of gravity location, must be installed at a judicious place inside the profiler.

Centre of buoyancy when fully immersed:

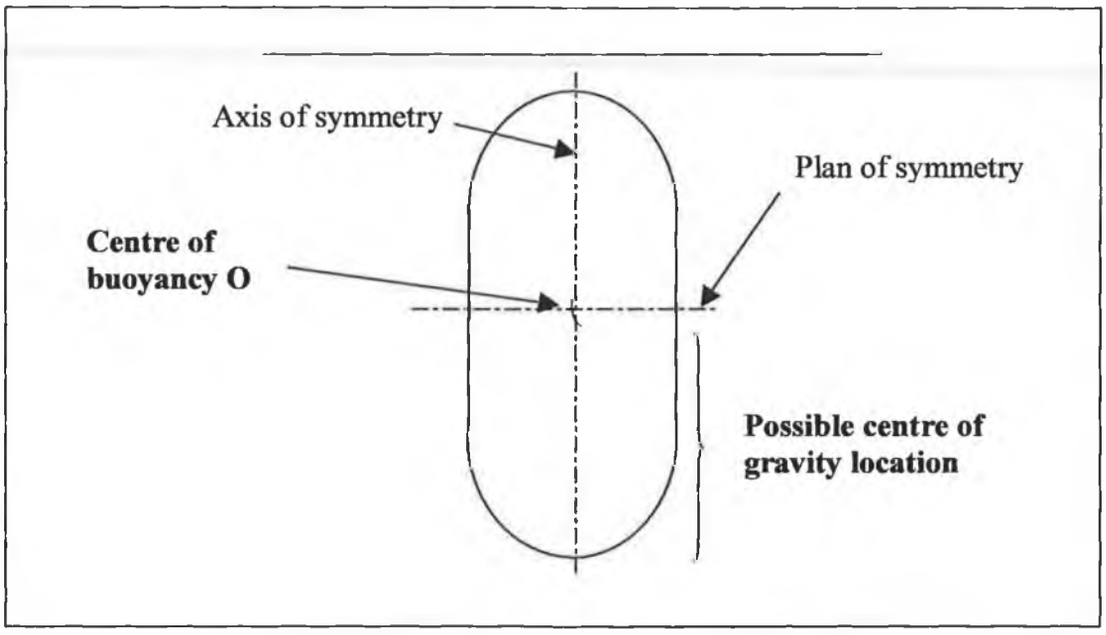

Figure IX-1

Centre of buoyancy when floating:

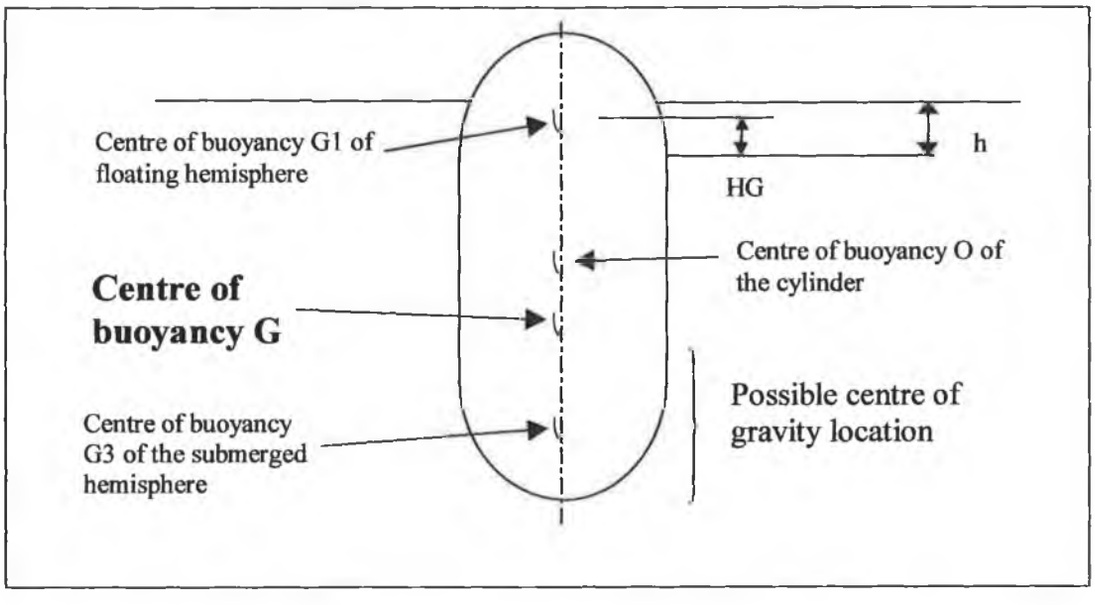

Figure IX-2

Using Mathematica, as shown below, the determination of the centre of buoyancy (when floating) is achieved.

```
Clear[r, l, ρ, mass,
 buoyancy, h, HG, mass1, mass2, mass3, OG1, OG2, OG3, OG]
r = 0.175;
l = 0.8;
ρ = 1030;
mass = 100.0;
buoyancy = (2/3 × π × r^2 × h + π × r^2 × l + 2/3 × π × r^3) × ρ;
DETERMINATION OF h;
h = h /. First[Solve[buoyancy - mass == 0, h]]
DETERMINATION OF THE CENTRE OF BUOYANCY OF THE SPHERICAL ZONE HG;
HG = (∫_0^h y × (r^2 - y^2) dy) / (∫_0^h (r^2 - y^2) dy)

mass1 = (2/3 × π × r^2 × h) × ρ;
mass2 = (π × r^2 × l) × ρ;
mass3 = (2/3 × π × r^3) × ρ;
OG1 = 1/2 + HG;
OG2 = 0;
OG3 = -(1/2 + 3/8 × r);
DETERMINATION OF THE DISTANCE OF THE TOTAL CENTRE OF BUOYANCY BELOW G;
OG = (mass1 × OG1 + mass2 × OG2 + mass3 × OG3) / (mass1 + mass2 + mass3)
```

```
0.150768
```

```
0.0629929
```

```
-0.00765497
```

To be stable in any circumstance, the centre of gravity of the profiler must be at least 7.65 millimetres below the point (O). The design of the profiler, having a centre of gravity below this point (G), must be achieved. This means that most of the mass of the profiler must be located in the lower profiler half.

Having the full design (excluding the batteries and the electronic components), the centre of gravity can be evaluated (figure IX-3).

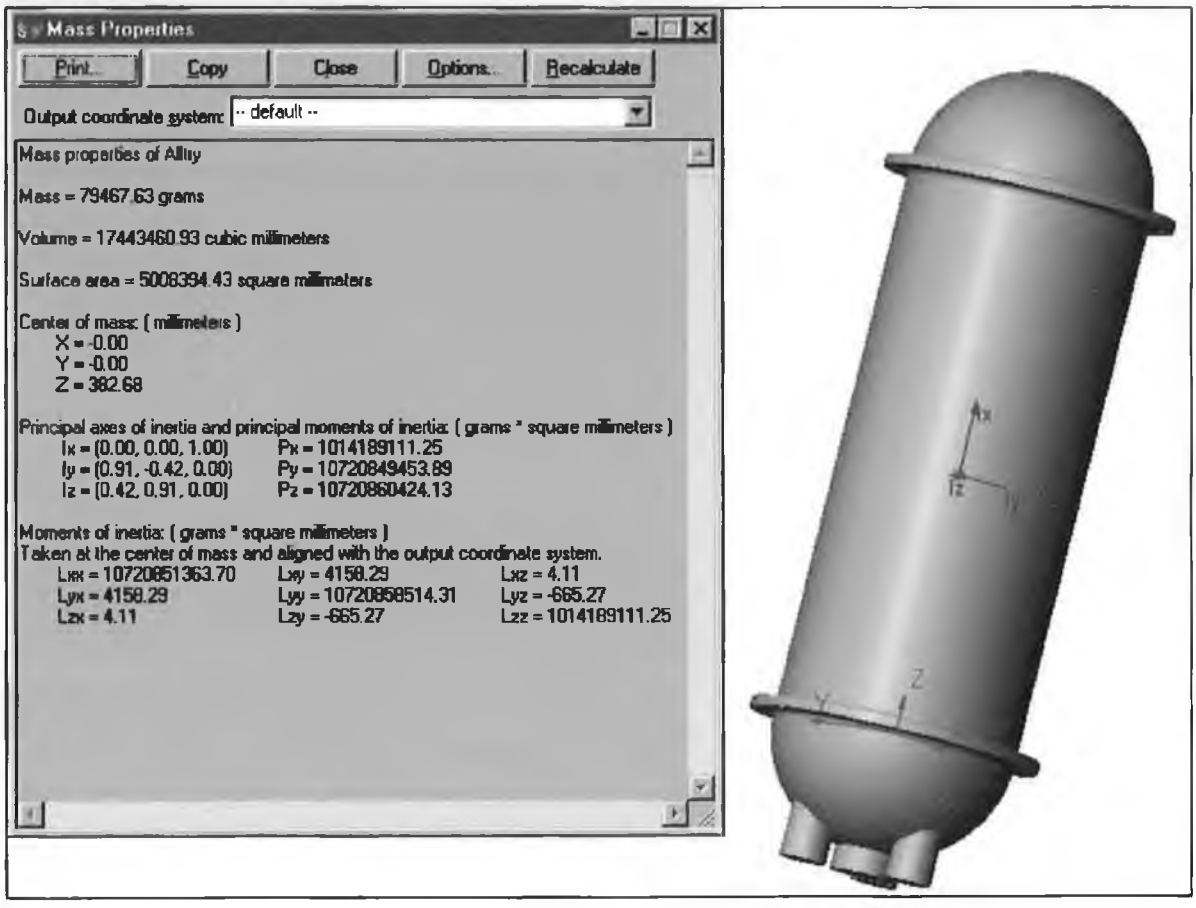

Figure IX-3 Evaluation of the centre of gravity

Key: □: Centre of gravity location

□: Origin

Bold numbers: refer to figure IX-3

The overall centre of gravity is 17.32mm (400-**382.68**) below the point (O). However, the battery (11.35kg) and all the electronics components (relatively light) must be added and other weight if necessary to reach 100.8kg (refer to chapter IV).
Therefore, from the 21.33 kg to add (100.8-**79.467**), the components should be located as low as possible in order to avoid the centre of gravity to rise.

In this case, the profiler will be stable in any circumstance, ensuring no risk for it to capsize.

Figure IX-4 summarises the different centres of buoyancy location and also the location of the centre of gravity:

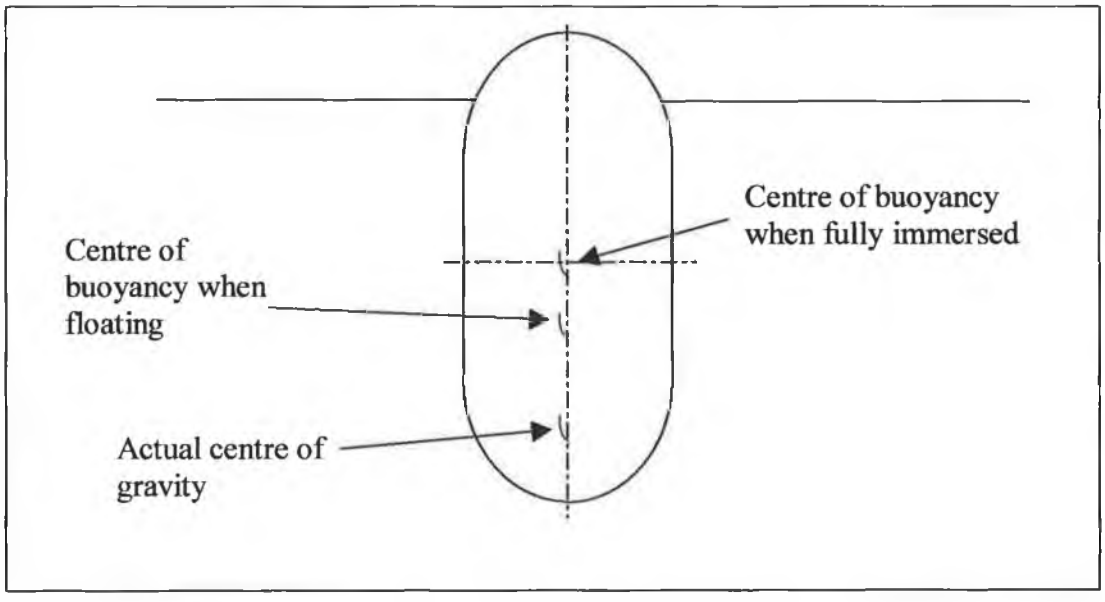

Figure IX-4

3-CONCLUSION

In order to have a stable profiler, its centre of gravity must be below the centre of buoyancy when floating (G). It is also of particular interest to design a profiler having its centre of gravity as close as possible to the bottom hemispheric surface. Indeed the lower (large distance between the centre of buoyancy and the centre of gravity) the centre of gravity is, the shorter the settling time of the profiler (when oscillating) is. Moreover there will be absolutely no risk that the profiler capsizes.

Therefore no problem will be encountered about the stability as far as the batteries and the electronics components are located below (G) in the lower half part of the profiler. If the electronics components (generally very light) are lighter than 9.98kg (21.33kg-11.35kg), additional weight must be added in order to reach 100.8kg. Once again this weight must be located in the lower half of the profiler.

Note that in some cases like boats, the centre of gravity is above the centre of buoyancy. In this case, the metacentric height must be calculated.

CHAPTER X:
OVERALL CONCLUSION

This project gave me the opportunity to learn about oceanography and to implement several engineering fields such as design methodology, mathematics, stress analysis, control system and software packages.

Different conclusions can be drawn from the present thesis:

First of all, emphasis has been laid on the complexity to model mathematically the dynamics of the profiler. Solving the dynamics equation was only possible by making assumptions such as no surface waves and constant water currents. Obviously, only real conditions could give accurate results. However these tests would be very expensive and due to the unpredictability of the sea, no generalisation could be made. The current magnitude in both vertical and horizontal directions has been simplified in order to solve the dynamics equation of the profiler. Furthermore during one cycle, the profiler will not horizontally drift beyond a "virtual cylinder" of 1.8 kilometres ($0.25 m.s^{-1} \times 2 \times 60 \times 60 s$) radius. This is acceptable and very localised compared to the vastness of the oceans.

Secondly, it has been demonstrated that a pump capacity of 2.1kg of water is sufficient for the profiler to dive and resurface at a velocity of $0.05 m.s^{-1}$. This was achieved in chapter IV using the simplified second order differential equation. However, considering all the simplifications, another kilogram of water is recommended to be added to the overall pump capacity.

Thirdly, a reciprocating pump (made of three pistons) has been chosen to pump and discharge water. According to this design, the selection of the motor was driven by two important parameters:

- Since the energy required is large, efficient devices must be used. Unfortunately, this also leads to an increase in price. A differential pump (made of washers or springs) was interesting in order to reduce the energy required. However in our case, it can not be achieved because it would be too cumbersome.

- The torque is deeply responsible for the choice of the motor. Only few DC motors are able to overcome the torque occurring at 200m deep. A reduction of the piston diameter would decrease the torque. Unfortunately, this would lead to an increase of the piston length, hence an increase of the profiler volume (in order to keep the capacity of 3.1kg of water). This would also lead to an increase of the pumping or discharging time, hence a slower motor response. Therefore a good compromise had to be found between the radius, the length and the number of pistons.

Next, the hydrodynamics and the mechanical strength of the external shape had to be studied. A cylindrical shape having two hemispheric ends is the most appropriate shape. Indeed the hemispheric ends allow a low drag coefficient, hence a low drag force acting on the profiler. Concerning the mechanical strength, only spherical and cylindrical shapes are able to withstand high pressure. Indeed, as seen in chapter VII, the optimised "shamrock" shape (with a reduced volume) having flat sides could not be chosen due to unacceptable large deflections.

All these chapters were studied in parallel. Indeed one parameter change was influencing some others. For example, a modification of the external shape would modify the dynamics of the profiler and also the quantity of water required. However, the dynamics of the profiler has been done first in order to determine theoretically the quantity of water required. Therefore the whole pump design could follow.

Among the several possible materials, the composite material fibreglass + epoxy is certainly the best material and the most used over the last decade. Indeed it offers good mechanical strength (to withstand high pressure), a low density (to have a light profiler) and is fully corrosion resistant. As a comparison, steel would be too heavy; aluminium would be too expensive due to the manufacturing of the lower part, middle part and upper part (refer to appendix E).

Concerning the control design of the profiler velocity, the pressure difference method is much more appropriate for our application. Indeed no approximated formulae are

used since sensors evaluate the actual pressure, which leads to a more accurate output profiler velocity. It has also been seen that the motor has a fast response; the settling time is reached after 0.014 seconds for the slowest configuration. It is necessary for the settling time to be short in order to get an accurate and efficient output profiler velocity. Finally, the theoretical determination of the stability could not be proven due to the non-linear term (amplifier saturation). However, simulating the motor response (using Simulink) has shown that the system is stable. This proves that the whole system will work efficiently.

The first time that the profiler is launched into the sea, an external switch might be necessary in order to turn on the pump system before it operates on its own. Even if this has not been studied throughout the present thesis, it is very easy to achieve by drilling a hole in the external shape and inserting a switch.

The profiler might seem expensive. Indeed, including the cost of the three motors, the three ball screws, the batteries and the cost of manufacturing, the price of the profiler is about £15000. However this is mainly due to the cost of the motors. Indeed these motors are rare and use the best magnetic material in order to get high performances. Moreover these motors are able to work in conditions where most of the motors would fail. As a comparison to the motor price (£3500 each), a stepper motor having the same working characteristics would cost £5622 (from API Motion company).
Finally, even if the overall cost (£15000) is high, it seems relatively low compared with a ship charter cost (up to £50,000 per day).

Finally, throughout this thesis, it has been demonstrated that a profiler having a $0.05 m.s^{-1}$ velocity is able to work efficiently and able to achieve two hundred cycles. However, if deeper or more cycles are required, another source of energy must be used. Indeed, even if the alkaline battery is efficient, it would become too cumbersome since more energy would be required. Going down to about 500m would be possible. However it seems very difficult to probe deeper using this design since it might be impossible to find an appropriate motor.

BIBLIOGRAPHY:

[1] OPEN UNIVERSITY COURSE TEAM, 1995, *Ocean Circulation*, Pergamon press.

[2] POND S. & PICKARD G.L, 1983, *Introductory Dynamical Oceanography*, 2nd edition, Butterworth-Heinemann.

[3] MICHAEL J.KENNISH Ph.D., *Practical handbook of marine science*, 2nd edition, CRC Press

[4] Federov K. N., 1978, *The thermohaline fine structure of the ocean*. Pergamon, Oxford,

[5] CAROL M LALLI & TIMOTHY PARSONS, 1997, *Biological Oceanography: An Introduction*, 2nd edition, Butterworth-Heinemann Publishers

[6] WELLER ROBERT A. & PRICE JAMES F., *Langmuir Circulation Within The Oceanic Mixed Layer*, Deep-Sea Res., 35, 711-747, 1988.

[7] *Thermocline Graph*, Florida International University
http://www.coexploration.org/bermuda/html/thermocline_graph.html

[8] SUMMERHAYES C.P. & THORPE S.A, 1996, *Oceanography An illustrated Guide*, Manson publishing.

[9] *S-PALACE Instrument Description*, Woods Hole Oceanographic Institution
http://hrp.whoi.edu/floats/inst1.html

[10] CENGEL YUNUS A. & BOLES MICHAEL A., 1989, *Thermodynamics An Engineering Approach*, McGraw-Hill

[11] B.R. CLAYTON & R.E.D. BISHOP, 1982, *Mechanics of Marine Vehicle*, E. & F.N. Spon Ltd,

[12] M Grant Gross, *Oceanography*, 7th edition, Maxwell Mac Millan internationnal publishing , 1990

[13] BARRETT LOUIS C.& WYLIE C. RAY, 1995, *Advanced Engineering Mathematics*, 6th edition, McGraw-Hill

[14] GLYN JAMES, 1996, *Modern Engineering Mathematics*, 2nd edition, Addison-Wesley

[15] GRACZYK T., JASTRZEBSKI T. & BREBBIA C.A., 1995, *Marine technology and transportation*, Computational mechanics publications.

[16] DOUGLAS J.F, GASIOREK J.M & SWAFFIELD J.A, 1995, *Fluid mechanics*, 3rd edition, Addison Wesley Longman limited.

[17] JAMES WALDIE, "The Propulsion System for an Autonomous Underwater Vehicle Mission to Europa", *The Existence and Physical Properties of the European Ocean,* RMIT University, Melbourne, Australia
http://home.vicnet.net.au/~nbrotar/Europam.htm#Cur

[18] MASSEY B.S., 1989, *Mechanics of fluids*, 6th edition, Chapman & hall.

[19] JOHN J. BERTIN & MICHAEL L., 1989, *Aerodynamics for engineers*, 2nd edition, Prentice-Hall International

[20] W.R. DERRICK & S.I. GROSSMAN,1987, *Introduction to differential equations with boundary value problems*, 3rd edition, West publishing company,

[21] STEPHEN WOLFRAM, *The Mathematica Book*, 3rd edition, Mathematica Version 3, Cambridge University Press

[22] STEINMEYER CATALOGUE, 1996, *Power transmission Ball screws.*

[23] THOMSON SAGINAW CATALOGUE, 1996, *Advanced linear actuator guide.*

[24] JACK HOWELL & RICHARD BUCKIUS, 1992, *Fundamentals of engineering thermodynamics*, McGraw-Hill,

[25] J.E. SHIGLEY & C.R. MISHKE, 1996, *Standard handbook of machine design*, 2nd edition, Mc Graw-Hill,

[26] *New ultra-hard, low-friction coating is slicker than Teflon*, ARGONNE, Ill. (Oct. 3, 1997) Argonne National Laboratory, University of Chicago

[27] Plas-Tech Coatings, Inc, DuPont Teflon® industrial coatings
http://www.plastechcoatings.com/teflon.htm

[28] KOLLMORGEN CATALOGUE, 1996, *Direct Drive DC motors.*

[29] MULUKUTLA S. SARNA, 1985, *ELECTRIC MACHINES Steady-state theory and dynamic performance,* international edition, West publishing company.

[30] ROSENBLATT J. & FRIEDMAN H., 1984, *Direct and Alternating current Machinery,* 2nd edition, Bell & Howell Company.

[31] SAY M.G., 1973, *Electrical Engineer's Reference book*, 13th edition, Butterworths.

[32] CROMPTON T.R, 1982, *Small batteries secondary cells volume 1*, The MacMillan press Ltd.

[33] CROMPTON T.R, 1982, *Small batteries primary cells volume 2*, The MacMillan press Ltd.

[34] ROBERT GIBSON, *Corrosion Resistance Using Polymers as an Alternative to Metals* - UNDERWATER MAGAZINE, p31-34, vol. 3, 1999

[35] PARRISH A., 1973, *Mechanical Engineer's Reference Book*, 11th edition, Butterworths

[36] SHREIR L.L, 1978, *Corrosion volume1 Metal/Environment Reactions*, 2nd edition, Newnes-Butterworths.

[37] UHLIG HERBERT H., 1971, *Corrosion and corrosion control*, 2nd edition, John Wiley & Sons Inc.

[38] BAUMEISTER AVALLONE BAUMEISTER, *Standard Handbook for Mechanical Engineers*, 8th edition, McGraw-Hill book company

[39] FONTANA MARS G./GREENE NORBERT D. , 1982 ,*Corrosion Engineering,* 2nd edition, Mc-Graw Hill Inc.

[40] O.C. ZIENKIEWICZ, & Y.K. CHEUNG, *The finite element method in structural and continuum Mechanics*, McGRAW-HILL Inc.

[41] *Ansys user manual, revision 5.0*, Swanson Analysis System, Inc.

[42] 1992,*A finite element Primer*, Nafems , Galsgow,

[43] SAEED MOAVENI, 1999, Finite Element Analysis: Theory and Application with ANSYS, Prentice Hall Press

[44] S.TIMOSHENKO & S. WOINOWSKY-KRIEGER, 1959, *Therory of plates and shells*, 2nd edition, McGraw-Hill Inc.

[45] BEER FERDINAND P. & JOHNSTON E. RUSSEL Jr, 1985, *Mechanics of Materials*, McGraw Hill book company

[46] BENHAM PP., CRAWFORD RJ. & ARMSTRONG CG., 1996, *Mechanics of Engineering Materials*, 2nd edition, Longman

[47] SMALLWOOD DAVID, BACHMAYER RALF AND WHITCOMB LOUIS, September 1999, *A New Remotely Operated Underwater Vehicle For Dynamics And Control Research*, Submitted for consideration to the 11th International Symposium on Unmanned Untethered Submersible Technology, Durham, NH. September 1999

[48] LOUIS L WHITCOMB, *Dynamics and Control of Underwater Robotic Vehicles*, G.W.C. Whiting School of Engineering, Johns Hopkins University, *http://robotics.me.jhu.edu/~www/*

[49] EHRIC LEONARD NAOMI, September 1995, *Compensating For Actuator Failures: Dynamics And Control Of Underactuated Underwater Vehicles.*

[50] CAMPA GIAMPIERO, SHARMA MANU, CALISE ANTHONY J. AND INNOCENTI MARIO, *Neural Network Augmenation Of Linear Controllers With Application To Underwater Vehicles.*

[51] KATSUHIKO OGATA, 1997, *Modern Control Engineering*, 3rd edition, Prentice Hall, International edition.

[52] DORF RICHARD C.& BISHOP ROBERT H., 1998, *Modern Control Systems*, 8th edition, Addison-Wesley.

[53] DONALD G. FINK & DONALD CHRISTIANSEN, Electronics Engineers' Handbook, 2nd edition, Mc Graw-Hill book company, 1982

[54] BOLTON W., 1992, *Control Engineering,* Longman Group UK.

[55] E.H. WERNINCK, 1978, *Electric motor handbook*, McGraw Hill

[56] NISE NORMAN S.,1995, *Control Systems Engineering*, 2nd edition, The Benjamin/Cummings Publishing company, Inc.

APPENDIX A:

INTERNATIONAL EQUATION OF STATE OF SEA-WATER

INTERNATIONAL EQUATION OF STATE OF SEA WATER, 1980:

Determination of the seawater density according to its salinity (S), temperature (T), and pressure p (in bars):

$$\rho(S,T,p) = \frac{\rho(S,T,0)}{\left(1-\left(\frac{p}{K(S,T,p)}\right)\right)}$$

Where:

$$\rho(S,T,0)= 999.842594 + 6.793952\times10^{-2}\times T - 9.095290\times10^{-3}\,T^2 + 1.001685\times10^{-4}T^3 - 1.120083\times10^{-6}\,T^4 + 6.536336\times10^{-9}\,T^5 + (8.24493\times10^{-1} - 4.0899\times10^{-3}T + 7.6438\times10^{-5}\,T^2 - 8.2467\times10^{-7}\,T^3 + 5.3875\times10^{-9}\,T^4)\times S + (-5.72466\times10^{-3} + 1.0227\times10^{-4}\,T - 1.6546\times10^{-6}\,T^2)S^{3/2} + 4.8314\times10^{-4}\,S^2$$

$$K(S,T,p)= 19652.21+148.4206\times T - 2.327105\times T^2 +1.360477\times10^{-2}\,T^3 - 5.155288\times10^{-5}\,T^4 + S\times(54.6746 - 0.603459\times T + 1.09987\times10^{-2}\,T^2 - 6.1670\times10^{-5}\,T^3) - S^{3/2}(7.944\times10^{-2} + 1.6483\times10^{-2}\,T - 5.3009\times10^{-4}\,T^2) + p\times[3.239908 + 1.43713\times10^{-3}\,T + 1.16082\times10^{-4}\,T^2 - 5.77905\times10^{-7}\,T^3 + S\times(2.2838\times10^{-3} - 1.0981\times10^{-5}\,T - 1.6078\times10^{-6}\,T^2) + S^{3/2}\,(1.91075\times10^{-4})] + p^2\times[8.50935\times10^{-5} - 6.12293\times10^{-6}\,T + 5.2787\times10^{-8}\,T^2 + S\times(-9.9348\times10^{-7} + 2.0816\times10^{-8}\,T + 9.1697\times10^{-10}\,T^2)]$$

APPENDIX B:

BALL SCREW VELOCITY AND TIME PER DUTY

In order to determine the ball screw velocity and its duration per duty (i.e. each important depth), three different parameters, which are the "displacement to mass conversion", "the pressure to torque conversion" and "the depth to velocity conversion", must be determined.

Displacement to mass conversion:

We wish to stop the simulation after pumping 1 or 1.1 kg of water (depending on the depth). The output of the motor is the velocity ω in rad.s^{-1}. Hence first of all ω must be integrated to get a displacement (say θ) in radians. Then multiplying θ by the lead screw and divide it by 2π gives the piston displacement in metres. Finally this value is multiplied by the piston area and by the water density to get the actual mass in kg:

$$\text{mass} = \left(\frac{\int \omega dt \times \text{lead}}{2 \times \pi} \right) \times \pi \times r^2 \times \rho_{\text{water}}$$

$$\text{mass} = \frac{\theta \times 0.004}{2 \times \pi} \times \pi \times 0.028^2 \times 1030$$

$$\text{mass} = 0.00161 \times \theta$$

Pressure to torque conversion:

The torque disturbance (N.m) must be taken into consideration since it has a great influence. As seen in chapter VI, the torque equation is:

$$\text{Torque} = \frac{\text{Force} \times \text{lead}}{2 \times \pi \times \eta} = \frac{(\text{Pressure} \times \text{piston area}) \times \text{lead}}{2 \times \pi \times \eta}$$

$$\text{Torque} = \frac{\text{Pressure} \times \pi \times 0.028^2 \times 0.004}{2 \times \pi \times 0.9}$$

$$\text{Torque} = 1.74 \times 10^{-6} \times \text{pressure}$$

Depth to velocity conversion:

Depending on the depth, the appropriate velocity must be selected. The easiest way to find the velocity ratio is to simulate the motor response when the torque disturbance is first at the sea surface and then at 200 meters deep. Assuming no torque disturbance at 1m deep, as shown next page, the maximum motor velocity is 12.51rad.s^{-1} (datum collected from the MATLAB "velocity.mat" file).

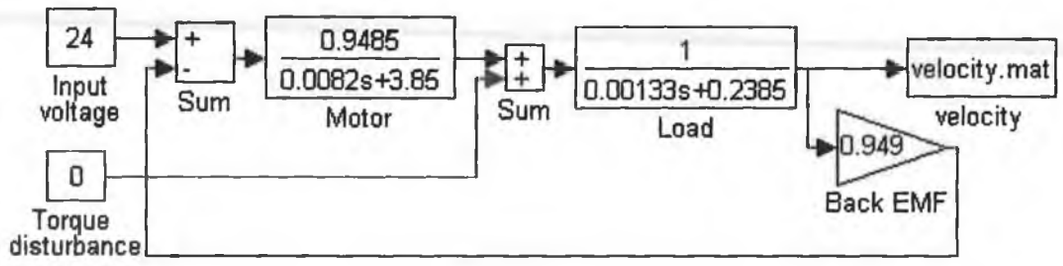

Then in the following graph, when the torque disturbance is the highest, the velocity becomes 5.0661rad.s^{-1}.

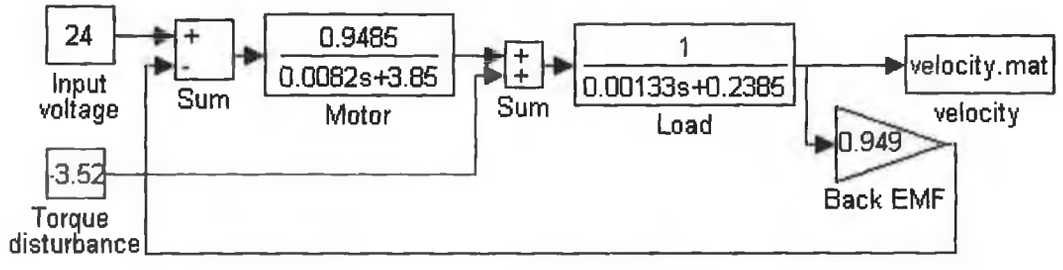

Note: 3.52N.m is the torque occurring at 200 metres deep.

The negative sign means that the motor must overcome the torque (when water must be released).

Hence the depth to velocity conversion is:

$$\frac{\text{Vmax} - \text{Vmin}}{200} = \frac{12.51 - 5.0661}{200} = 0.0372\,\text{s}^{-1}.$$

These values are found using a 24 volts supply, assuming no error due to the feedback.

Then the time required and the velocities in each of the four cases can be simulated.

Graph representing the motor velocity (i.e. ball screw velocity) and time required to pump 1.1 kilograms of water at 1 metre deep:

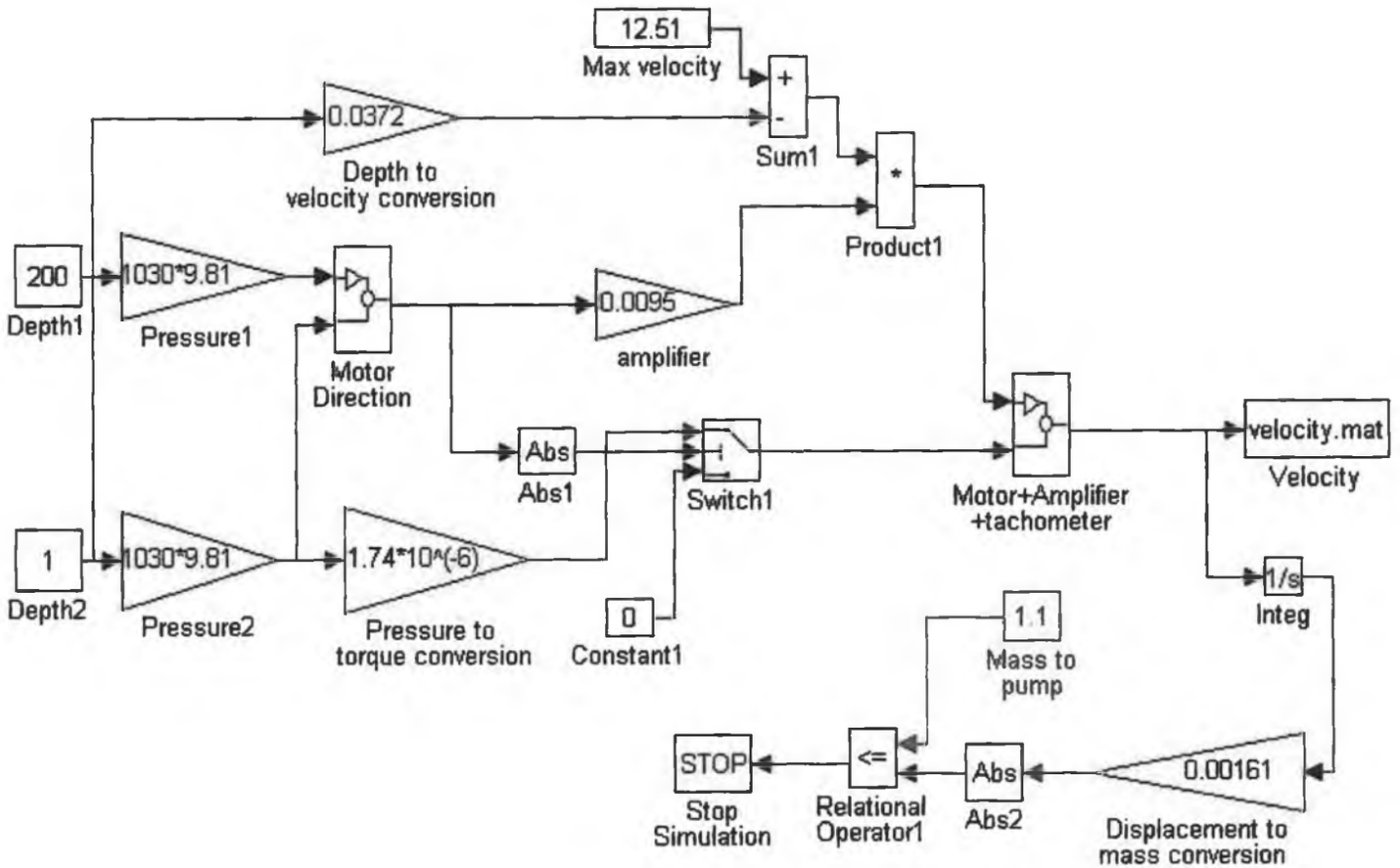

Time and velocity at 1m deep to pump 1.1kg of water:

Data collected from the "velocity.mat" file. The simulation is stopped when 1.1kg is pumped.

Note: depth 1 is randomly selected but it must be larger than depth 2 to allow the pumping.

[...]

Columns 64 through 70

TIME:	55.8516	55.8526	55.8536	55.8546	55.8556	55.8566	55.8576
VELOCITY:	**12.2268**	12.2268	12.2268	12.2268	12.2268	12.2268	12.2268

Columns 71 through 77

55.8586	55.8596	55.8606	55.8616	55.8626	55.8636	55.8646
12.2268	12.2268	12.2268	12.2268	12.2268	12.2268	12.2268

Columns 78 through 84

55.8656	55.8666	55.8676	55.8686	55.8696	55.8706	55.8716
12.2268	12.2268	12.2268	12.2268	12.2268	12.2268	12.2268

Columns 85 through 91

55.8726	55.8736	55.8746	55.8756	55.8766	55.8776	55.8786
12.2268	12.2268	12.2268	12.2268	12.2268	12.2268	12.2268

Columns 92 through 96

55.8796	55.8806	55.8816	55.8826	**55.8836**
12.2268	12.2268	12.2268	12.2268	12.2268

Then: velocity = 12.2268 rad.s^{-1} ≈ 117 rev.min^{-1}

Time ≈ 56 seconds

(values rounded up to the following integer)

Graph representing the ball screw velocity and time required to pump 1 kilogram of water at 100 metres deep:

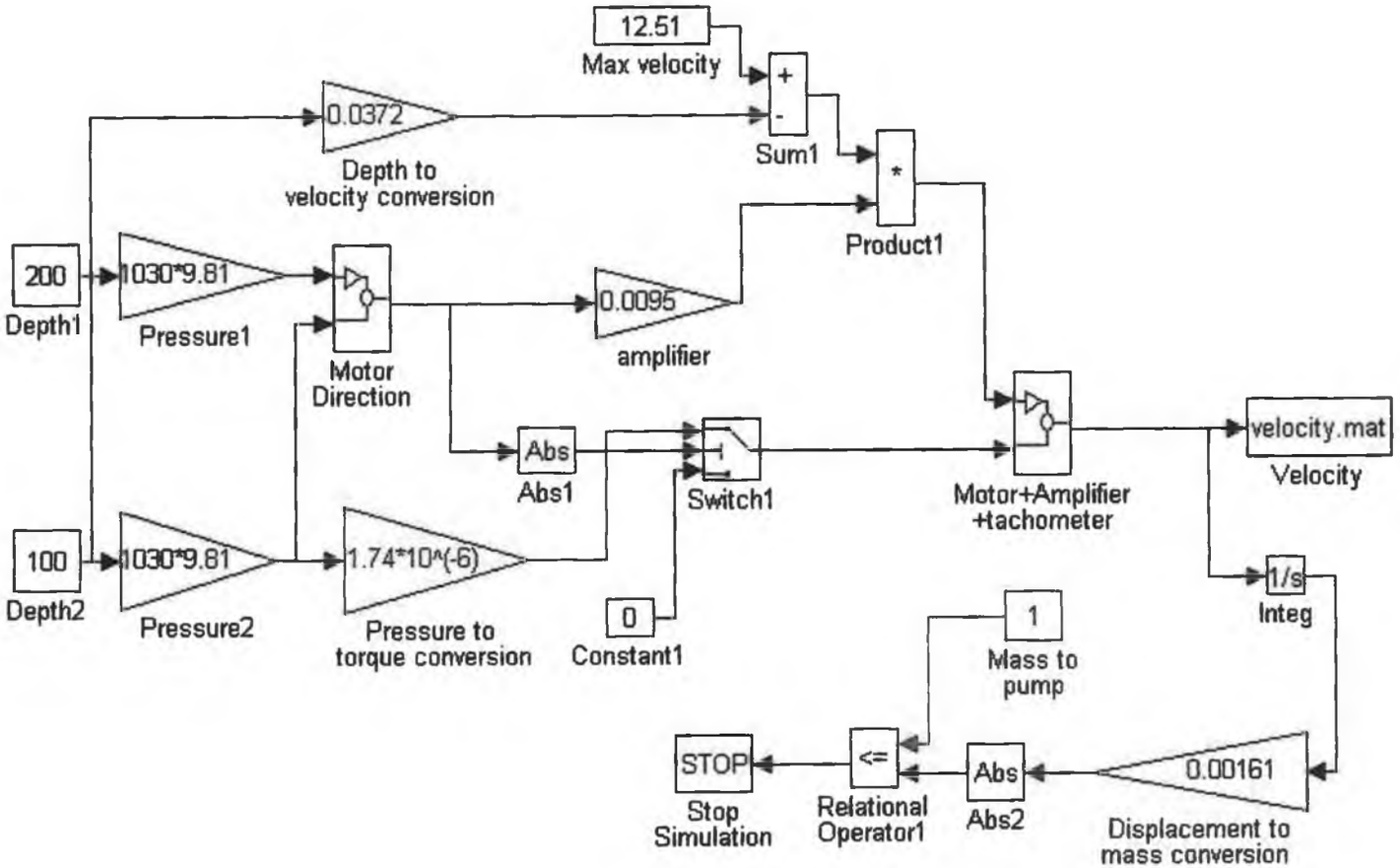

Time and velocity at 100m deep to pump 1kg of water:

[...]

Columns 22 through 28

71.4403	71.4413	71.4423	71.4433	71.4443	71.4453	71.4463
8.6898	8.6898	8.6898	8.6898	8.6898	8.6898	8.6898

Columns 29 through 35

71.4473	71.4483	71.4493	71.4503	71.4513	71.4523	71.4533
8.6898	8.6898	8.6898	8.6898	8.6898	8.6898	8.6898

Columns 36 through 42

71.4543	71.4553	71.4563	71.4573	71.4583	71.4593	71.4603
8.6898	8.6898	8.6898	8.6898	8.6898	8.6898	8.6898

Columns 43 through 49

71.4613	71.4623	71.4633	71.4643	71.4653	71.4663	71.4673
8.6898	8.6898	8.6898	8.6898	8.6898	8.6898	8.6898

Columns 50 through 56

71.4683	71.4693	71.4703	71.4713	71.4723	71.4733	71.4743
8.6898	8.6898	8.6898	8.6898	8.6898	8.6898	8.6898

Columns 57 through 61

71.4753	71.4763	71.4773	71.4783	**71.4793**
8.6898	8.6898	8.6898	8.6898	8.6898

Then: velocity = 8.6898 rad.s^{-1} ≈ 83 rev.min^{-1}

Time ≈ 72 seconds

Graph representing the ball screw velocity and time required to release 1.1 kilograms of water at 200 metres deep:

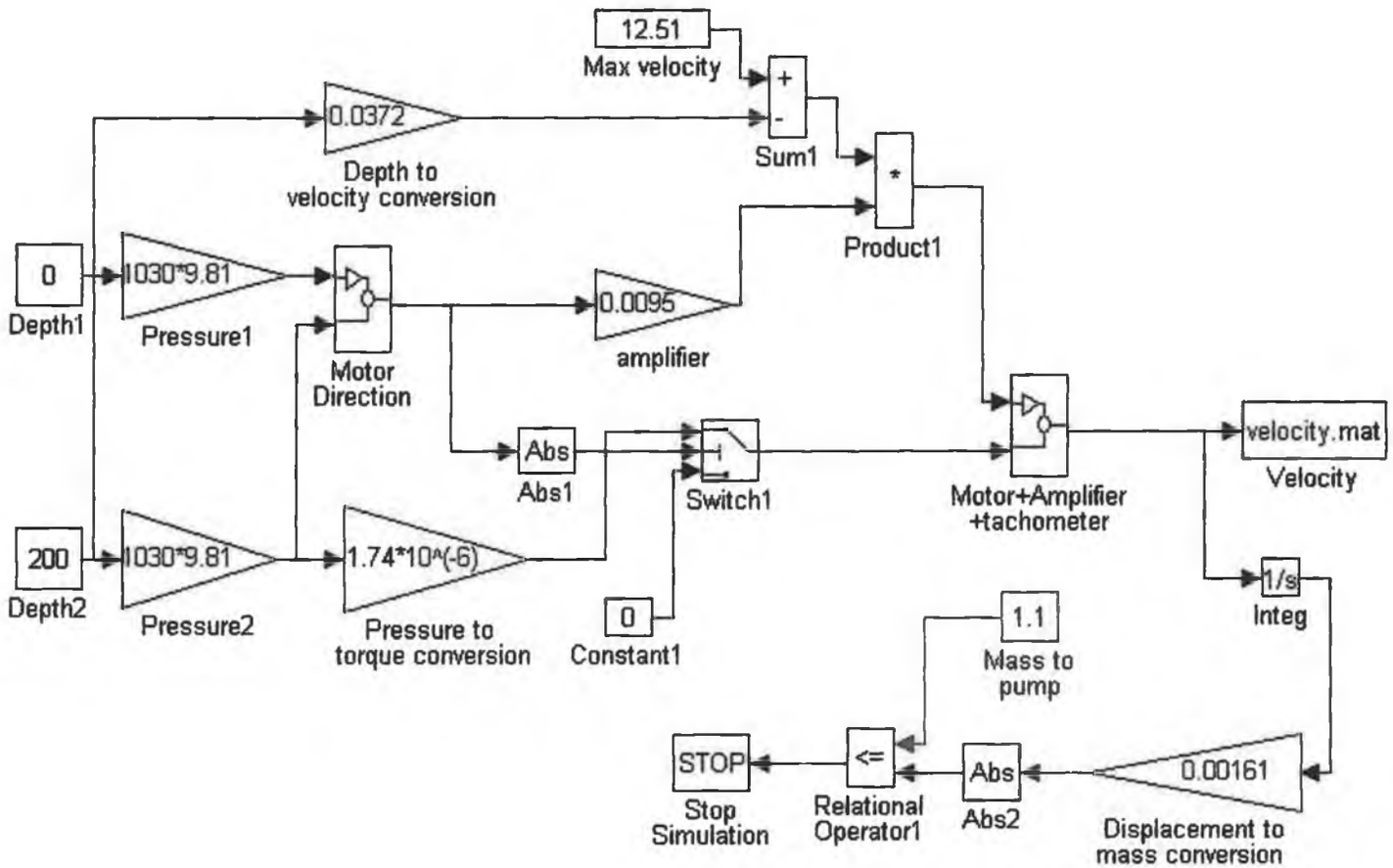

Time and velocity at 200m deep to release 1.1kg of water:

[...]

Columns 57 through 63

141.6441	141.6451	141.6461	141.6471	141.6481	141.6491	141.6501
-4.8224	-4.8224	-4.8224	-4.8224	-4.8224	-4.8224	-4.8224

Columns 64 through 70

141.6511	141.6521	141.6531	141.6541	141.6551	141.6561	141.6571
-4.8224	-4.8224	-4.8224	-4.8224	-4.8224	-4.8224	-4.8224

Columns 71 through 77

141.6581	141.6591	141.6601	141.6611	141.6621	141.6631	141.6641
-4.8224	-4.8224	-4.8224	-4.8224	-4.8224	-4.8224	-4.8224

Columns 78 through 84

141.6651	141.6661	141.6671	141.6681	141.6691	141.6701	141.6711
-4.8224	-4.8224	-4.8224	-4.8224	-4.8224	-4.8224	-4.8224

Columns 85 through 91

141.6721	141.6731	141.6741	141.6751	141.6761	141.6771	141.6781
-4.8224	-4.8224	-4.8224	-4.8224	-4.8224	-4.8224	-4.8224

Columns 92 through 97

141.6791	141.6801	141.6811	141.6821	141.6831	**141.6841**
-4.8224	-4.8224	-4.8224	-4.8224	-4.8224	-4.8224

Then: the negative signs mean that the motor is rotating in the other direction

velocity = 4.8224 rad.s^{-1} ≈ 47 rev.min^{-1}

Time ≈ 142 seconds

Graph representing the ball screw velocity and time required to release 1 kilogram of water at 100 metres deep:

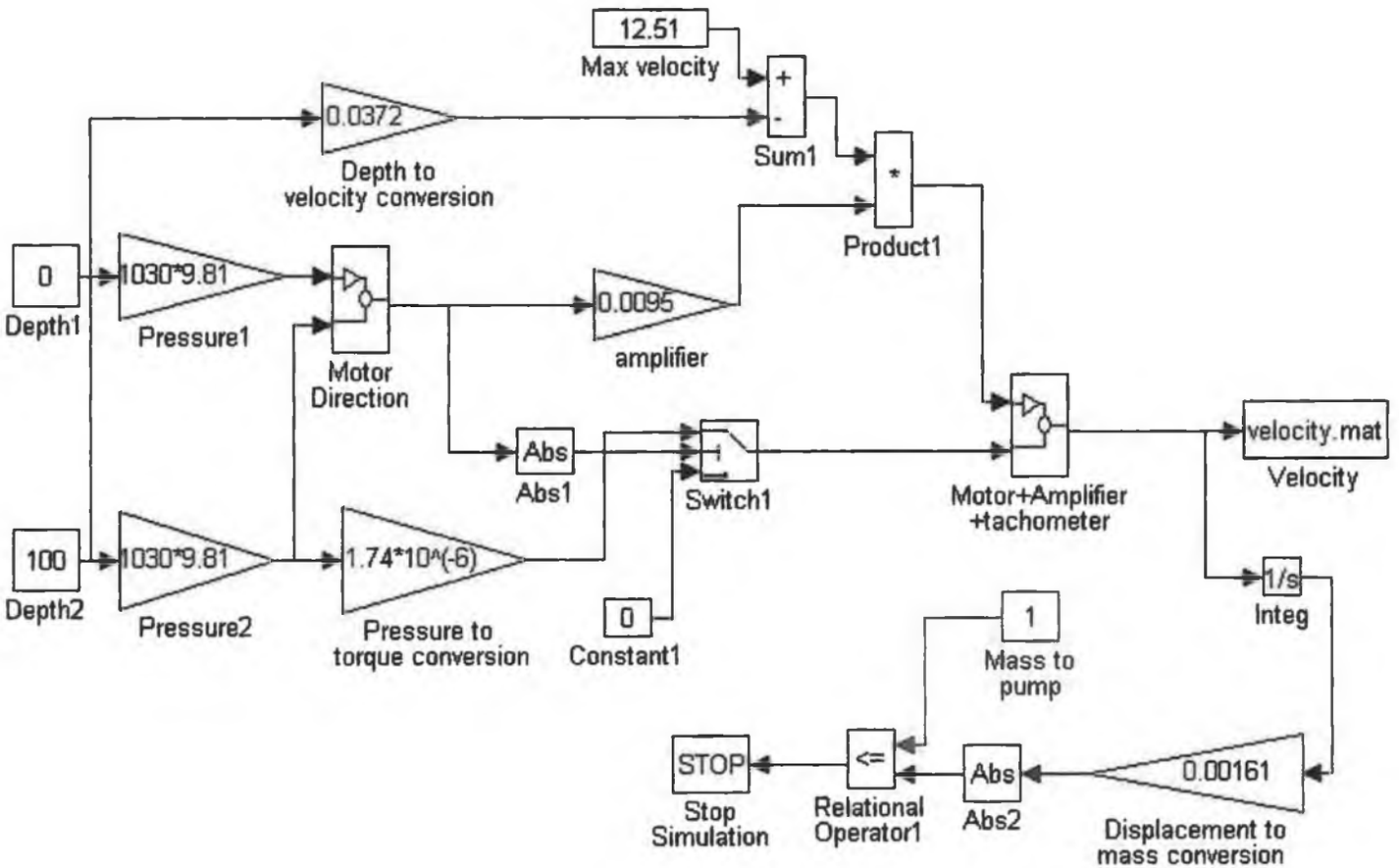

Time and velocity at 100m deep to release 1kg of water:

[...]

Columns 36 through 42

72.6776	72.6786	72.6796	72.6806	72.6816	72.6826	72.6836
-8.5425	-8.5425	-8.5425	-8.5425	-8.5425	-8.5425	-8.5425

Columns 43 through 49

72.6846	72.6856	72.6866	72.6876	72.6886	72.6896	72.6906
-8.5425	-8.5425	-8.5425	-8.5425	-8.5425	-8.5425	-8.5425

Columns 50 through 56

72.6916	72.6926	72.6936	72.6946	72.6956	72.6966	72.6976
-8.5425	-8.5425	-8.5425	-8.5425	-8.5425	-8.5425	-8.5425

Columns 57 through 63

72.6986	72.6996	72.7006	72.7016	72.7026	72.7036	72.7046
-8.5425	-8.5425	-8.5425	-8.5425	-8.5425	-8.5425	-8.5425

Columns 64 through 70

72.7056	72.7066	72.7076	72.7086	72.7096	72.7106	72.7116
-8.5425	-8.5425	-8.5425	-8.5425	-8.5425	-8.5425	-8.5425

Columns 71 through 73

72.7126	72.7136	**72.7146**
-8.5425	-8.5425	-8.5425

Then: velocity = 8.5425 rad.s^{-1}≈ 82 rev.min^{-1}

Time ≈ 73 seconds

APPENDIX C:

TIME AND AMPERAGE REQUIRED PER DUTY

Graph representing the amperage required when pumping 1.1 kilograms of water at 1 metre deep (depth1 is randomly selected but must be higher than depth 2):

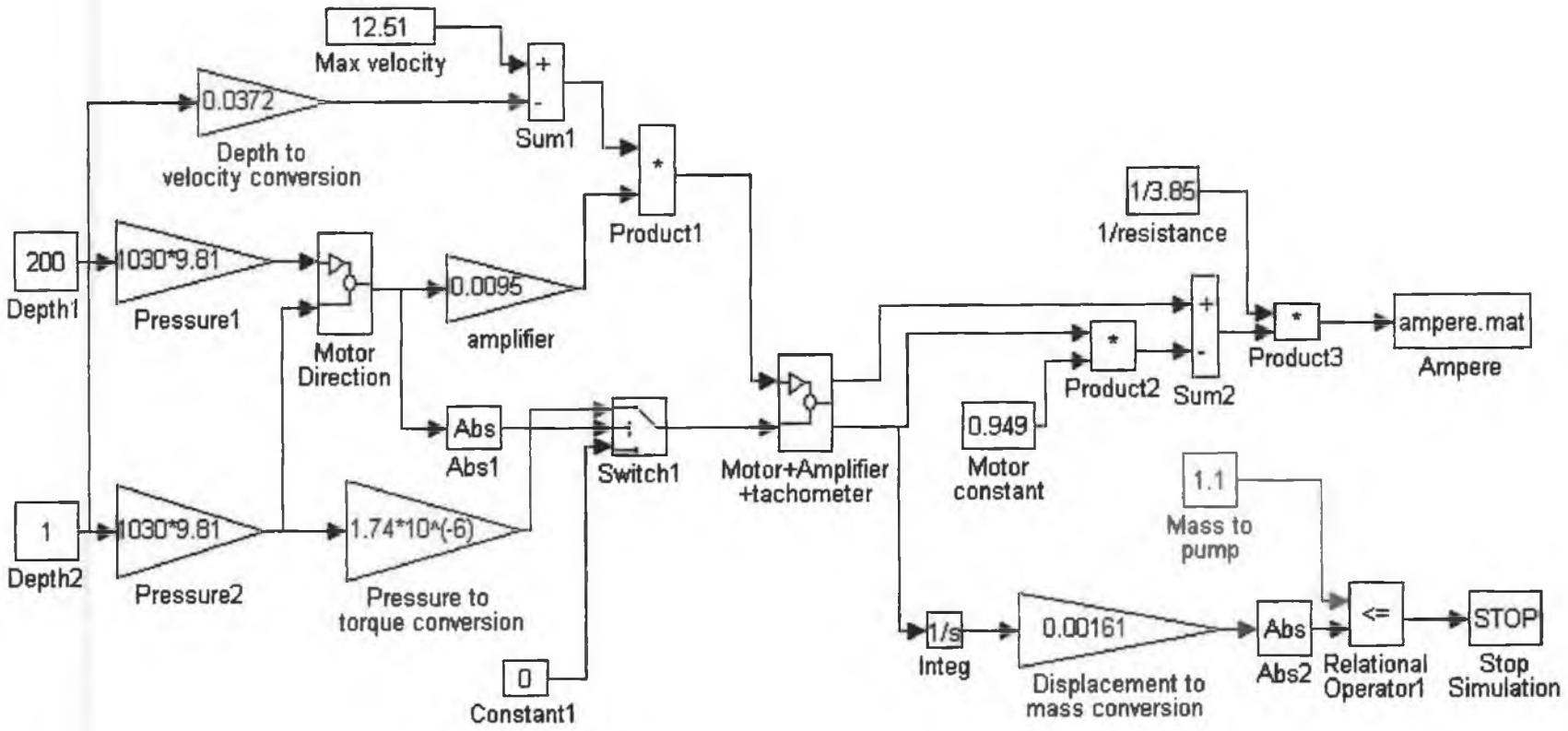

Determination of the amperage required and its duration in order to find out the battery capacity per duty (for more information about the block diagrams, refer to appendix 1).

Time and amperage required when pumping 1.1kg of water at 1m deep:

[...]

Columns 57 through 63

TIME:	55.8446	55.8456	55.8466	55.8476	55.8486	55.8496	55.8506
AMPERAGE:	**3.0559**	3.0559	3.0559	3.0559	3.0559	3.0559	3.0559

Columns 64 through 70

55.8516	55.8526	55.8536	55.8546	55.8556	55.8566	55.8576
3.0559	3.0559	3.0559	3.0559	3.0559	3.0559	3.0559

Columns 71 through 77

55.8586	55.8596	55.8606	55.8616	55.8626	55.8636	55.8646
3.0559	3.0559	3.0559	3.0559	3.0559	3.0559	3.0559

Columns 78 through 84

55.8656	55.8666	55.8676	55.8686	55.8696	55.8706	55.8716
3.0559	3.0559	3.0559	3.0559	3.0559	3.0559	3.0559

Columns 85 through 91

55.8726	55.8736	55.8746	55.8756	55.8766	55.8776	55.8786
3.0559	3.0559	3.0559	3.0559	3.0559	3.0559	3.0559

Columns 92 through 96

55.8796	55.8806	55.8816	55.8826	**55.8836**
3.0559	3.0559	3.0559	3.0559	3.0559

Then: amperage = 3.0559A

time = 55.8836≈55.9 seconds

Graph representing the amperage required when pumping 1 kilogram of water at 100 metres deep:

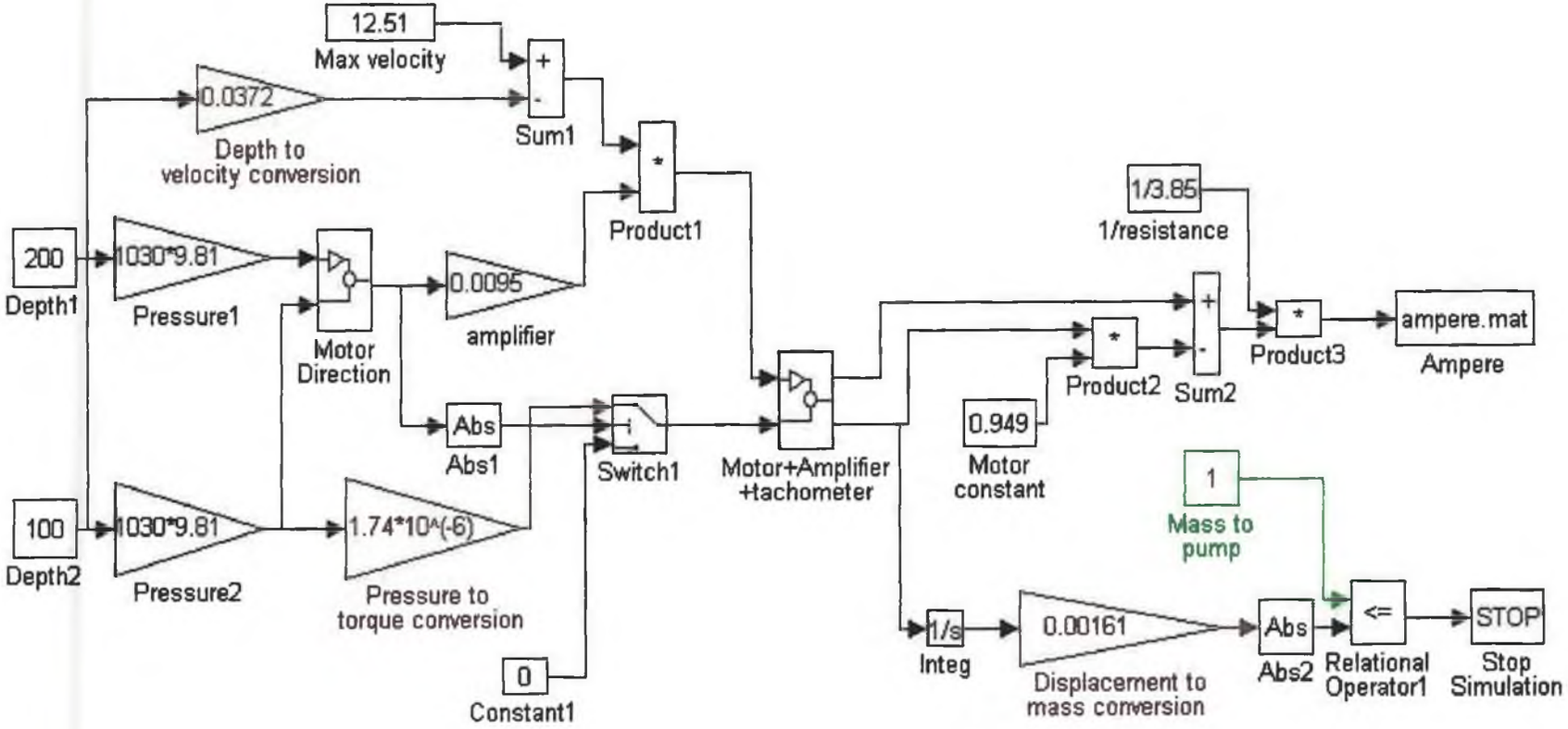

Time and amperage required when pumping 1kg of water at 100m deep:

[…]

Columns 29 through 35

71.4473	71.4483	71.4493	71.4503	71.4513	71.4523	71.4533
0.3314	0.3314	0.3314	0.3314	0.3314	0.3314	0.3314

Columns 36 through 42

71.4543	71.4553	71.4563	71.4573	71.4583	71.4593	71.4603
0.3314	0.3314	0.3314	0.3314	0.3314	0.3314	0.3314

Columns 43 through 49

71.4613	71.4623	71.4633	71.4643	71.4653	71.4663	71.4673
0.3314	0.3314	0.3314	0.3314	0.3314	0.3314	0.3314

Columns 50 through 56

71.4683	71.4693	71.4703	71.4713	71.4723	71.4733	71.4743
0.3314	0.3314	0.3314	0.3314	0.3314	0.3314	0.3314

Columns 57 through 61

71.4753	71.4763	71.4773	71.4783	**71.4793**
0.3314	0.3314	0.3314	0.3314	0.3314

Then: amperage = 0.3314A

time = 71.4793≈71.5 seconds

Graph representing the amperage required when releasing 1.1 kilograms of water at 200 metres deep:

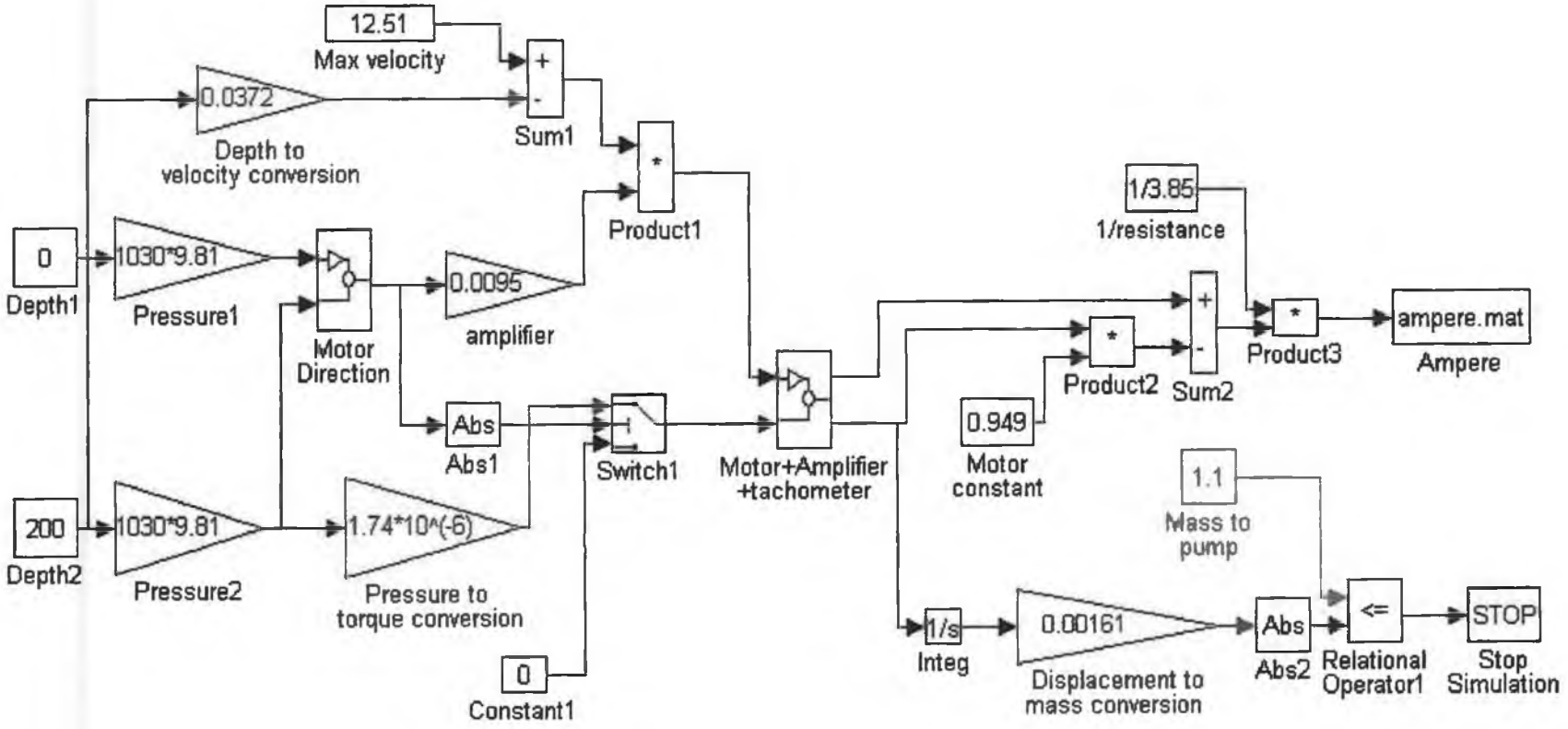

Time and amperage required when releasing 1.1kg of water at 200m deep:

[…]

Columns 57 through 63

141.6441	141.6451	141.6461	141.6471	141.6481	141.6491	141.6501
-4.9198	-4.9198	-4.9198	-4.9198	-4.9198	-4.9198	-4.9198

Columns 64 through 70

141.6511	141.6521	141.6531	141.6541	141.6551	141.6561	141.6571
-4.9198	-4.9198	-4.9198	-4.9198	-4.9198	-4.9198	-4.9198

Columns 71 through 77

141.6581	141.6591	141.6601	141.6611	141.6621	141.6631	141.6641
-4.9198	-4.9198	-4.9198	-4.9198	-4.9198	-4.9198	-4.9198

Columns 78 through 84

141.6651	141.6661	141.6671	141.6681	141.6691	141.6701	141.6711
-4.9198	-4.9198	-4.9198	-4.9198	-4.9198	-4.9198	-4.9198

Columns 85 through 91

141.6721	141.6731	141.6741	141.6751	141.6761	141.6771	141.6781
-4.9198	-4.9198	-4.9198	-4.9198	-4.9198	-4.9198	-4.9198

Columns 92 through 97

141.6791	141.6801	141.6811	141.6821	141.6831	**141.6841**
-4.9198	-4.9198	-4.9198	-4.9198	-4.9198	-4.9198

Then: amperage = 4.92A

time = 141.6821≈141.7 seconds

Graph representing the amperage required when releasing 1 kilogram of water at 100 metres deep:

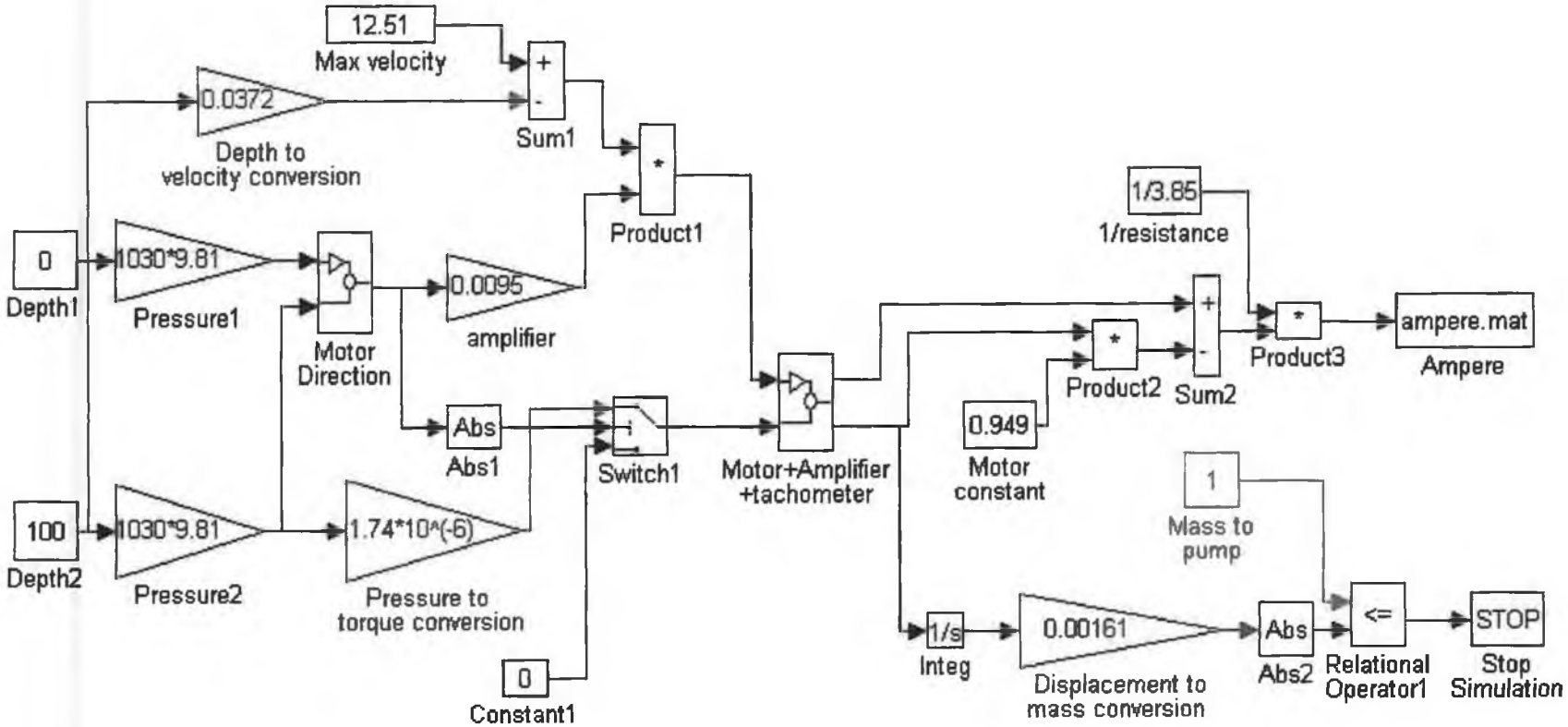

Time and amperage required when releasing 1kg of water at 100m deep:

[…]

Columns 43 through 49

72.6846	72.6856	72.6866	72.6876	72.6886	72.6896	72.6906
-4.0016	-4.0016	-4.0016	-4.0016	-4.0016	-4.0016	-4.0016

Columns 50 through 56

72.6916	72.6926	72.6936	72.6946	72.6956	72.6966	72.6976
-4.0016	-4.0016	-4.0016	-4.0016	-4.0016	-4.0016	-4.0016

Columns 57 through 63

72.6986	72.6996	72.7006	72.7016	72.7026	72.7036	72.7046
-4.0016	-4.0016	-4.0016	-4.0016	-4.0016	-4.0016	-4.0016

Columns 64 through 70

72.7056	72.7066	72.7076	72.7086	72.7096	72.7106	72.7116
-4.0016	-4.0016	-4.0016	-4.0016	-4.0016	-4.0016	-4.0016

Columns 71 through 73

72.7126	72.7136	**72.7146**
-4.0016	-4.0016	-4.0016

Then: amperage = 4A

time = 72.7136≈72.72 seconds

APPENDIX D:

OUTPUT CHARACTERISTICS OF THE MOTOR

Determination of the characteristics of the motor response:

These characteristics include the settling time and the percentage overshoot. They must be as small as possible in order to reach the stable state very quickly.

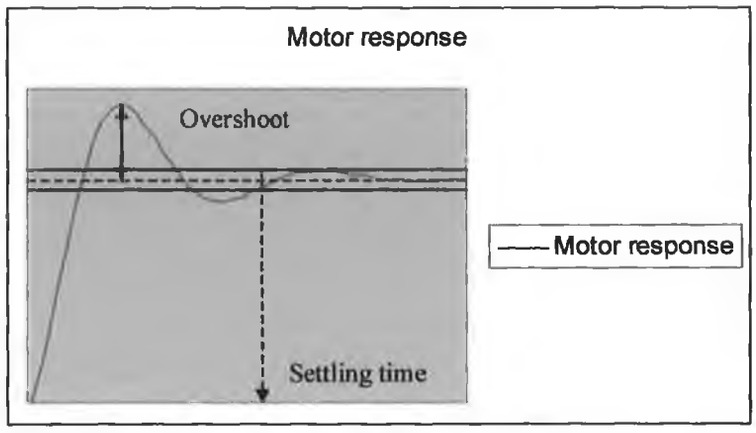

Determination of the settling time T_s:

T_s is determinate when the output v is (within 2%):

Final value× (1-0.02)<velocity<final value×(1+0.02)

Form the velocity we can find the settling time.

Determination of the percentage overshoot PO:

$$PO = \left(\frac{\text{Maximal velocity - final velocity}}{\text{final velocity}} \right) \times 100$$

Key:

□ : Maximal velocity

□ : Settling time

□ : Final velocity

Block diagram giving the output velocity at 1 metre deep. Concerning the other states, only depth1and depth2 have to be changed.

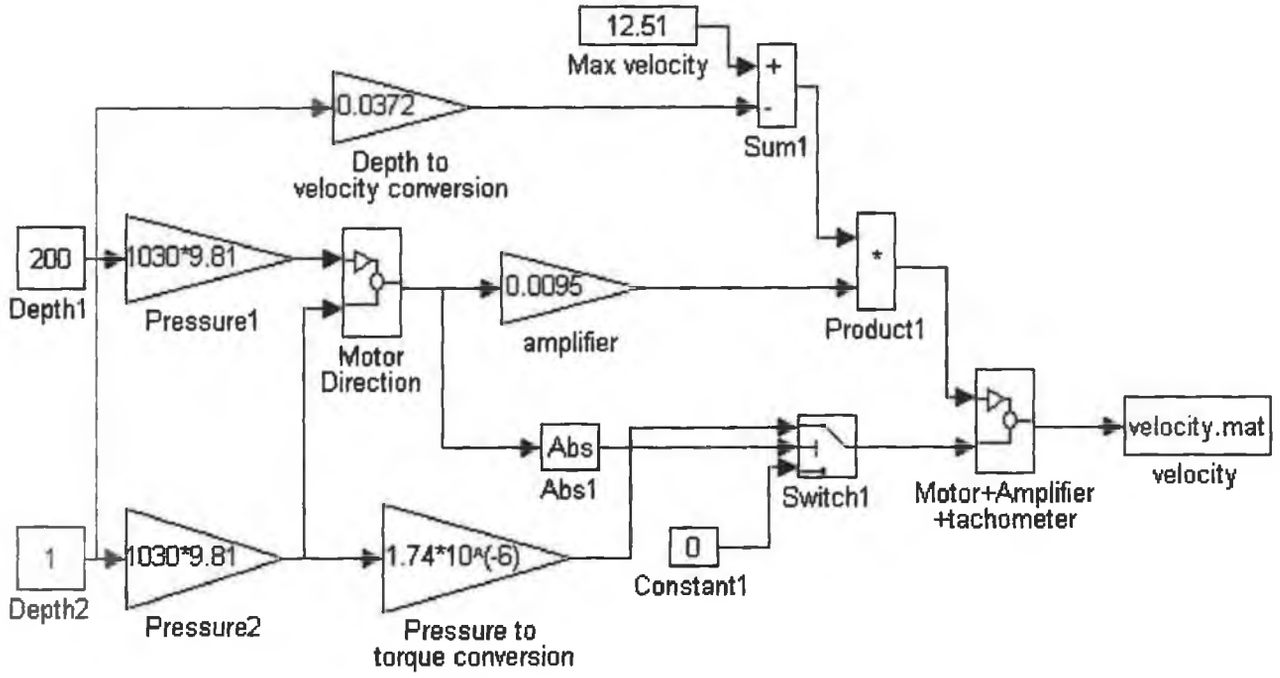

Overshoot and settling time (within 2% of the final value) at 1m deep:

Columns 1 through 7

TIME	0	0.0001	0.0010	0.0019	0.0029	0.0039	0.0049
VELOCITY	0	0.0115	0.8682	2.5005	4.6560	6.7384	8.5306

Columns 8 through 14

0.0059	0.0069	0.0079	0.0082	0.0086	0.0089	0.0091
9.9543	11.0132	11.7533	11.9384	12.1333	12.2189	12.2893

Columns 15 through 21

0.0094	0.0096	0.0098	0.0101	0.0102	0.0112	0.0122
12.3378	12.3121	12.2631	12.2021	12.1667	12.0376	12.0329

Columns 22 through 28

0.0132	0.0142	0.0146	0.0149	0.0151	0.0154	0.0156
12.0938	12.1815	12.2179	12.2399	12.2517	12.2500	12.2366

Columns 29 through 35

0.0159	0.0163	0.0173	0.0176	0.0179	0.0183	0.0187
12.2192	12.2042	12.2135	12.2244	12.2343	12.2371	12.2299

Columns 36 through 42

0.0190	0.0196	0.0200	0.0203	0.0207	0.0211	0.0215
12.2216	12.2206	12.2274	12.2324	12.2306	12.2257	12.2226

Columns 43 through 49

0.0219	0.0223	0.0228	0.0233	0.0237	0.0242	0.0246
12.2252	12.2287	12.2292	12.2263	12.2247	12.2264	12.2281

Columns 50 through 56

0.0255	0.0259	0.0265	0.0270	0.0277	0.0282	0.0289
12.2267	12.2257	12.2268	12.2276	12.2267	12.2262	12.2270

Columns 57 through 63

0.0294	0.0301	0.0307	0.0313	0.0320	0.0327	0.0336
12.2272	12.2266	12.2266	12.2270	12.2269	12.2266	12.2269

Columns 64 through 70

0.0343	0.0350	0.0359	0.0366	0.0375	0.0385	0.0393
12.2269	12.2267	12.2269	12.2268	12.2268	12.2269	12.2268

Columns 71 through 77

0.0402	0.0412	0.0421	0.0431	0.0441	0.0451	0.0461
12.2268	12.2268	12.2268	12.2268	12.2268	12.2268	12.2268

Columns 78 through 81

0.0471	0.0481	0.0491	0.0500
12.2268	12.2268	12.2268	12.2268

11.982<v<12.471 Then Ts=0.0086 seconds

PO=0.91%

Overshoot and settling time at 100m deep (pumping):

Columns 1 through 7

0	0.0001	0.0010	0.0020	0.0030	0.0032	0.0035
0	0.1412	2.1595	4.7143	7.5564	8.2966	8.9077

Columns 8 through 14

0.0036	0.0037	0.0045	0.0047	0.0048	0.0049	0.0050
9.2192	9.3695	9.3683	9.1426	8.9512	8.7790	8.6083

Columns 15 through 21

0.0052	0.0053	0.0062	0.0066	0.0068	0.0070	0.0072
8.3557	8.2306	7.9998	8.2051	8.3948	8.5897	8.7738

Columns 22 through 28

0.0074	0.0076	0.0078	0.0079	0.0081	0.0083	0.0086
8.9409	8.9839	8.9562	8.8747	8.7538	8.6107	8.4991

Columns 29 through 35

0.0087	0.0089	0.0091	0.0093	0.0095	0.0098	0.0100
8.4772	8.4937	8.5526	8.6363	8.7410	8.8281	8.8272

Columns 36 through 42

0.0102	0.0104	0.0106	0.0109	0.0111	0.0113	0.0115
8.7877	8.7226	8.6462	8.5905	8.5973	8.6324	8.6847

Columns 43 through 49

0.0118	0.0121	0.0123	0.0125	0.0128	0.0132	0.0134
8.7401	8.7609	8.7470	8.7142	8.6731	8.6397	8.6533

Columns 50 through 56

0.0137	0.0139	0.0143	0.0146	0.0148	0.0151	0.0155
8.6797	8.7100	8.7245	8.7119	8.6907	8.6698	8.6664

Columns 57 through 63

0.0157	0.0160	0.0164	0.0167	0.0170	0.0173	0.0177
8.6780	8.6945	8.7070	8.7027	8.6915	8.6801	8.6793

Columns 64 through 70

0.0180	0.0184	0.0189	0.0192	0.0196	0.0200	0.0204
8.6874	8.6960	8.6955	8.6886	8.6837	8.6861	8.6912

Columns 71 through 77

0.0208	0.0212	0.0216	0.0221	0.0226	0.0230	0.0235
8.6941	8.6913	8.6877	8.6874	8.6904	8.6920	8.6902

Columns 78 through 84

0.0239	0.0247	0.0252	0.0258	0.0263	0.0270	0.0275
8.6884	8.6899	8.6909	8.6898	8.6889	8.6899	8.6904

Columns 85 through 91

0.0282	0.0287	0.0293	0.0299	0.0306	0.0312	0.0319
8.6896	8.6893	8.6900	8.6900	8.6895	8.6897	8.6899

Columns 92 through 98

0.0327	0.0334	0.0342	0.0350	0.0357	0.0366	0.0375
8.6897	8.6897	8.6899	8.6897	8.6897	8.6898	8.6897

Columns 99 through 105

0.0383	0.0393	0.0403	0.0412	0.0421	0.0431	0.0441
8.6898	8.6898	8.6897	8.6898	8.6898	8.6897	8.6898

Columns 106 through 112

0.0451	0.0461	0.0471	0.0481	0.0491	0.0501	0.0511
8.6898	8.6898	8.6898	8.6898	8.6898	8.6898	8.6898

8.516<v<8.864 Then Ts=0.0091 seconds

PO=7.82%

Overshoot and settling time at 200m deep:

Columns 1 through 7

0	0.0001	0.0010	0.0018	0.0027	0.0037	0.0047
0	0.2518	1.5224	1.6442	1.0331	-0.0362	-1.2045

Columns 8 through 14

0.0057	0.0067	0.0077	0.0087	0.0097	0.0100	0.0102
-2.2833	-3.1847	-3.8844	-4.3940	-4.7426	-4.8051	-4.8562

Columns 15 through 21

0.0103	0.0106	0.0108	0.0110	0.0112	0.0114	0.0124
-4.8815	-4.8930	-4.8772	-4.8435	-4.8023	-4.7796	-4.7059

Columns 22 through 28

0.0134	0.0144	0.0154	0.0157	0.0160	0.0163	0.0166
-4.7119	-4.7589	-4.8215	-4.8369	-4.8402	-4.8308	-4.8178

Columns 29 through 35

0.0170	0.0176	0.0181	0.0184	0.0187	0.0190	0.0194
-4.8069	-4.8063	-4.8157	-4.8244	-4.8298	-4.8295	-4.8236

Columns 36 through 42

0.0197	0.0203	0.0208	0.0212	0.0216	0.0220	0.0227
-4.8176	-4.8184	-4.8257	-4.8264	-4.8231	-4.8198	-4.8218

Columns 43 through 49

0.0231	0.0239	0.0244	0.0251	0.0256	0.0263	0.0269
-4.8243	-4.8228	-4.8216	-4.8225	-4.8231	-4.8222	-4.8220

Columns 50 through 56

0.0275 0.0281 0.0287 0.0294 0.0300 0.0309 0.0315

-4.8227 -4.8227 -4.8222 -4.8224 -4.8226 -4.8224 -4.8224

Columns 57 through 63

0.0323 0.0331 0.0339 0.0348 0.0356 0.0365 0.0374

-4.8226 -4.8224 -4.8224 -4.8225 -4.8224 -4.8224 -4.8225

Columns 64 through 70

0.0384 0.0393 0.0403 0.0413 0.0423 0.0433 0.0443

-4.8224 -4.8225 -4.8225 -4.8224 -4.8225 -4.8224 -4.8224

Columns 71 through 77

0.0453 0.0463 0.0473 0.0483 0.0493 0.0503 0.0513

-4.8225 -4.8224 -4.8224 -4.8225 -4.8224 -4.8224 -4.8224

Columns 78 through 84

0.0523 0.0533 0.0543 0.0553 0.0563 0.0573 0.0583

-4.8224 -4.8224 -4.8224 -4.8224 -4.8224 -4.8224 -4.8224

Columns 85 through 86

0.0593 0.0600

-4.8224 -4.8224

4.726<v<4.919 Then Ts=0.0144 seconds

PO=1.46%

Overshoot and settling time at 100m deep (releasing):

Columns 1 through 7

0	0.0001	0.0010	0.0018	0.0028	0.0038	0.0048
0	0.1208	0.3643	-0.3691	-1.7512	-3.3432	-4.8350

Columns 8 through 14

0.0058	0.0068	0.0078	0.0088	0.0098	0.0101	0.0103
-6.0939	-7.0789	-7.8014	-8.2995	-8.5984	-8.6095	-8.5912

Columns 15 through 21

0.0105	0.0108	0.0110	0.0120	0.0130	0.0140	0.0150
-8.5568	-8.5169	-8.4921	-8.4315	-8.4440	-8.4932	-8.5518

Columns 22 through 28

0.0155	0.0158	0.0162	0.0164	0.0174	0.0177	0.0182
-8.5549	-8.5437	-8.5338	-8.5300	-8.5415	-8.5489	-8.5487

Columns 29 through 35

0.0185	0.0189	0.0193	0.0198	0.0202	0.0206	0.0210
-8.5427	-8.5374	-8.5387	-8.5448	-8.5464	-8.5435	-8.5403

Columns 36 through 42

0.0217	0.0221	0.0226	0.0231	0.0235	0.0240	0.0245
-8.5413	-8.5439	-8.5440	-8.5419	-8.5411	-8.5426	-8.5435

Columns 43 through 49

0.0251	0.0256	0.0263	0.0268	0.0275	0.0280	0.0287
-8.5424	-8.5417	-8.5427	-8.5430	-8.5423	-8.5422	-8.5427

Columns 50 through 56

0.0293	0.0299	0.0307	0.0313	0.0323	0.0330	0.0337
-8.5427	-8.5423	-8.5425	-8.5426	-8.5424	-8.5425	-8.5426

Columns 57 through 63

0.0347	0.0355	0.0363	0.0373	0.0382	0.0391	0.0401
-8.5424	-8.5425	-8.5425	-8.5424	-8.5425	-8.5425	-8.5425

Columns 64 through 70

0.0411	0.0420	0.0430	0.0440	0.0450	0.0460	0.0470
-8.5425	-8.5425	-8.5425	-8.5425	-8.5425	-8.5425	-8.5425

Columns 71 through 77

0.0480	0.0490	0.0500	0.0510	0.0520	0.0530	0.0540
-8.5425	-8.5425	-8.5425	-8.5425	-8.5425	-8.5425	-8.5425

Columns 78 through 83

0.0550	0.0560	0.0570	0.0580	0.0590	0.0600
-8.5425	-8.5425	-8.5425	-8.5425	-8.5425	-8.5425

8.372<v<8.713 Then Ts=0.0098 seconds

PO=0.784%

APPENDIX E:

NOMENCLATURE

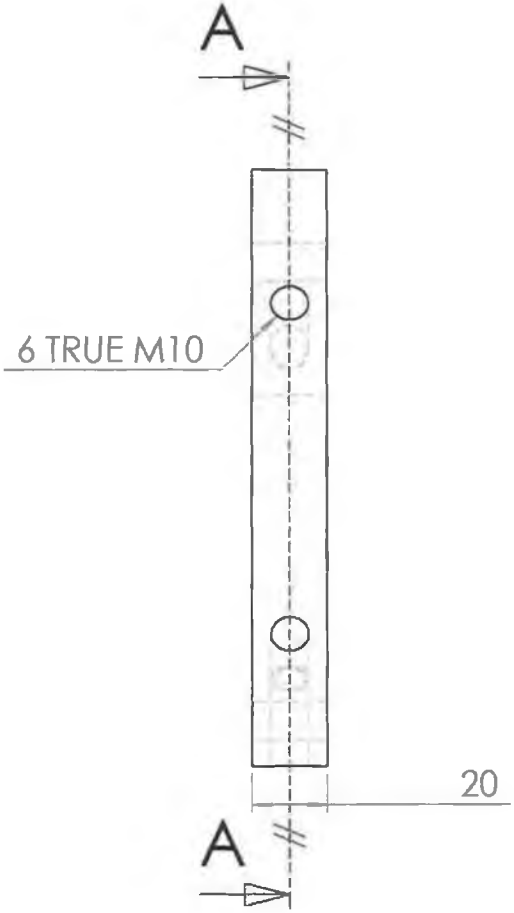

A-A

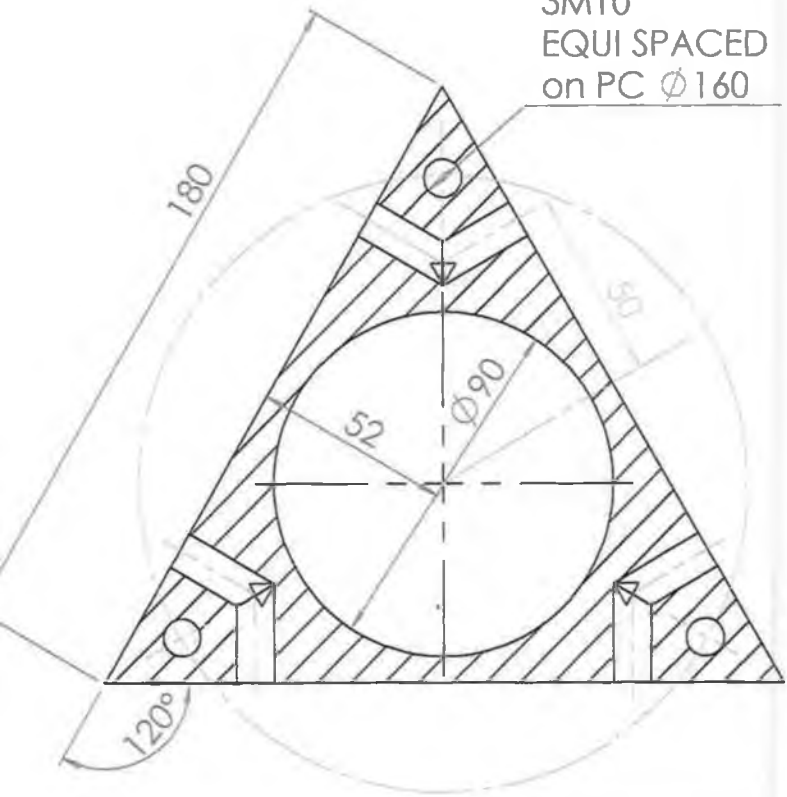

MATERIAL: STEEL ALL TOLERANCES ±0.2 UNLESS SPECIFIED OTHERWISE	NAME: SENSOR SUPPORT
	ALL DIMENSIONS IN MILLIMETRES DESIGNER: SEBASTIEN QUEHIN April 200
	QUANTITY:1 SCALE: 1/2 G.M.I.T

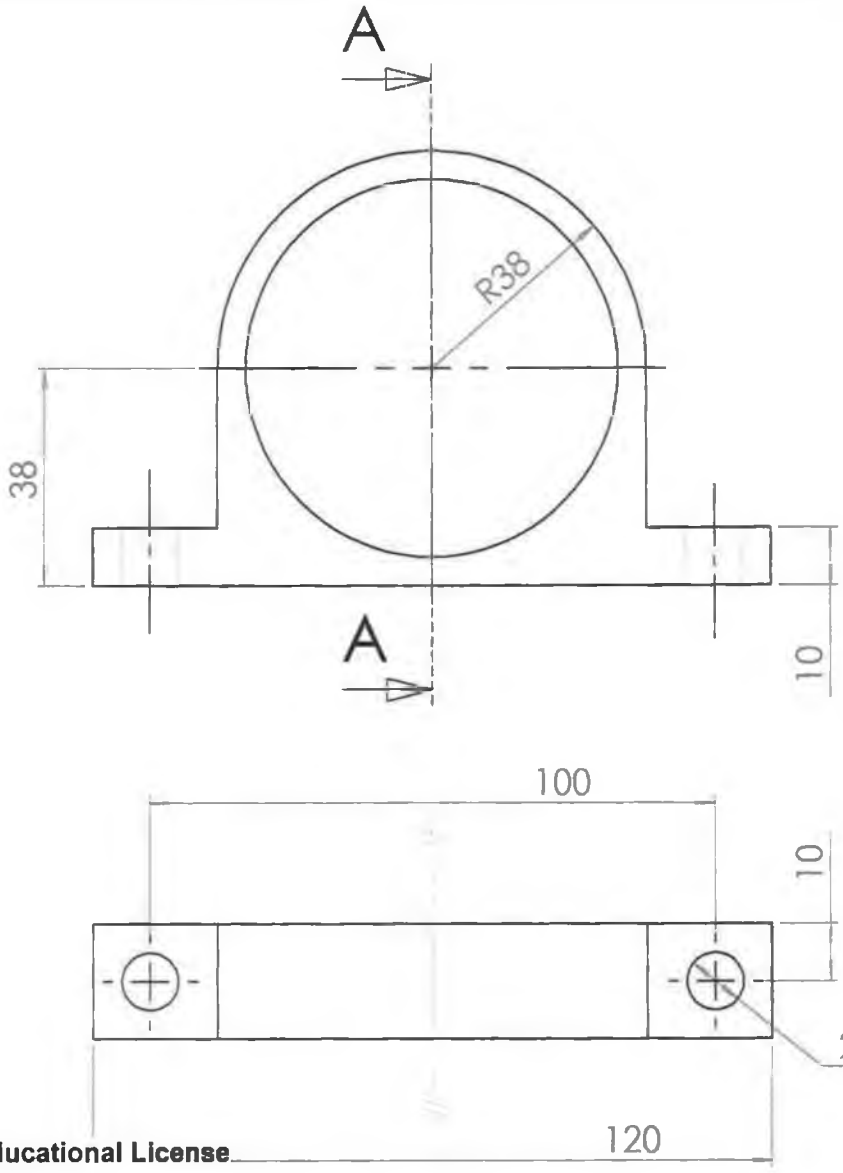

A-A

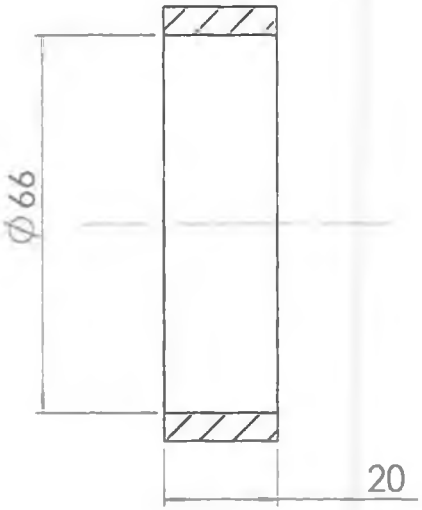

MATERIAL: STEEL ALL TOLERANCES ±0.2 UNLESS SPECIFIED OTHERWISE	NAME: CYLINDER SUPPORT
	ALL DIMENSIONS IN MILLIMETRES DESIGNER: SEBASTIEN QUEHI April 20(
	QUANTITY:3 SCALE: 3/4 G.M.I.T

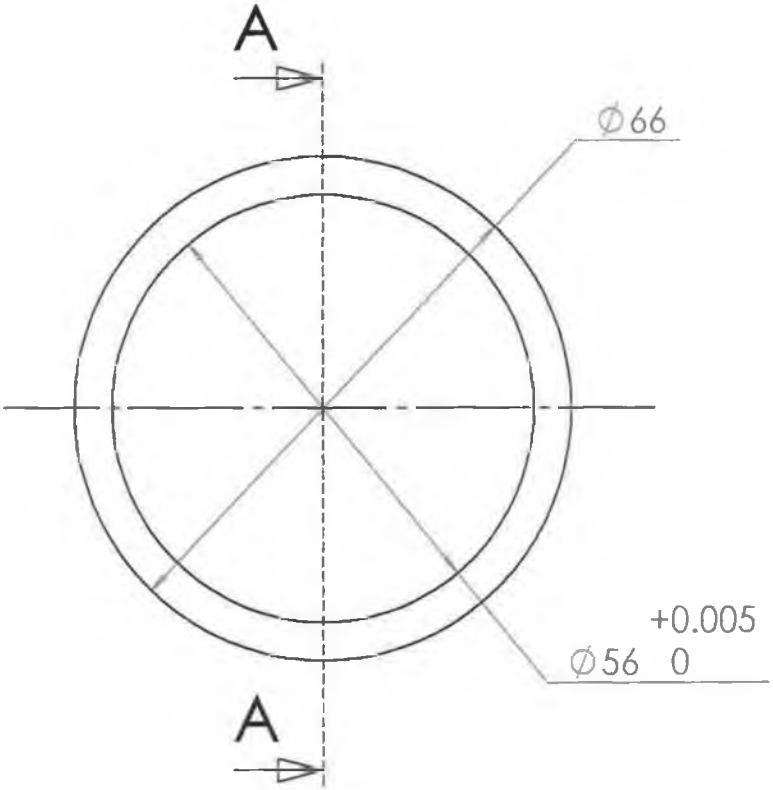

A-A

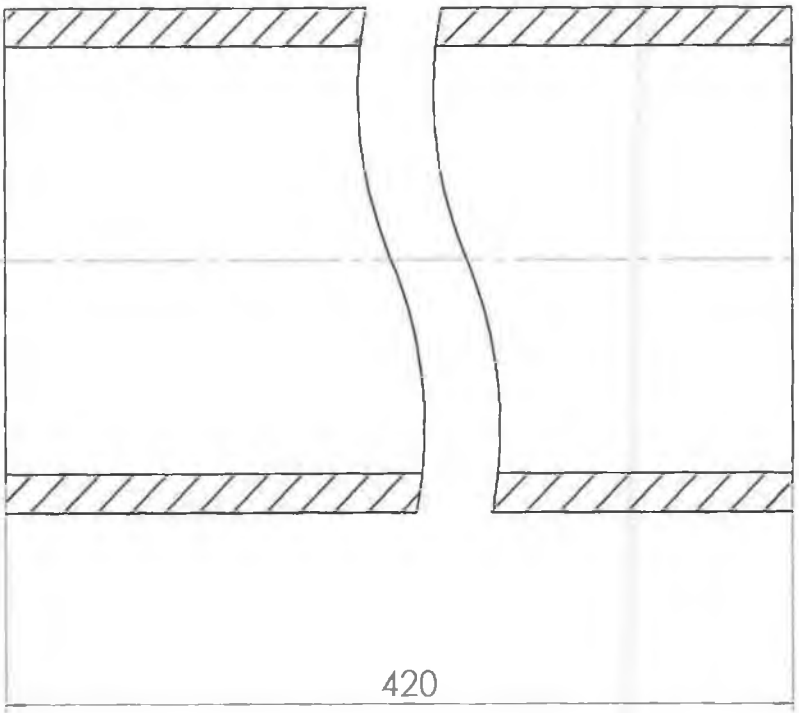

MATERIAL: STEEL+COATING	NAME: CYLINDER
ALL TOLERANCES ±0.2 UNLESS SPECIFIED OTHERWISE	
ALL DIMENSIONS IN MILLIMETRES	DESIGNER: SEBASTIEN QUEHI April 200
QUANTITY:3 SCALE: 1/1	G.M.I.T

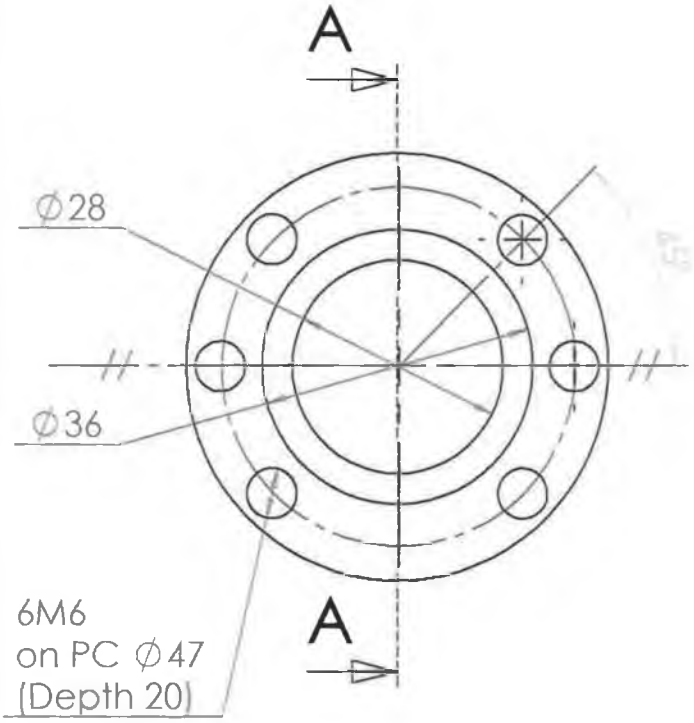

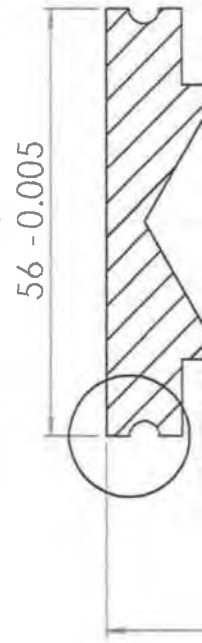

DETAIL B (2 : 1)

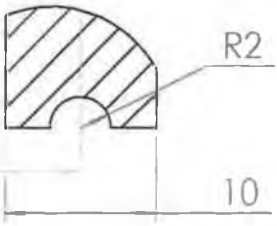

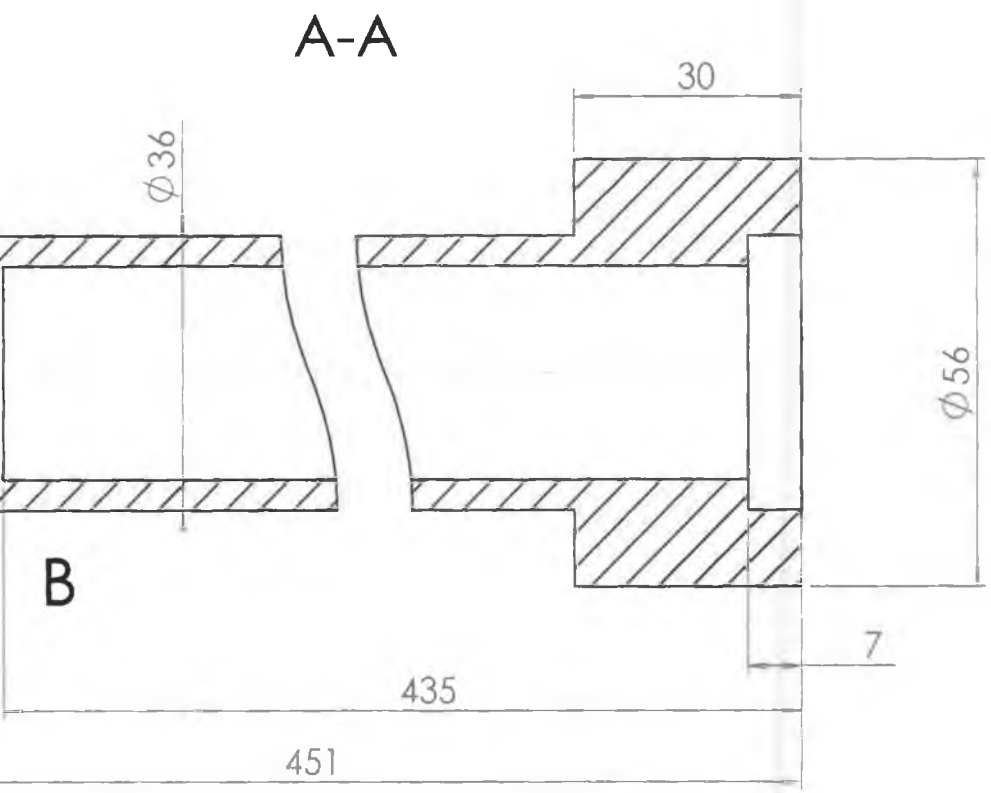

MATERIAL: STEEL	NAME: PISTON	
ALL TOLERANCES ±0.2 UNLESS SPECIFIED OTHERWISE		
	ALL DIMENSIONS IN MILLIMETRES	DESIGNER: SEBASTIEN QUEHI April 200
	QUANTITY:3 SCALE: 1/1	G.M.I.T

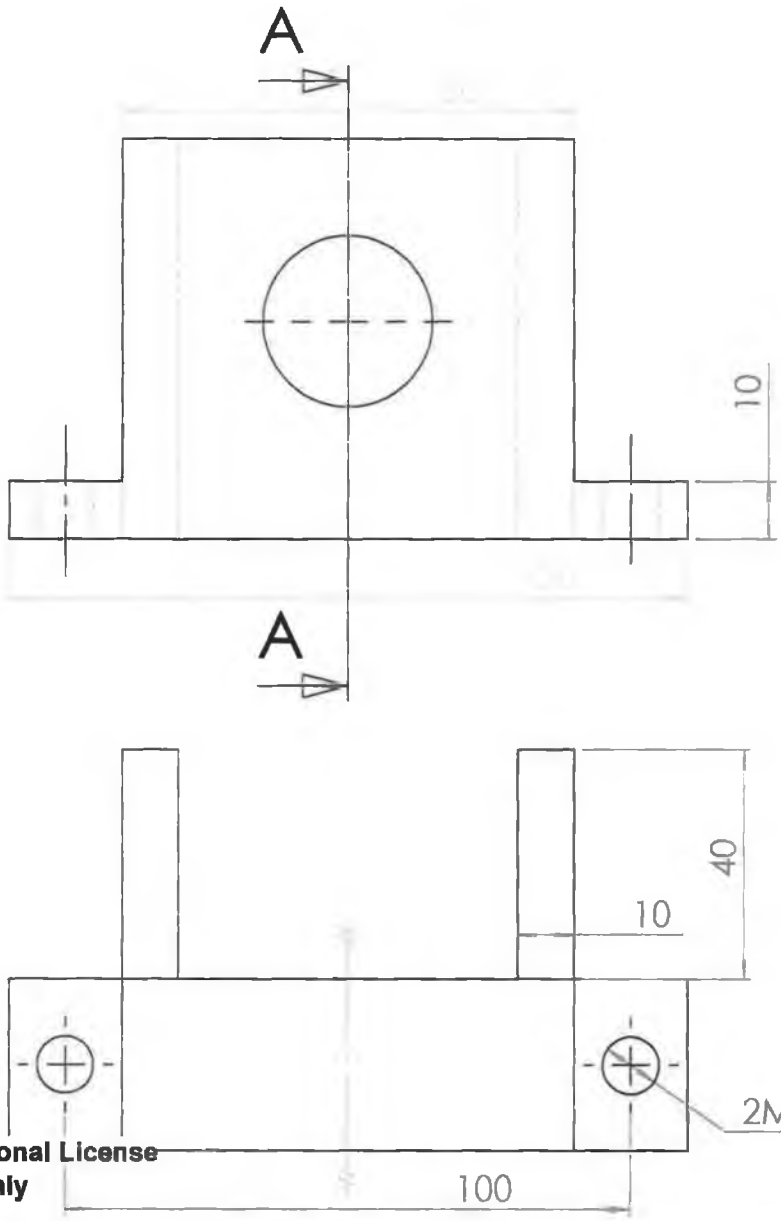

A-A

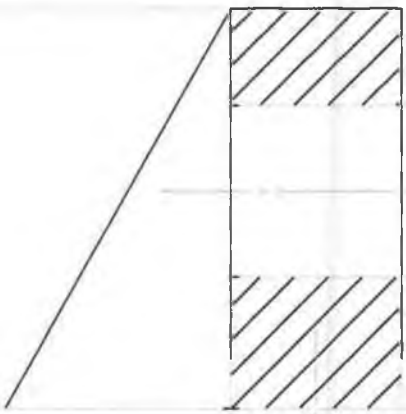

MATERIAL: STEEL ALL TOLERANCES ±0.2 UNLESS SPECIFIED OTHERWISE	NAME: BEARING SUPPORT
	ALL DIMENSIONS IN MILLIMETRES DESIGNER: SEBASTIEN QUEHIN April 200
	QUANTITY:3 SCALE: 3/4 G.M.I.T

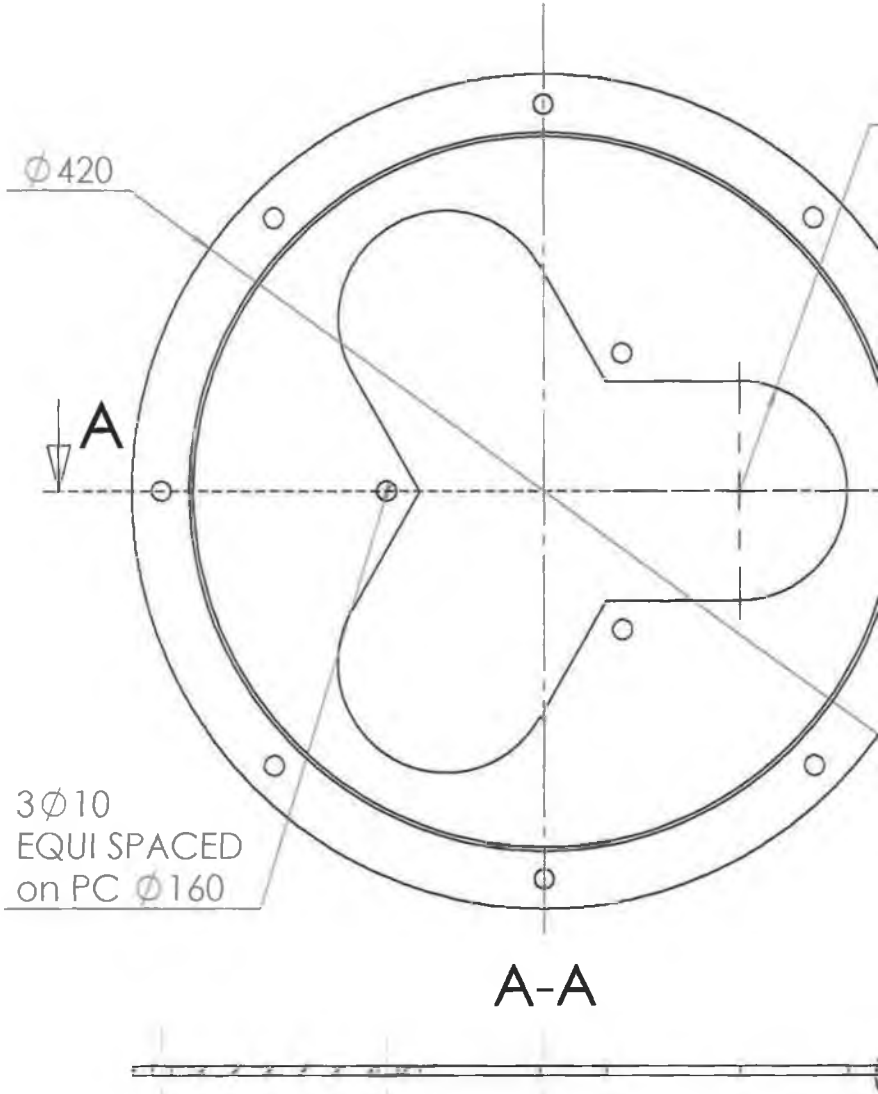

3R55
EQUI SPACED on PC ∅200

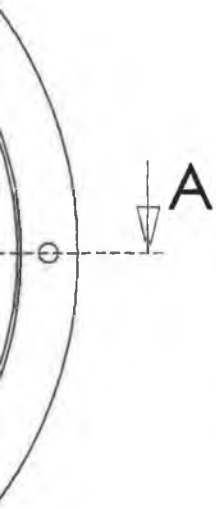

A

DETAIL B (2 : 1)

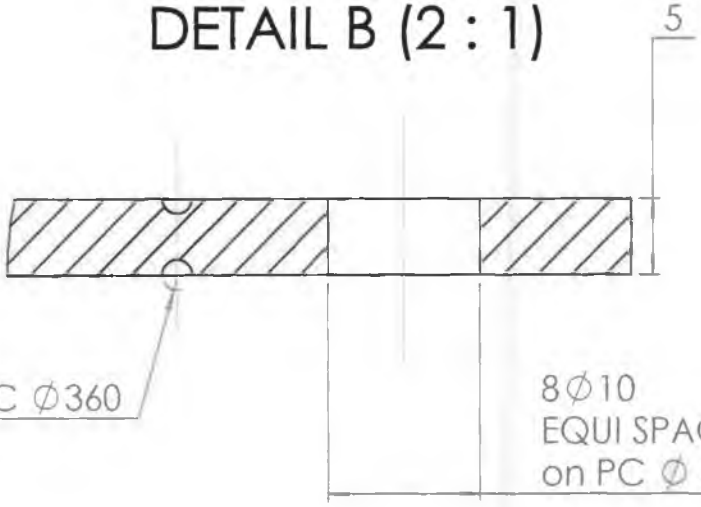

B

MATERIAL: STEEL ALL TOLERANCES ±0.2 UNLESS SPECIFIED OTHERWISE	NAME: LOWER PLATE
	ALL DIMENSIONS IN MILLIMETRES DESIGNER: SEBASTIEN QUEHIN April 200
	QUANTITY:1 SCALE: 1.3/5 G.M.I.T

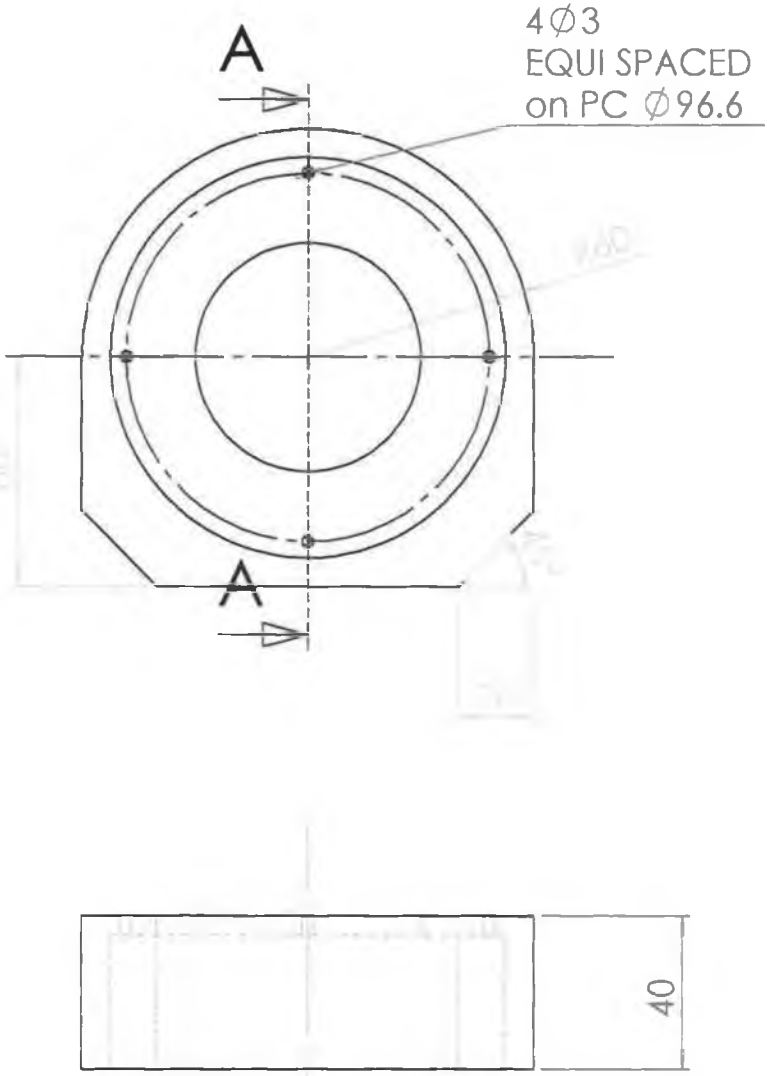

A-A

MATERIAL: STEEL	NAME: MOTOR SUPPORT
ALL TOLERANCES ±0.2 UNLESS SPECIFIED OTHERWISE	
ALL DIMENSIONS IN MILLIMETRES	DESIGNER: SEBASTIEN QUEHI April 200
QUANTITY:3 SCALE: 1/2	G.M.I.T

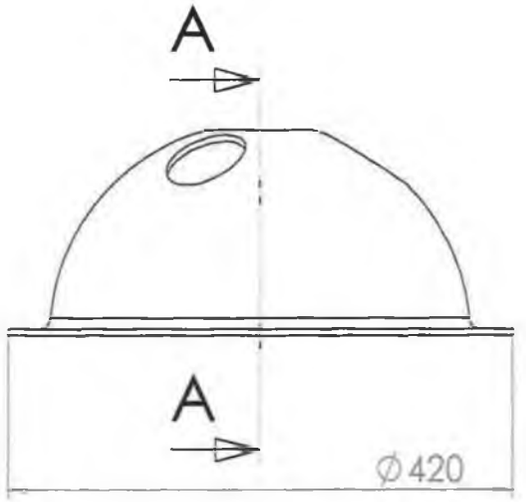

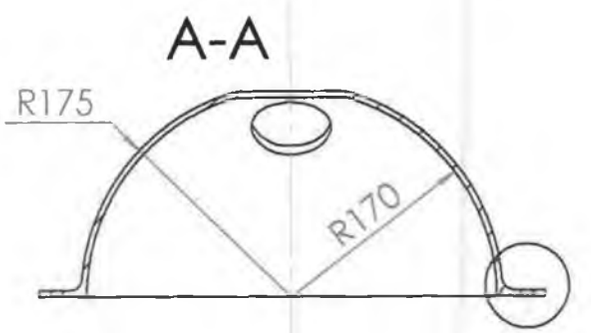

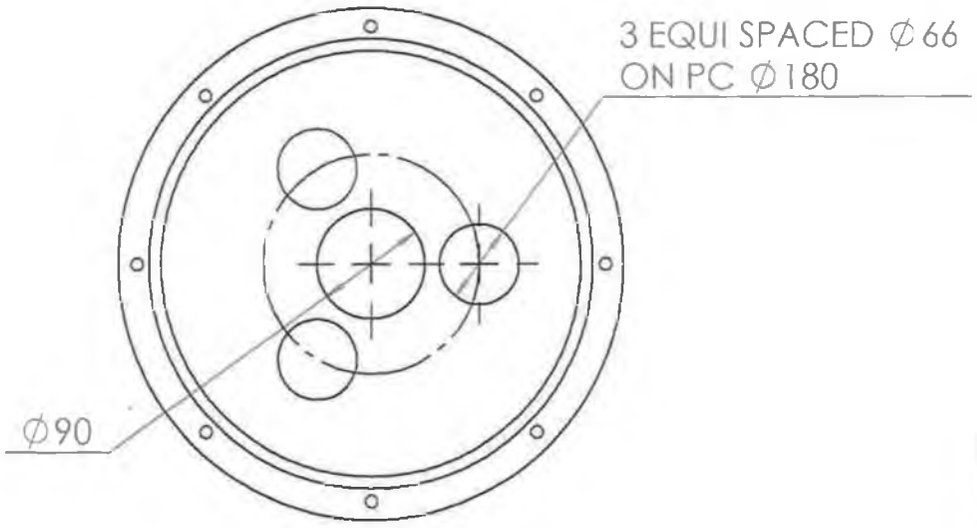

DETAIL B (1 : 1)

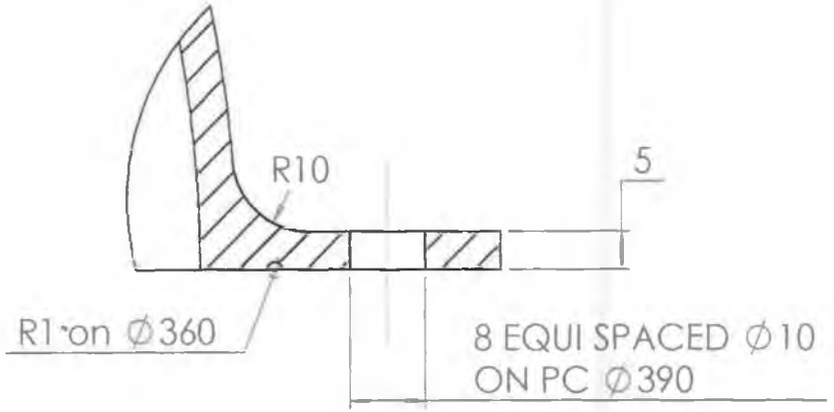

MATERIAL: EPOXY+FIBREGLASS

ALL TOLERANCES ±0.2 UNLESS SPECIFIED OTHERWISE

NAME: LOWER PLATE

ALL DIMENSIONS IN MILLIMETRES

DESIGNER: SEBASTIEN QUEHI April 20

QUANTITY:1 SCALE: 0.8/5 G.M.I.T

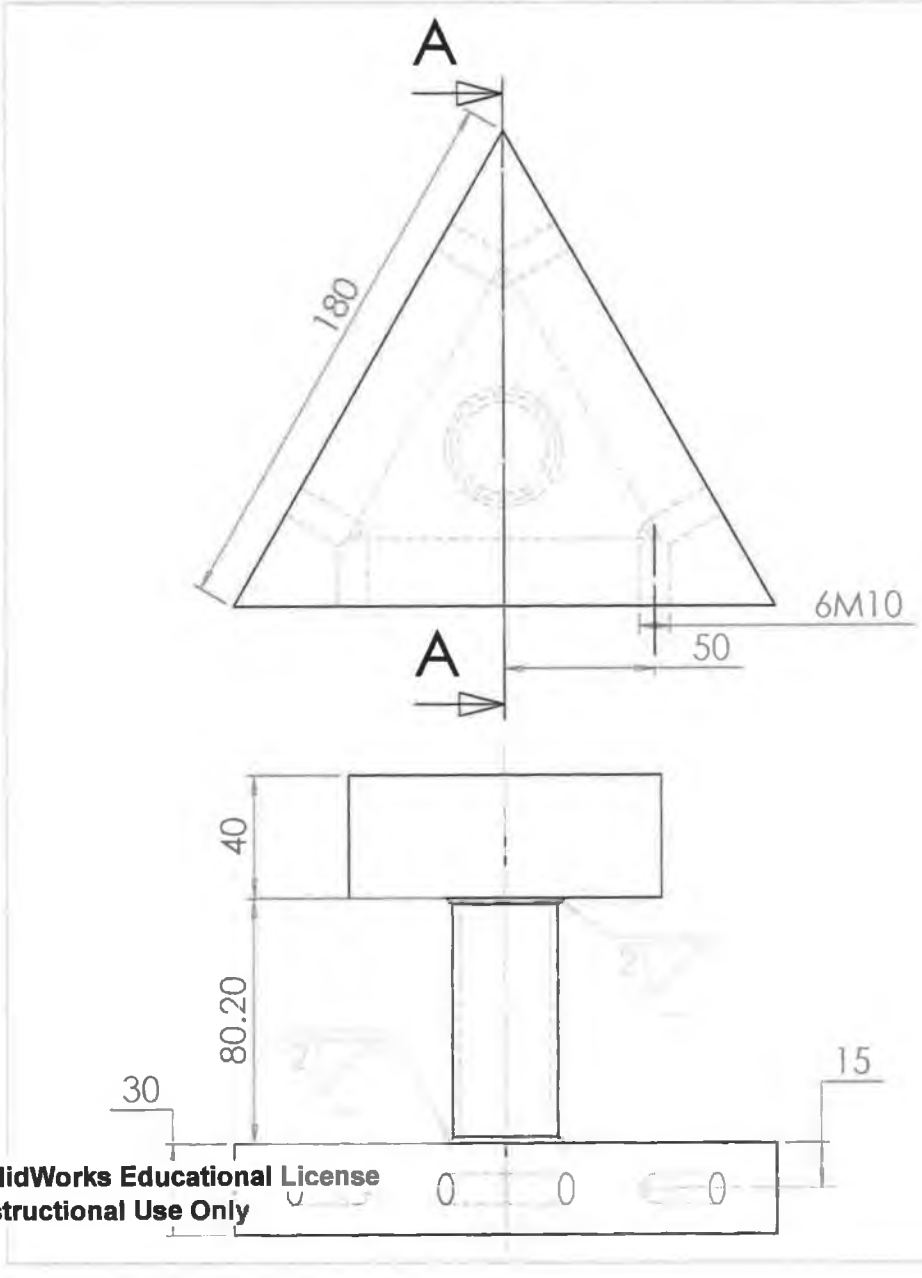

A-A

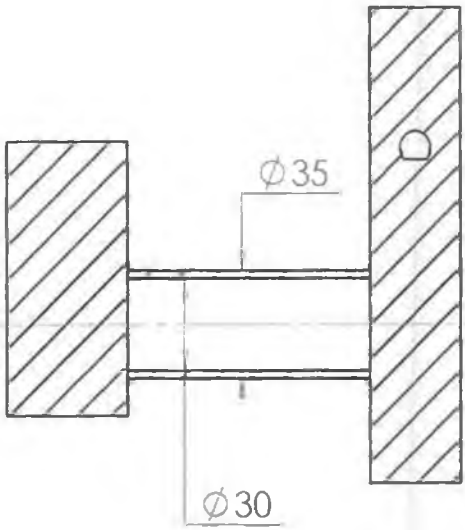

MATERIAL: STEEL ALL TOLERANCES ±0.2 UNLESS SPECIFIED OTHERWISE	NAME: CONNECTING PART
	ALL DIMENSIONS IN MILLIMETRES DESIGNER: SEBASTIEN QUEHI April 200
	QUANTITY:1 SCALE: 0.4/1 G.M.I.T

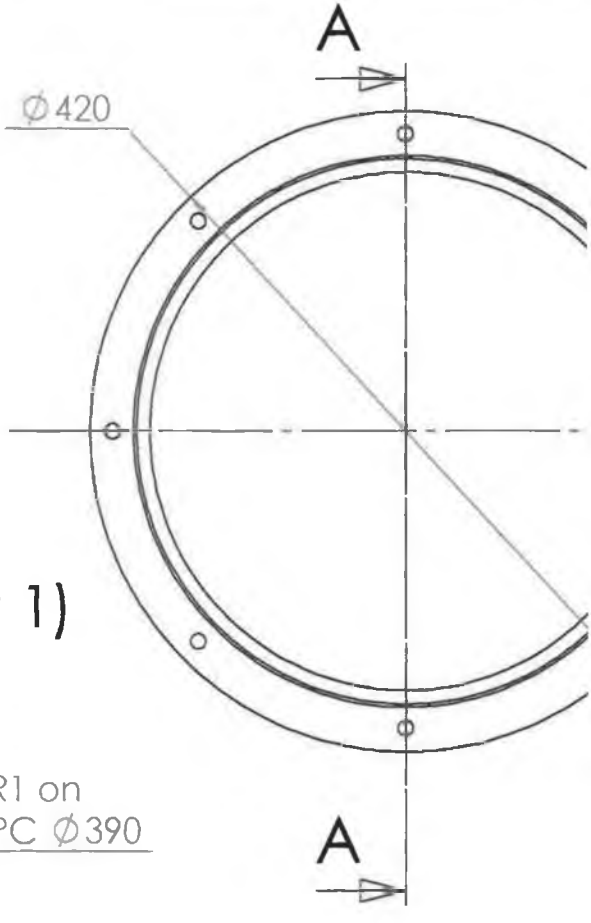

DETAIL B (1.5 : 1)

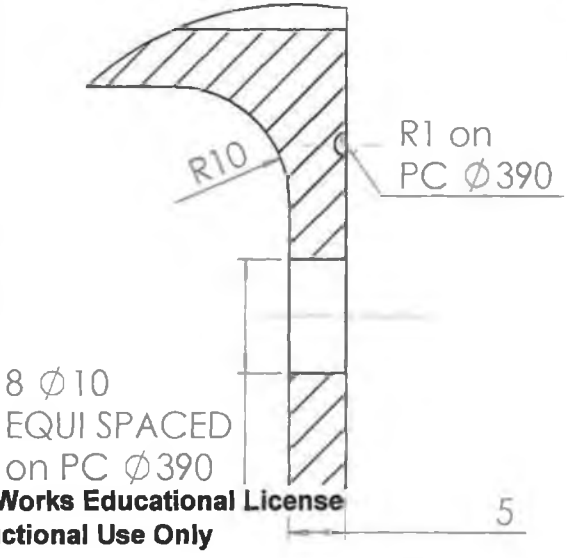

A-A

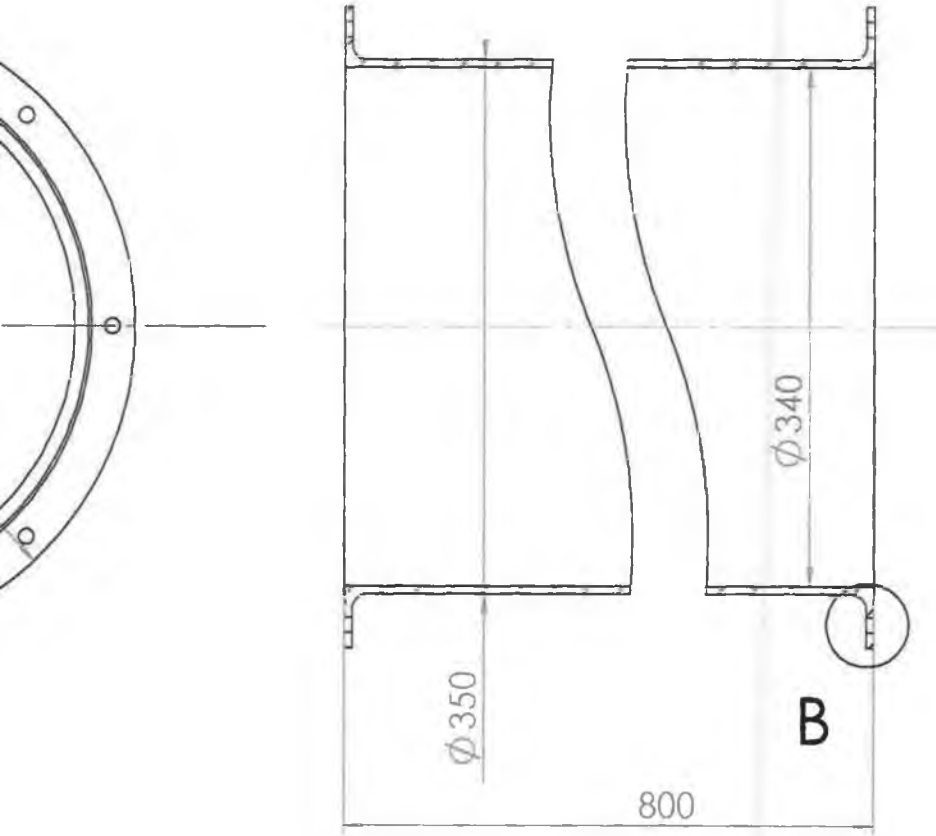

MATERIAL: EPOXY+FIBREGLASS

ALL TOLERANCES ±0.2 UNLESS SPECIFIED OTHERWISE

NAME: MIDDLE PART

ALL DIMENSIONS IN MILLIMETRES

DESIGNER: SEBASTIEN QUEHI April 200

QUANTITY:1 SCALE: 1/5 G.M.I.T

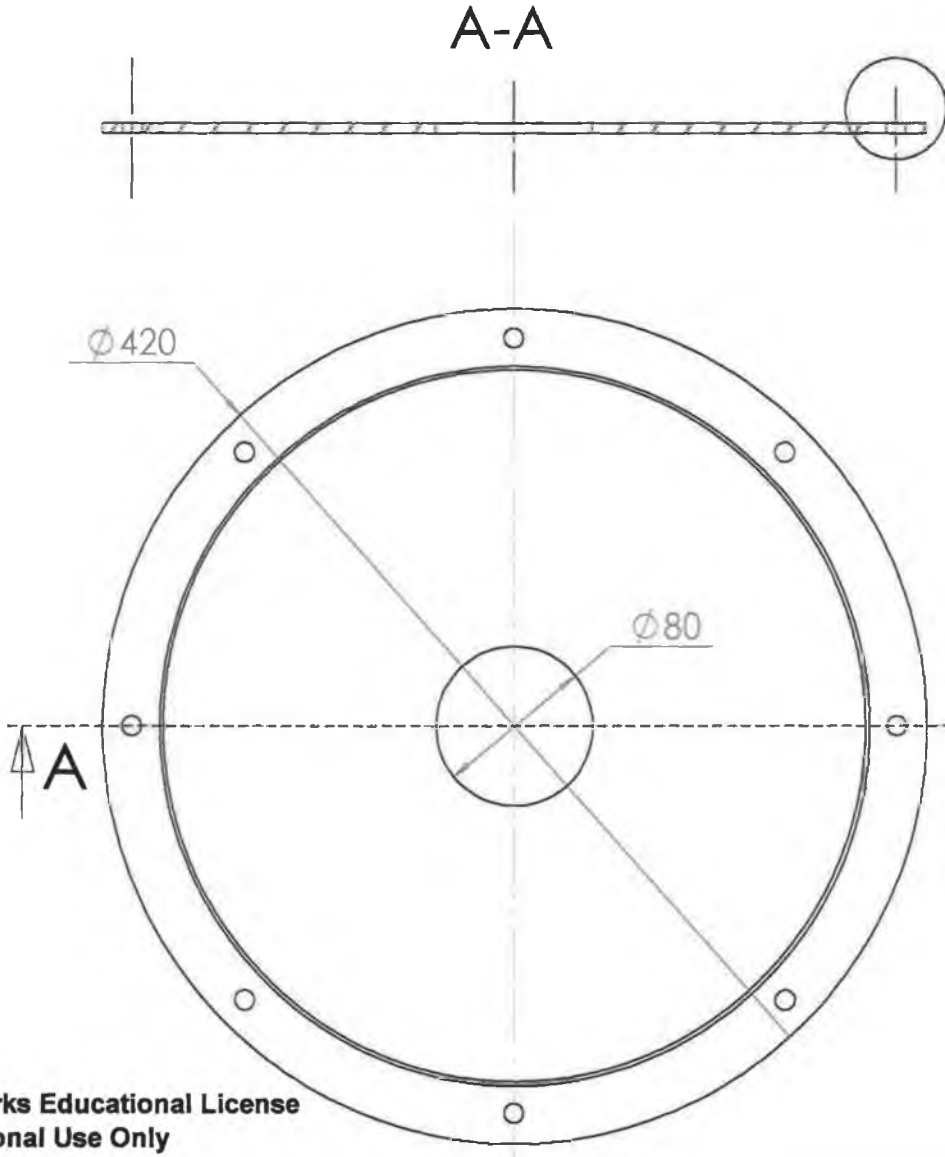

B

DETAIL B (2 : 1)

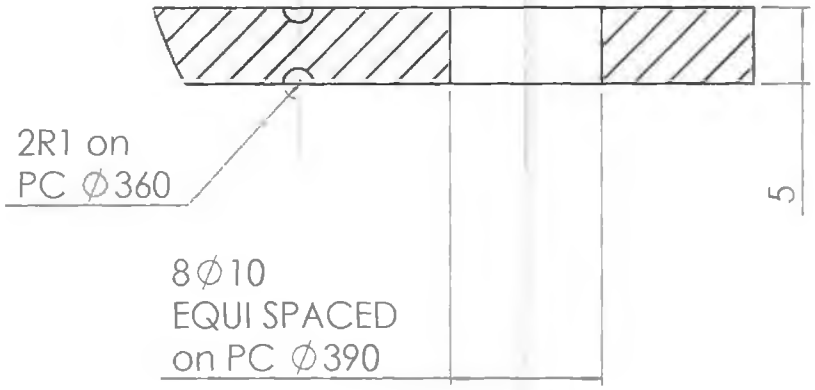

A

MATERIAL: STEEL	NAME: UPPER PLATE
ALL TOLERANCES ±0.2 UNLESS SPECIFIED OTHERWISE	
ALL DIMENSIONS IN MILLIMETRES	DESIGNER: SEBASTIEN QUEHI April 200
QUANTITY:1	SCALE: 1.3/5 G.M.I.T

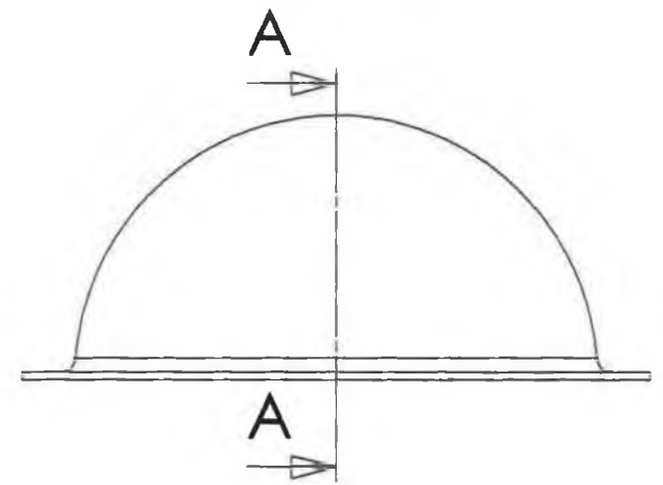

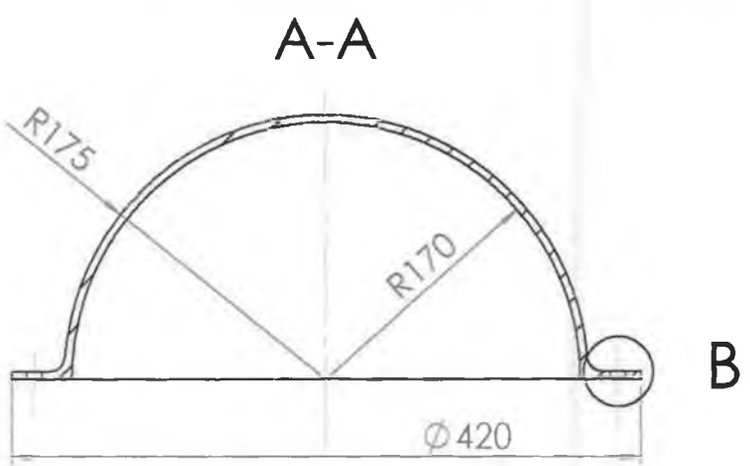

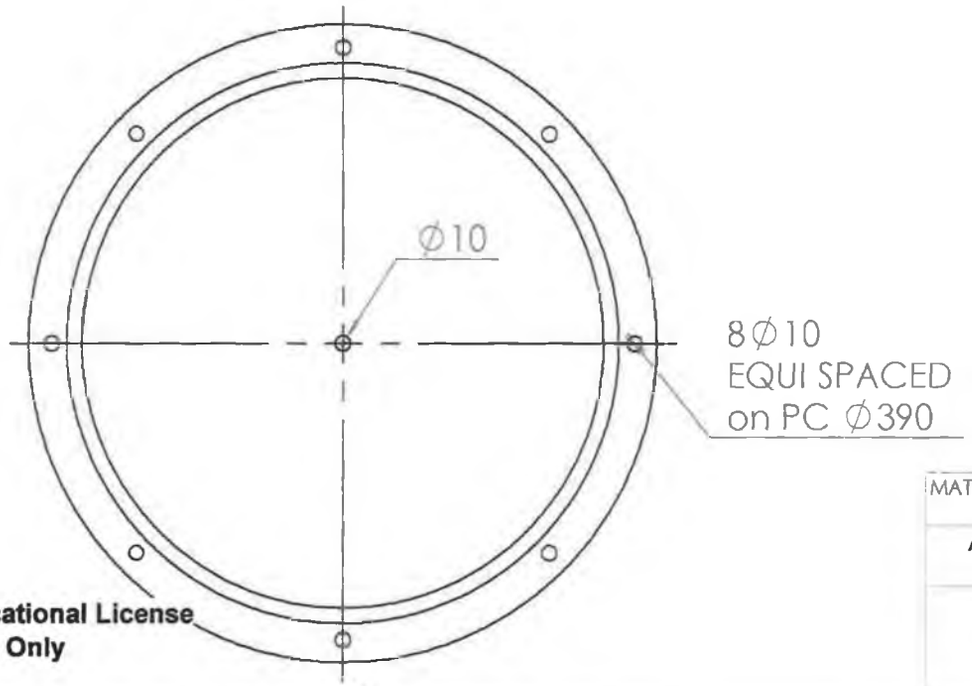

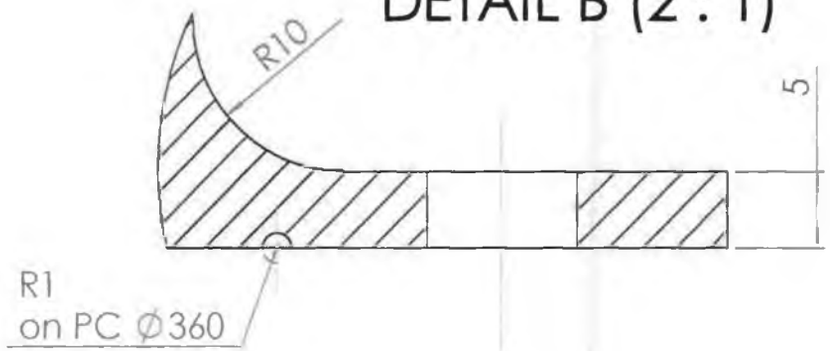

MATERIAL: EPOXY+FIBREGLASS

ALL TOLERANCES ±0.2 UNLESS SPECIFIED OTHERWISE

NAME: UPPERT PART

ALL DIMENSIONS IN MILLIMETRES

DESIGNER: SEBASTIEN QUEHI April 200

QUANTITY:1 SCALE: 1/5 G.M.I.T

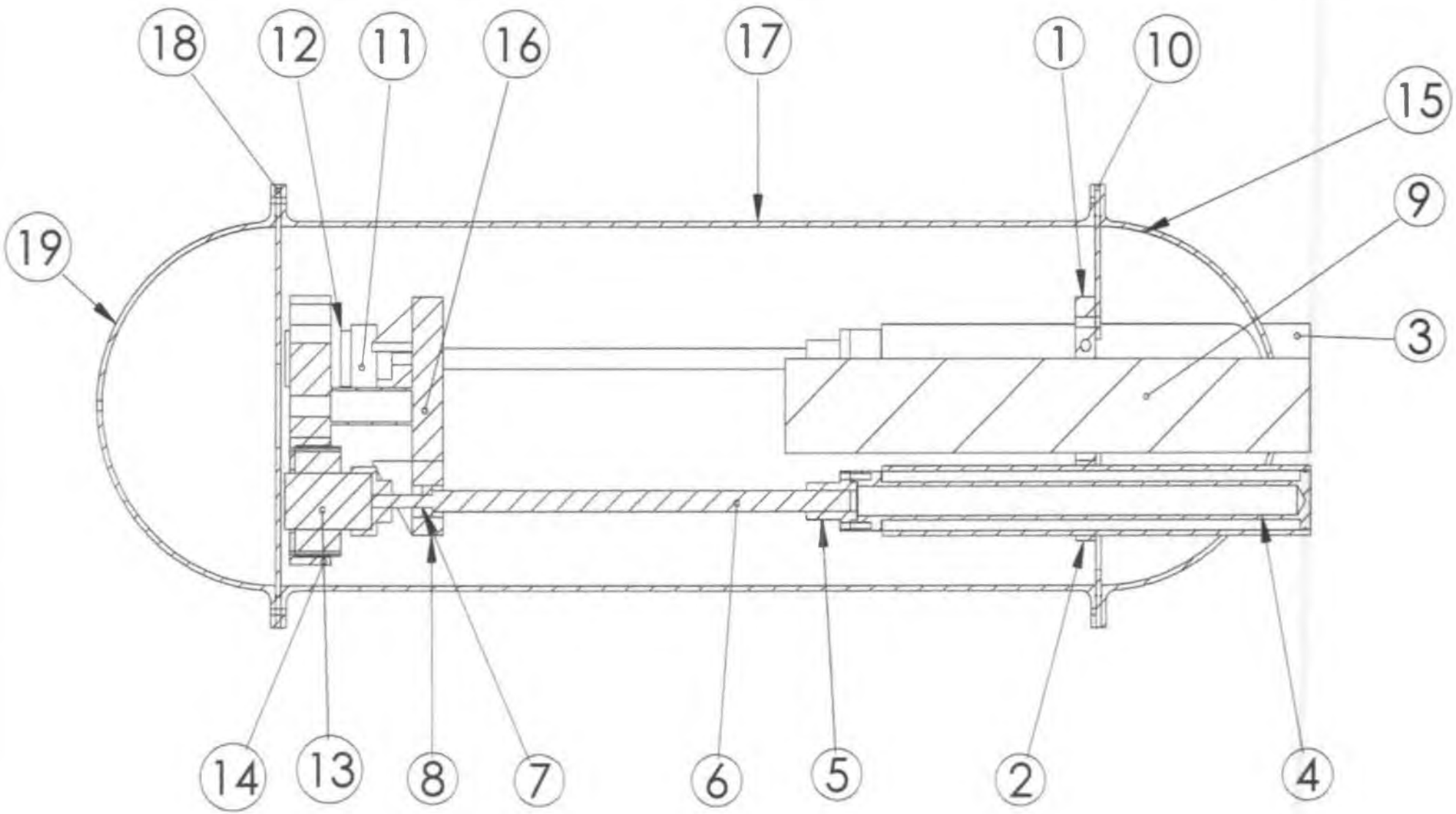

TION OF THE DEVICE SCALE 1.5 : 8 SEBASTIEN QUEHIN

No.	Element name	Comments
1	Sensor support	
2	Cylinder support	
3	Cylinder	-Teflon coating on the internal surface -Standard tube
4	Piston	
5	Nut	From Steinmeyer catalogue
6	Ball screw	From Steinmeyer catalogue
7	Bearing	Any supplier
8	Bearing support	
9	Sensor	Supplied by Sea Sense Ltd.
10	Lower plate	
11	Coupling	Any suplier/ Can also be manufacture
12	Shaft	
13	Motor	From Kollmorgen catalogue
14	Motor support	
15	Lower part	Made of epoxy and fibreglass
16	Connecting part	
17	Middle part	Made of epoxy and fibreglass
18	Upper plate	
19	Upper part	Made of epoxy and fibreglass